POLITECNICO
DI TORINO

CHALMERS
UNIVERSITY OF TECHNOLOGY

Drivers' comfort zone boundaries when overtaking pedestrians

Analysis of naturalistic driving and field test data

Master's thesis in Automotive Engineering

GABRIELE PANERO

POLITECNICO DI TORINO - ITA
CHALMERS UNIVERSITY OF TECHNOLOGY - SWE

MASTER'S THESIS IN AUTOMOTIVE ENGINEERING

Drivers' comfort zone boundaries when overtaking pedestrians

Analysis of naturalistic driving and field test data

GABRIELE PANERO

Department of Mechanics and Maritime Sciences
DIMEAS - Dipartimento di Ingegneria Meccanica e Aerospaziale

CHALMERS UNIVERSITY OF TECHNOLOGY - SWE
POLITECNICO DI TORINO - ITA

Drivers' comfort zone boundaries when overtaking pedestrians
Analysis of naturalistic driving and field test data
GABRIELE PANERO

© GABRIELE PANERO, 2018

Master's thesis 2018:66
Department of Mechanics and Maritime Sciences
DIMEAS - Dipartimento di Ingegneria Meccanica e Aerospaziale
Chalmers University of Technology - SWE
Politecnico di Torino - ITA

Telephone: +46 (0)31-772 1000

Cover:
Logo of Politecnico di Torino and Chalmers university of technology

Chalmers Reproservice

Drivers' comfort zone boundaries when overtaking pedestrians
Analysis of naturalistic driving and field test data
GABRIELE PANERO

Abstract

In the European Union, while pedestrian fatalities decreased over the past decade, their relative percentage in respect to all traffic fatalities slightly increased. Worldwide, the share of the pedestrian problem, in road accident injury, has not shown any significant change or improvement in the last few years. Furthermore, considering the constantly increasing tendency towards vehicle automation, it is even more important to understand, quantify, and model road users comfort zone boundaries. Comfort zone boundaries turn out to be relevant regions for enabling automated vehicles to drive in such a way that users feel both safe and comfortable.

Considering that safety research has thus far been focused on the interaction between drivers and pedestrian in the intersection scenario, the aim of this project has been to provide information about relevant safety metrics in the longitudinal scenario, i.e. when pedestrians are overtaken by a vehicle.

Thus, the work described in this thesis involved quantifying the comfort zone boundaries when drivers overtake a pedestrian, both from the driver and the pedestrian's perspective. Driver comfort zone boundaries were estimated from naturalistic data in the UDRIVE database. As well drivers' behaviour was observed from a pedestrian viewpoint using a wearable data logger, which has been set up and employed in an experiment performed on the road. The analysis of 68 events from the UDRIVE naturalistic driving study and 481 overtaking manoeuvres from the road experiment has allowed to estimate the comfort zone boundaries, by mean of the application of Bayesian regression models.

Driver behaviour was shown to be influenced by the presence of oncoming vehicles, as well as by the walking direction of the pedestrian. Also, the steering input for the last phase of the overtaking manoeuvre, was surprisingly performed by drivers before the vehicle had passed the pedestrian.

Overtaking maneuvers are complicated events, resulting usually in outcomes that cannot easily be predicted and are sometimes completely unexpected. However, this study showed how specific factors influence drivers' comfort zone boundaries while overtaking a pedestrian. The two data sets investigated resulted to be complementary, allowing to have a complete understanding of the event. Findings are relevant for active system development, and Euro NCAP safety features assessment related to the collision pedestrian longitudinal adult (CPLA) scenario. Safety factors have been compared with previous study related to bicycle overtaking events.

Keywords: Driver behaviour, Active Safety, Human factors, Comfort Zone Boundaries, Field of safe travel, Driver – Pedestrian interaction, Euro NCAP, Naturalistic Driving Data, ROS, LiDAR

Preface

This master thesis work has been carried within the Master of Science degree in Automotive Engineering at Chalmers University of Technology in Göteborg, Sweden. The activity has been carried out within the ERASMUS + student exchange program, as final project of the home university Politecnico di Torino, MSc in Automotive Engineering. The whole project was performed during the spring semester (from January to June 2018) within the Vehicle and Traffic Safety Centre at Chalmers - SAFER. The activity is related to the "Driver Interaction with Vulnerable Road Users" (DIV) research project. The whole activity has been supported by Autoliv AB and Toyota Motor Europe. The project has been conducted by mean of a parallel and joint activity carried out by the author of this document and the Master student, Alexander Rasch, author of the thesis project entitled: "Modeling driver behaviour in longitudinal car-to-pedestrian scenarios". A special mention has to be given to the active cooperation with Alexander throughout the whole duration of the project.

Acknowledgements

First and foremost, I would like to express my gratitude to the examiner Marco Dozza, at the outset for his proposal and recommendation (about this project activity), for all precious suggestions, feed-backs and for his willingness in making it possible to accomplish the field experiment. A special acknowledgement to Christian-Nils Åkerberg Boda, who in the capacity of supervisor has always proven an amazing leader, being ready in helping and in proposing advise during the course of the project.

I must express my gratitude toward the thesis project partner Alexander Rasch, with whom I had the pleasure of sharing my time and improving my knowledge.

I would also like to express my gratitude to the secondary supervisor Nils Lubbe, for his outstanding positive attitude and willingness to help.

A special thank goes to Jordanka, Erik and Helena for their help during UDRIVE analysis in particular for suggestion in using SALSA tool; a special mention to Andràs for his help with STRADA, to Esko for his help with Ubuntu laptop, to Autoliv/Veoneer for giving the possibility of equipping a test-car and for having supported this thesis activity. I am also grateful to Alberto and Kevin for the interesting discussion we had about driver modelling following the Bayesian approach. I extend my gratitude to everyone in SAFER who has always been very kind, letting me possible to always feel like at home. It is amazing how everybody is playing a role in providing a pleasant and sound environment to work and learn. A special mention to the advisor Andrea Tonoli of the Italian university Politecnico di Torino.
Finally, I would like to thank my wonderful girlfriend Giada, for her ever-present support. I would like to show my thankfulness to my family, who always made me feel their love and enthusiasm even if I was very far from home. To my brilliant mother Brunella, to my generous and down-to-earth father Adriano, to my awesome brother Fabio: thank you for having made it possible this experience.

A special thank to my friends, to everyone I met during these years of study and to everyone from all over around the world that made this period the best experience I could have ever imagined.

Also to you, who are reading this thesis work: thank you!

Gabriele Panero

Nomenclature

Abbreviations

ADAS	Advanced driver assistance systems
AEB	Automated emergency braking
CAD	Computed aided design
CAN	Controller area network
CPLA	Collision pedestrian longitudinal adult
CZB	Comfort zone boundaries
DAS	Data acquisition system
DATMO	Detection and tracking of moving objects
DBM	Driver behavior modeling
FCW	Forward collision warning
FoST	Field of safe travel
FT	Field test
GPS	Global positioning system
IMU	Inertial measurement unit
LiDAR	Light detection and ranging
ME	MobilEye
NCAP	New car assessment program
NDS	Naturalistic driving study
pcl	Point cloud library
PCW	Pedestrian collision warning
RANSAC	Random sample consensus
ROI	Region of interest
ROS	Robotic operative system
RPi	Raspberry Pi
SALSA	Smart automation for large data sets analysis
STRADA	Swedish traffic accident data acquisition
UDRIVE	European naturalistic Driving and Riding for Infrastructure & Vehicle safety and Environment
VRU	Vulnerable road user

Overtaking scenario specific variables

LC	Lateral clearance
mAG	Minimum approaching gap
mC	Minimum clearance between driver and pedestrian
mDS	Minimum distance steering
mRG	Minimum returning gap
$T2P$	Time to pedestrian
THW	Time headway
TTC	Time to collision

Contents

1 Introduction

Since the automobile transportation is still increasing in all countries all over around the world, cyclists, pedestrians and motorcyclists, also called vulnerable road users (VRUs) will be more exposed to traffic crashes. Actually, over 400.000 pedestrians die every year, and half of these deaths occur in low income countries [1].

Concerning the location of pedestrian crashes, some studies show that this type of crash occurs often in areas with higher population density such as large towns. In fact, in 2007 approximately 73% of pedestrian fatalities occurred in urban areas due to the high amount of pedestrians. On the other hand, some others studies report that the fatality rate of pedestrian crashes in rural areas, with lower population density, was higher than the fatality rate in urban areas. Indeed pedestrians are more than 2.3 times more likely to die from a pedestrian crash in a rural area than in an urban area [1]. Reasons for this phenomenon are related to the fact that vehicles move more likely with higher speeds in rural areas. Also, less pedestrian facilities, such as sidewalks, are available to prevent possible collision in a longitudinal driver-pedestrian scenario. Moreover the quality of emergency services in these areas is lower than in urban areas.

Furthermore, considering the constantly increasing tendency towards car automation, there is an ever more importance to understand and quantify road users comfort zone boundaries [2]. These are defined as a spatiotemporal region surrounding the vehicle, in which no discomfort is felt or predict while driving [3]. Comfort zones result to be relevant variables for enabling automated vehicles and active safety features to perform in such a way that users feel both safe and satisfied. In this context, independent organizations (e.g. Euro NCAP) are encouraging significant safety improvements to new car design and, at the same time, they are providing independent assessment of safety performances of vehicles available on the market. Hence, a detailed quantification of the factors influencing motorist's behaviour in the particular scenario of pedestrian overtaking has the potential benefit of indicating which are the physical parameters that need to be evaluated during a testing protocol.

1.1 Purpose

The objectives of this activity aim to understand how to identify and analyze overtaking manoeuvres of pedestrians from the UDRIVE database, which refers to a naturalistic driving data collection in the European union. Moreover, with the intention of quantifying the driver behaviour with a complementary data set, a field data measurements has been performed in the road traffic. The field data collection activity has also been focused on the development of a logger platform, which could enable data recording also for future studies. Comfort zone boundaries are evaluated and a driver model has been devised, in order to estimate the influence of specific factors (characterizing the scene) on drivers' performance.

1.1.1 Research questions and hypotheses

The overall activity of driver behaviour quantification has been based on the following research questions:

Q1 - Does the lateral position of a pedestrian influence the lateral distance (leeway) a car is giving to him/her, while passing?

Q2 -Do drivers perform the steering-away phase even if a pedestrian is perceived out of the lane (i.e. on the curb)?

Q3 - Does the "eye-contact" influence driver behaviour?

Q4 - Does the oncoming traffic presence reduce the leeway between a motorized vehicle and a pedestrian?

Q5 - Is the overtaking speed influenced by the presence of oncoming vehicles?

In order to answer to the research questions some hypotheses have been formulated:

H1 - "If a pedestrian is closer to the middle of the lane, the clearance decreases"

H2 - "If a pedestrian is outside of the lane, drivers do not perform the steer away phase"

H3 - "If a pedestrian is facing the traffic, the "eye-contact" reduces the lateral clearance"

H4 - "If oncoming traffic is present, the lateral clearance is reduced"

H5 - "If oncoming traffic is present, drivers reduce vehicle speed"

The results and discussion section of this thesis have been structured based on these hypotheses. Those are associated to three main factors characterizing the overtaking event. Hypotheses one and two relate to the pedestrian walking position. Hypothesis three is related to the pedestrian walking direction, while hypotheses four and five refer to the oncoming traffic factor.

1.2 Credibility and restrictions

The naturalistic data set offers a unique opportunity in analyzing the driver behaviour thanks to the unobtrusive way of its data collection. Hence, drivers behave in a natural manner, providing information about their usual driving style. As well, the field test data collection allowed to record data associated to drivers' natural way of performing the manoeuvre, since no driver was previously informed about the collection. Therefore the ecological validity of the events analyzed is quite relevant.

However, restrictions are present. These are mainly related to the accuracy of the pedestrian position measurement sensor available in UDRIVE. The MobilEye system (implemented on the car data logger for object detection and tracking) has been prone to lots of miss-detection (traffic-sign classified as pedestrians), hence manual annotation needed to be performed. Indeed the annotation procedure could be source of subjectivity, even though both annotators adopted an objective approach. Concerning the field data-collection, limitation of results could be related to the equipment used by the pedestrian, who was wearing a reflective vest during the collection. As well, the human body motion while walking had a relevant impact in the phases individuation of the overtaking manoeuvre.

1.3 Outline

Chapter two - Background A overall review is presented about pedestrian crash statistic, human factors, ADAS systems and naturalistic driving studies.

Chapter three - Approach and Methodology A detailed description of the activity is presented. Two specific sections are adopted: in the first it is described the analysis performed on the naturalistic data set; while in the second section it is presented the activity associated to a field test experiment. Eventually, the implementation of a comfort boundary regression model is specified in a dedicated section.

Chapter four - Results Main findings are grouped with respect to the three activities carried out in this project as stated in the methodology. An overview of the results is given through tables and figures.

Chapter five - Discussion Results are discussed considering answers to the research questions. Relevant implications on safety systems are given. Also, advantages and disadvantages are outlined related to each part of the adopted methodology.

Chapter six - Conclusion and future work A summary of the activity is given, with a special mention to possible future projects linked to driver VRU interaction in the longitudinal scenario.

2 Background

In this chapter it is given a quite comprehensive overview on different topics analyzed in this thesis project. This includes terminology definition as well as description of the data collections available and the theoretical background of some technologies there implemented. This could help the reader to get acquainted with several areas of research covered hereafter. The chapter starts with the presentation of general crash statistics concerning mainly the pedestrian category between road users. Moreover, it will be outlined a general description of the specific manoeuvre analyzed in this thesis project, together with basic principles of driver-pedestrian interaction. The literature discussed provides a general insight into why overtaking manoeuvres of VRUs are interesting and what variables in such overtaking manoeuvres need to be kept under review. Lastly, it will be given a description of the safety features rating systems currently in force.

2.1 Crash statistics

According to World Bank estimates [4], about 1.2 million people are annually killed in road accidents around the world, of whom one third are pedestrians, where typically pedestrians account for the major proportion of road-traffic injuries and fatalities in low- and medium-income countries. To be more precise, worldwide over 400,000 pedestrians die every year, with over half of these deaths occurring in low-income countries [5]. It stands out that with greater wealth comes greater motorization and that fatal pedestrian crashes are higher in low-income countries, despite the fact that overall fatal motor vehicles crashes are higher in high-income countries [1]. In the United States in 2015 there were 5,376 pedestrians killed in traffic crashes, a 9.5 percent increase with respect to the previous year. This figure accounts for the 15% of all traffic fatalities. Furthermore 90% of pedestrians were killed in traffic crashes that involved single vehicles [6]. It is worth to mention that 71% of pedestrian fatalities occurred at non-intersections while only 19% took place at intersections. This percentage had also been reported by Clifton et al. in [7]. These researchers state that nearly 60% of the VRU involved in a crash and just under 70% of those killed in a crash were not in crosswalks, suggesting the importance of pedestrian compliance to traffic laws as well as availability of marked crossing in promoting pedestrian safety. Moreover, in USA approximately 73% of pedestrian fatalities occurred in urban areas, largely because of the greater number of pedestrian trips in urbanized areas [8]; in Europe it is shown the same trend [9].

Concerning the European Union a deeper analysis reveals that almost 6000 pedestrians (5730 in 2016 CARE records) and 2000 bicyclists are killed annually, which is approximately 27% of all fatalities [10]. In Sweden, approximately 45 pedestrians (and 20 bicyclists) are killed annually [11] which account for 15% (and 9%) of all road fatalities respectively. Out of all pedestrians and bicyclists admitted to hospital in Sweden in 2013, 262 pedestrians and 2155 bicyclists were estimated to suffer from long term disability [11]. It is worth noting that during the decade 2005-2014,in the European Union, pedestrian fatalities were reduced by 35%, while the total number of fatalities was reduced by almost 42%.

In the following a detailed description of pedestrian fatalities based on different parameters [12] is outlined:

- fatalities based on AGE-group and GENDER:

The percentage of pedestrian fatalities is higher for children and the elderly than for other age groups. Although a high percentage of child fatalities were pedestrians, they only represent 4% of the total pedestrian fatalities. Moreover, more than one third of pedestrian fatalities (36%) were female, compared with less than one quarter (24%) when all traffic fatalities are considered.

- fatalities based on DAY of the Week and TIME of the day:
  More than 50% of all pedestrian fatalities occurred between 4pm and midnight. Pedestrian and total road fatality distributions by day of the week and time of the day are quite similar. However, relatively more pedestrians are killed in road accidents between 6pm and 9pm during the whole week and between midnight and 5am on Sundays.

- fatalities based on LIGHT CONDITION:
  45% of pedestrian fatalities in the EU occurred in darkness, whilst 36% of pedestrian fatalities was also recorded in daylight. Remaining 19% has been reported as unknown.

A detailed analysis of the Swedish traffic accident data acquisition (STRADA) has shown a decreasing trend of pedestrian injuries and fatalities over the decade 2006-2016. As depicted in Figure 2.1 and 2.2, the larger amount of events happened in urban areas. Moreover more than 40% of pedestrian fatalities were female, which is a higher value compared with the average percentage of all female fatally involved around Europe (36%). The amount of male involved as pedestrians is increased over a decade, however this trend is much more visible for bicycle users.

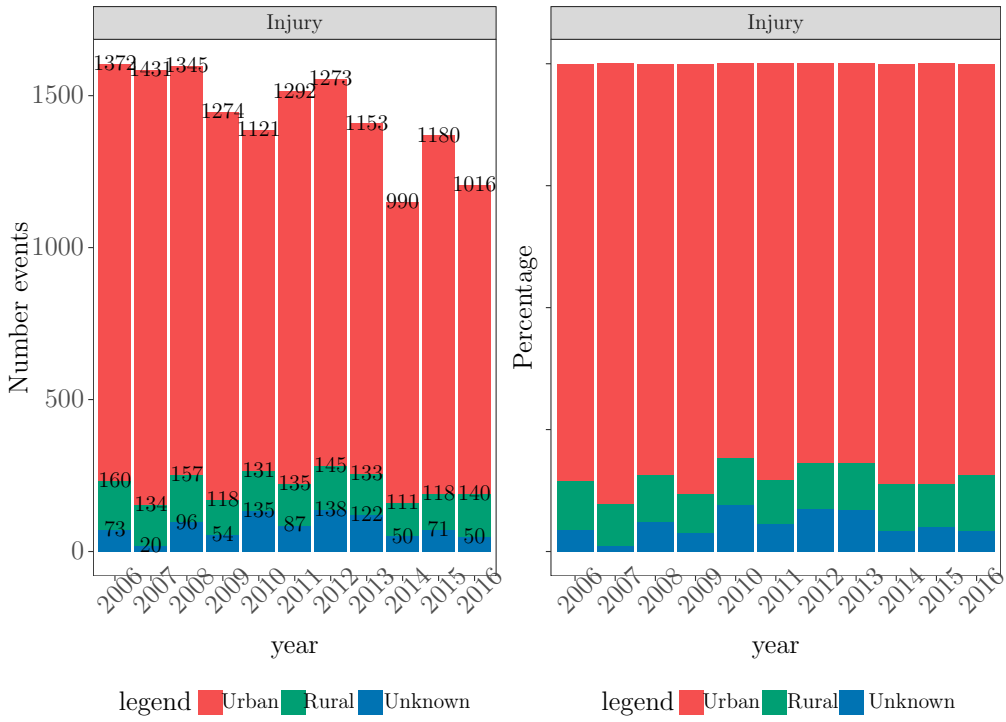

Figure 2.1: *Pedestrian injuries in decade 2006-2016, (left) number of events, (right) percentage per area. Data from STRADA*

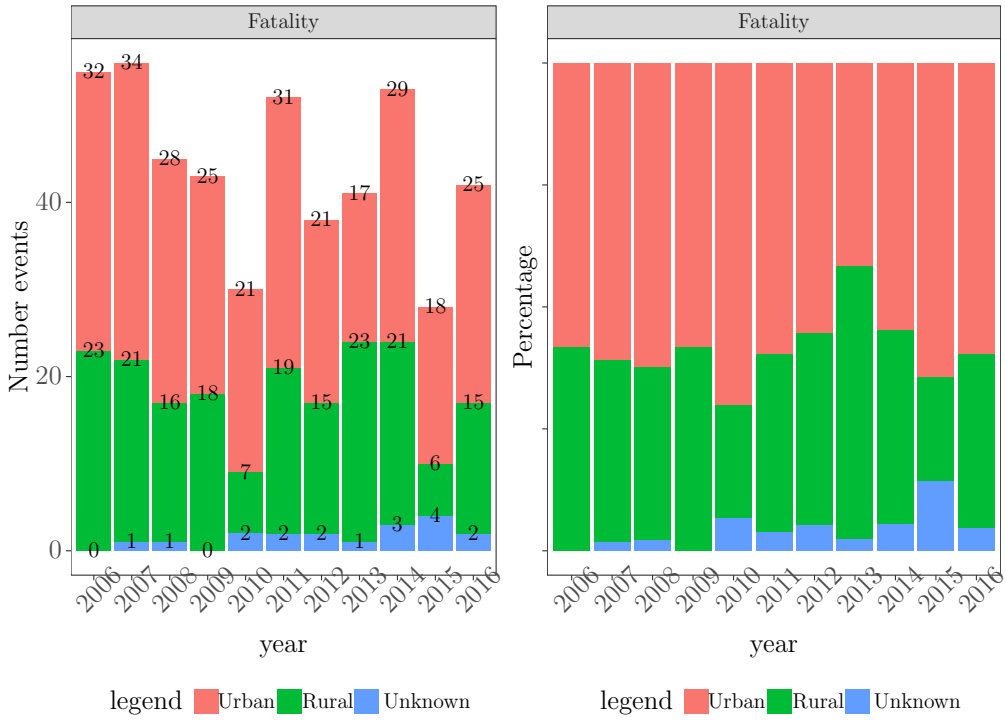

Figure 2.2: *Pedestrian fatalities in decade 2006-2016, (left) number of events, (right) percentage per area. Data from STRADA*

It is worth mentioning, that the higher percentage of people killed in rural areas (36% in 2016) compared to the percentage (12% in 2016) of people injured in the same area is consistent with what it has already been stated by Zegeer et al. [1]. It has been highlighted that although fewer pedestrian fatalities usually occur in rural areas, pedestrians are more than 2.3 times more likely to die from a crash in rural areas than in urban areas. This can be mainly due to the higher vehicle speed in non-urban environments. As a matter of fact, speed plays a critical role for pedestrian safety. Pedestrian injury severity is usually based on speed: the probability for a pedestrian to die is 85% when the striking vehicle is travelling at 40 mph (64.4 km/h). Probability drops to about 45% for a 30 mph (48.3 km/h) and if the speed is 20 mph (32.2 km/h) the percentage drops to a value of 5% [13].
However, that causes of such events are multiple and diverse. Not only the interaction between driver and pedestrian is crucial, but also the built environment plays an important role. In [14] it has been shown that more pedestrian crashes occur in areas with educational facilities and higher percentages of commercial land use.
An investigation in the Swedish database has allowed to analyze the trend of injured and killed pedestrians over the period 2003-2010 for the specific longitudinal scenario of pedestrian walking on the right side of the road. Data are represented in the column graph in Figure 2.3. This specific scenario accounts roughly for the 8% of all pedestrian injuries recorded in the database in the previously described 8 years period.

To summarize, the overall number of VRU involved (both for pedestrians and bicyclist) has decreased over years. However, as represented in Figure 2.4 considering the rate between the pedestrian casualties and the overall fatalities in Sweden, this value has increased over the past ten years. A steadily increasing rate from 12,4% (in 2006) to a peak of 19,6% (in 2014) highlights that even if lots of improvements have been done on general vehicle safety, the

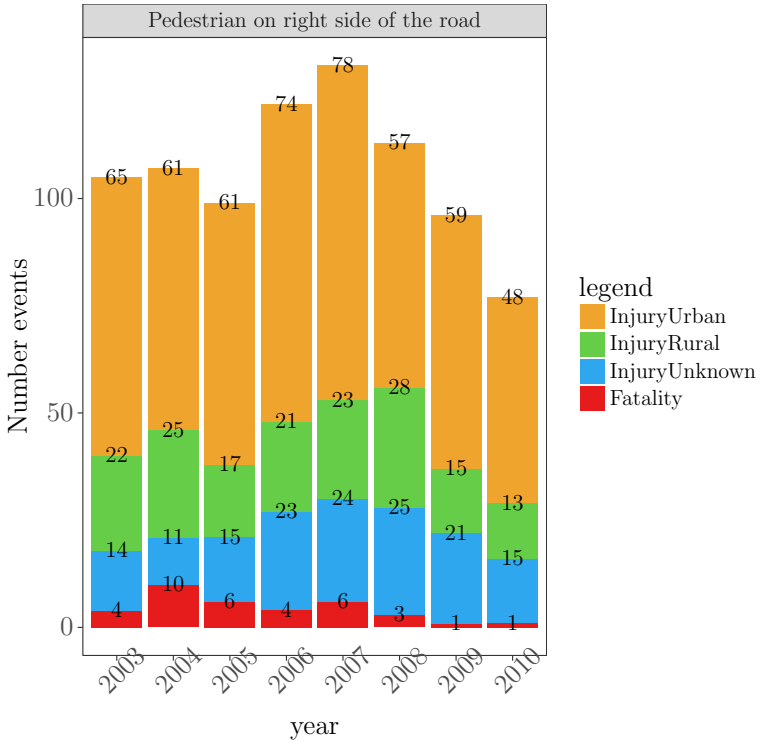

Figure 2.3: *Pedestrian events, both injured and killed, while walking in right side of the road. Data from STRADA*

interaction between motorists and pedestrian should be investigated to enhance road users' safety.

It has to be noted that the slightly increasing trend of the of pedestrian fatality rate over all traffic casualties is observed also in the whole Europe [12].

The aforementioned facts and figures bring out that, even if an important progress has been made over the last decades, there is still need of advancement in the VRU's safety. This with the purpose of promoting safety in the car to pedestrian interaction on a par with other scenarios. Accordingly, the purpose of this thesis work is focused on the quantification of human behaviour and comfort zone boundaries which may help the development of future Advanced Driver Assistance Systems (ADAS), which are supposed to predictively help drivers in a safer accomplishment of their task, hence reducing pedestrian casualties.

2.2 Overtaking manoeuvre

In the Cambridge dictionary [15] overtaking is defined as "to come from behind another vehicle or a person and move in front of them". With reference to the English Royal Society for the prevention of accidents, overtaking is defined as "one of the highest risk manoeuvres for both drivers and riders because it can put the overtaking vehicle into the path of oncoming traffic, often at high speeds. If there is a head-on collision, the speed of both vehicles combines to create a much more severe impact" [16]. It is worth considering that overtaking manoeuvres are usually dissimilar each other, mainly on the account of multiple road user present in the scene (e.g. oncoming traffic, leading vehicles) as well as environmental condition present while

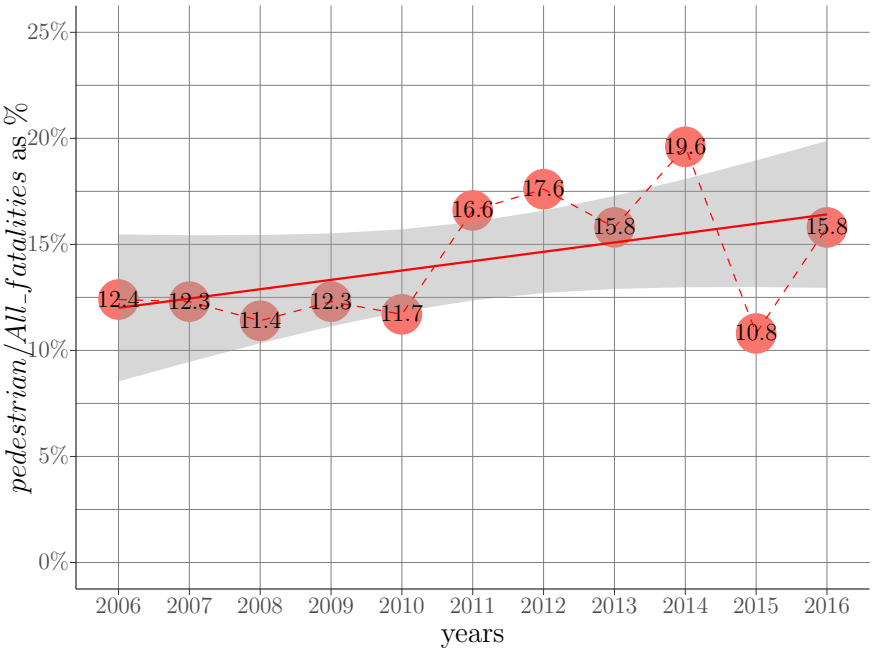

Figure 2.4: *Percentage of pedestrian fatalities related to all traffic fatalities in Sweden. A trend line is fitted through percentage evolution over years. The grey zone represents the 95% confidence interval of the trend line. Data from STRADA*

the overtaking is performed (e.g. nigh-time, lane width). Hence it is important to refer to definition and categorization of overtaking manoeuvres suggested in the literature.

2.2.1 Overtaking strategies

Overtaking manoeuvres are usually categorized in different strategies as follows [17] [18] [19] [20]:

- Flying
- Accelerative
- Piggy backing
- 2+

In the flying strategy a driver overtakes at a relatively constant speed. In the accelerative manoeuvre, a driver decelerates and/or adapts the vehicle's speed to the velocity of the leading road user; the overtaking occurs only when the driver has followed the leading road user for some time before passing. The piggy backing strategy is adopted by drivers who follow a lead overtaking vehicle, so that two or more cars in a row are involved in the overtaking of the same vehicles or VRU. In this scenario the lead driver may have selected either a flying or accelerative strategy. The 2+ manoeuvre occurs when the over-taker catches up with multiple road users, hence the minimal number of overtaken users is two.

2.2.2 Overtaking phases

The overtaking is a long, complex and diverse manoeuvre. Thus, different authors proposed various classification procedures segmenting the manoeuvre in three phases [21], four phases [19] or five phases [20] based on consideration related also to driver's intentions and actions. When reference is made to car overtaking another car three main driver actions may be identified [22]:

- Diverting from the lane
- Driving straight in the adjacent lane
- Returning to the lane

Hageman et al. in [20] extended the three phases approach to five phases when it is considered the overtaking of another vehicle. These are:

- Decision (based on driver behavioural state and environmental factors)
- Preparation (related to driver's perception and reaction time)
- Lane change (based on steering action and vehicle acceleration)
- Passing (influenced by presence of oncoming vehicles)
- Return to original lane

When the focus is made to a vehicle overtaking a bicyclist, the phases classification has been investigated and elaborated by Dozza and colleagues [19] [23] based on previous Master's thesis [24]. The former study evaluated the manoeuvre using an instrumented bicycle, while the latter analyzed the overtaking from a car perspective, utilizing NDS data. Thus, when it is considered an overtaken wheeled VRU four phases can be outlined:

- Approaching
- Steering away
- Passing
- Returning

It is worthwhile clarify the phases listed above.

Phase one – The approaching phase occurs when a vehicle reaches the bicycle, within the reading range of measurement sensors adopted in previous study, until the start of the next stage of the overtaking manoeuvre. In [25] the start of the first phase has been defined based on the time-stamp in which the bicycle was visible in the video-feed provided from a camera installed in the vehicle.

Phase two – It begins when the driver steers away/pull out the vehicle from its collision course to the VRU. In [24] the start of this phase was annotated whenever the car side was detected by the used measurement sensor (LiDAR) and it was expected to finish whenever the vehicle's front was at a longitudinal distance of 2 m behind the rear of the bicycle.

Phase three – the passing phase refers to the area behind and in front of the VRU in which the car is passing and overcoming the slower road user. For this phase two different definition have been established. Dozza et al. considered a zone which stretches from -2 m behind the bicycle rear wheel till +2 m in front of the bicycle front wheel. Considering naturalistic driving data Kovaceva et al. considered the same approach but using a longitudinal distance of ±3 m.

Phase four – the returning phase occurs by the time stamp in which the phase three ends to the extend that the vehicle returns to the same lane position it had before the overtaking maneuver [19]; while in [25] the end of phase four was considered when the distance driven since the start (of the same phase) reached 50 meters.

2.2.3 Overtaking terminology adopted in this study

In the current study, the classification elaborated in previous research studies would be considered. As far as the overtaking strategies it is concerned, hereafter it will be made reference to:

- Flying: overtaking performed with somewhat constant speed, with no brake intervention by the driver.
- Accelerative: overtaking in which the driver slowed down either by releasing the accelerator pedal or by braking.
- Piggy backing: overtaking in which multiple vehicles overtook the VRU. When it is analyzed the manoeuvre from a car perspective, the event is considered piggybacking whenever there is a leading vehicle, with respect to the EGO vehicle, at a time headway of 3 seconds. On the other hand, from a pedestrian point of view, vehicles were annotated as piggy backers whenever the manoeuvre was performed in succession following a leading vehicle. Also, in the automated annotation algorithm a vehicle was defined as piggy backer if its driver was passing the pedestrian with a time headway lower than 3 seconds with respect to the leading vehicle.
- 2+: whenever a driver was overtaking multiple VRU present in the scene.

However, it is important mentioning that, in the literature, no previous study has been executed concentrating on the driver interaction with a pedestrian while performing an overtaking manoeuvre. Therefore a definition of overtaking phases suitable for this specific scenario would be provided (see Section 3.1.3), since it rarely occurs that overtaking vehicles are driven straight, being completely in the adjacent lane, as proposed by Petrov et al. in [22] or by Hegeman et al in [20] for car overtaking another vehicle.

2.3 Human factors

In the following it will be presented a brief description of which parameters are influential in the driver-pedestrian interaction, considering mainly the notion of perception as well as a general introduction of the concept of the cortical mechanism of action-selection, which has the potential of describing the joint driver-vehicle system. Moreover, a general description of both field of safe travel (FoST) as well as comfort zone boundaries (CZB) will be reported.

2.3.1 What is behaviour?

Considering that the scope of this thesis project refers to quantifying driver's behaviour, a definition of behaviour is paramount. The definition of behaviour in a dictionary [26] states: "The way in which one acts or conducts oneself, especially towards others". Another lexicon [27] expresses the term as "a specific response of a certain organism to a specific stimulus or group of stimuli". Therefore, behaviour concerns actions and reactions triggered by the aim and goal of a person, and his adaptation to disturbances from the outside world [28]. From an automotive perspective, driver behaviour is a set of operations a driver performs in order to reach his targeted location. As well, behaviour refers to the set of action a motorist takes to cope with environmental factors interfering with the achievement of a pre-planned destination, in an appropriate and pleasant way.

2.3.2 Driver's perception of pedestrians

In a driver to pedestrian interrelation it is primary importance the detection. This refers mainly to driver perception of the scene around the road, together with its users. In virtue of the human vision system, drivers are enabled to detect traffic participants on the road, in a dynamic, constantly changing environment. However, pedestrian behaviour can influence driver's perception as well. In [29], it has been shown that pedestrians may increase their own safety by using appropriate nonverbal signals toward drivers. In a research study presented in [30] authors demonstrated that motorists drive more slowly after receiving a smile from a pedestrian who is at a pedestrian crossing. Those results are consistent with a mood-inducing explanation: more slowly behaviour can be linked to a better mood phenomenon given by a smile. Moreover, pedestrian appearance also plays an important role. In [31] while enhancing the difference between form perception and motion perception, authors show a significant interaction between clothing configuration and pedestrian motion. By mean of a synergistic relationship between reflective markings and pedestrian movements, benefits of highlighting the pedestrian's form are greater when the pedestrian is walking (e.g. pedestrians can be made both visible and conspicuous if some of the retro reflective material is shifted from the torso to the limbs).
Another important factor in the VRU detection, considering the pedestrian side, is related to an overestimation of their visibility, especially at night. In [32] it has been found that pedestrians wearing black clothing estimated that drivers would have seen them at a distance that was 7.06 times greater than the distance at which the drivers actually responded. Underestimation occurred only when the pedestrians wore bio-motion markings. The latter confirms that the reason why pedestrians under-use an effective intervention (the bio-motion configuration) is due to the fact that they do not realize and do not appreciate the actual benefit of reflective vests [33]. Considering driver's side, in [34] 95% of drivers in a common, but challenging, visual condition (due to low beams and oncoming glare present) failed to detect a pedestrian wearing dark clothing, despite knowing that there were pedestrians along the roadway and that their ability to respond to the pedestrians was being monitored. This suggests that under low visibility conditions drivers are frequently unable to recognize and respond to pedestrians from a safe distance. This highlights the criticality of the driver interaction with vulnerable road users in darkness.
However, not only daytime is influential in pedestrian perception, but also, as stated in [7], the traffic environment and driving experience are two dominant factors that affect the identification

of pedestrians. Thus, in non-urban environments, drivers focus more on pedestrians when they are on the road. Pedestrians on the curb are common in non-urban/rural environments and possibly, drivers effectively filter them out and focus primarily on pedestrians who are about to cross the road or stand in close proximity to the driven vehicle.
Furthermore, pedestrian detection could, in principle, be influenced by the age of the driver. In [35] the author shows that elderly drivers have a narrower useful field of view (UFV), thus influencing the hazard perception. Even if, identification of hazards by elderly experienced drivers came, in some cases, later than among experienced-drivers, the elderly drivers attempt to cope with hazards by controlling their driving speed. Hence, although the way in which they attend to elements in traffic is more restricted than the ones of younger drivers, reducing the vehicle speed to a more comfortable level is enabling the elderly drivers to have more time to process information, detect hazards, and respond to them.
Additionally, in [36] a detailed analysis of the time to collision (TTC) occurring in a pedestrian fatality has been performed. Steward et al. proposed that when drivers of road vehicles are in potential collision with pedestrians their perception of distance is based primarily on familiar size, resulting in overestimation of size and therefore of time-to-collision with child pedestrians. Hence, authors proposed a new definition of TTC without considering the optic flow $\tau = \frac{\theta}{\dot{\theta}}$ where θ refers to the visual angle and $\dot{\theta}$ refers to its rate of change. Following the notion of explosion of optic flow when a collision is imminent [37], it has been claimed that the dynamic characteristic of an explosion (just as much as a crash) is not speed but acceleration. Therefore, the proposed expression $TTC = \frac{2\dot{\theta}}{\ddot{\theta}}$ has the potential to be used also in the condition in which an object would be accelerating. This has to be considered as a suggestion that perception of imminent collision is far more sophisticated than previously understood. Even a brief view of an object could provide the necessary $\dot{\theta}$ and $\ddot{\theta}$ to judge time-to-collision. It is worth mentioning also that distance to a pedestrian is primarily based on apparent and familiar size (familiar size is the actual size as recollected from previous experience). Therefore [36] proved that if a child is misperceived as a larger person at a greater distance, time to collision will be overestimated. Hence, according to the authors, this perceptual error has to be considered the main reason that children have a much higher pedestrian accident rate than adults.

2.3.3 Driver behaviour modelling

The joint system composed by driver and vehicle needs to be quantified and qualified by means of models. The main objectives of driver behaviour modeling (DBM) are related to the prediction of driving maneuvers, driver intent, vehicle and driver state to improve transportation safety and the driving experience as a whole. The principal benefit of these models is related to the design of ADAS in vehicles; likewise DBM can help safety rating committees to objectively evaluate car safety systems. Broadly speaking the driving task can be decomposed in a subsequent action of navigation, guidance and control. Control can be generally defined as the ability to direct and manage the development of events [38] or, more specifically, the maintenance of a goal state in the face of disturbances [39].

However, in the literature, several models have been proposed; examples of these models are the hierarchical control model [40], the GADGET-Matrix model [41], and the DRIVABILITY [42] model. The former expresses the driver control of a vehicle as operational (actions performed over less than a second primarily in order to remain safe), tactical (manoeuvres, which lasts for several seconds, intended to achieve a short-term goal such as lane changes,

overtaking manoeuvres, and stops), and strategical (actions are triggered by the long-term goals of the driver, e.g. destination and route). The GADGET-Matrix extends the three previous levels, introducing a forth behavioural stance based on driver's general goals for life and skills for living. The DRIVABILITY is mainly focusing on the strategical level, as defined by Michon in the hierarchy of controls. Bekiaris defined five permanent and temporary contributors, which affect a driver's attitude:

- Individual Resources.
- Knowledge and Skills.
- Environmental Factors.
- Workload
- Risk Awareness.

Furthermore, within the framework of driver modelling a distinction needs to be performed between reactive and predictive models. The former refers to an observation after the action has been conducted, while the latter are required in order to identify driver's action on the onset of the behaviour in real time.

In addition, in the last decade a new trend based on the principle of competition between affordances [43], allow researchers to model driver behaviour with layered control architectures and optimal control motor primitives. Thus, proposed methods [44], [45] seeks to explain human sensorimotor behaviours in terms of models of the underlying brain architectures and processing.

The aforementioned list of driver model is quite comprehensive, to ensure that the reader has sufficient information to understand the aims and scope of this work.

Nevertheless, the overtaking manoeuvre has the potentiality to be related to a control analogy. As expressed in [46], the dynamic control properties of driver while steering are expressed by mean of an anticipatory and compensatory control. Also in pedestrian overtaking operation the driver-vehicle system has the potentiality to be associated to a feed-forward control. By definition feed-forward driven controllers use awareness of the environment as well as previous experience with the system, which a driver is supposed to control, to act directly on it, anticipating changes. In these conditions, the control is successful if the controller manages to perform a task in accordance with the desired goal. When this fails, it is made reference to deviation. According to [47] a deviation is the classification of a systems variable when the variable takes a value that falls outside a norm. With the notion of norm, which is always some kind of desired state, although the definition of these states can be of many different kinds, like a discrete state or a performance envelope. Thus, drivers are used to gather information about the system variable/variables in order to judge whether or not the system's performances are within the desired state and and expected conditions.

2.3.4 Field of safe travel

In order to relate driver's behaviour to the perceptual task required while driving, one of the main driver's activity is to conceive the imminent projected spatial FoST. As expressed by Gibson et al. in 1938 the "field of safe travel is a spatial field that is not fixed in a physical space [...] phenomenally, it is a sort of tongue protruding forward along the road, consisting,

at any given moment, the field of safe paths which the car may take unimpeded"[48]. More recently researchers in [49] proposed a FoST framework suggesting that at any moment a motorist is creating a mental viable field by integrating two perceptual entities:

- the possible available spatial fields for locomotion and
- the driver's mental image of ego-vehicle outer-line and motion dynamics.

Authors in [49] argue that the FoST framework may be used to explain as well as predict drivers' behaviour in different traffic/situation environments based on their prioritization between the above two perceptual entities, comparing the driving task to a locomotion guided chiefly by vision. However, is worth noting that it is critical to study the way in which drivers usually prioritize perceptual cues, due to the high interplay among these optical variables and motorist's expectancy.

2.3.5 Comfort zone boundaries

A different framework with respect to the previously introduced FoST has been proposed in [3]. Authors express the situational control framework, as the degree of control jointly exerted by a driver and a vehicle over the development of specific traffic condition. By reference to the principle of adaptive behaviour, driving task has been described as the selection of goal states as balance between excitatory and inhibitory forces [50]. The driver behaviour to a large extent is governed by physiological reactions to threatening situations, e.g. emotions, experienced by the driver in terms of unpleasant feelings. Somatic markers are emotional signals that link positive or negative values to opportunities for action and their outcomes. According to [51], the driver seek to maintain a state of zero discomfort. Discomfort includes feelings of immediate risk or threat (e.g. in a critical traffic condition), but could also be related to an excessive task demands. In [51], together with a comfort zone it is also laid out a safety zone. This can be defined as the region of driver-vehicle-environment (DVE) that contains all states that result in a successful outcome (i.e. control is maintained). The region of DVE space that overcomes the safety zone contains all states that result in a crash or some other non-recoverable loss of control. The safety zone boundary thus divides all possible states in the DVE space into two categories: those that result in successful outcome (control is maintained) and those that do not (control is lost beyond recovery). Furthermore, to preserve the state of zero discomfort suggested by [52], drivers generally escape goal states close to the boundary of the safety zone. Rather, they prefer goal states that have a certain minimum distance, or safety margin, to the boundary. Hence, the definition of comfort zone can be expressed as follow: "The region of DVE space for which no discomfort is felt or predicted by the driver and which the driver therefore prefers to stay within" [3]. The comfort zone thus represent the zone of comfortable action as sensed by the driver. Every time the comfort zone boundary is exceeded, a feeling of discomfort is experienced, resulting in adaptive behaviour in terms of corrective actions. Therefore, driver's adaptive behaviour can be conceptualized as a trajectory in the DVE space. The trajectory represents the outcome of the driving control process, where driver and vehicle, in the face of changing driving conditions, adapt the goal state in order to maintain a sufficient safety margin to the safety zone boundary. This process is clearly and objectively present every time a driver come across a pedestrian overtaking scenario involving oncoming vehicle. As represented in Figure 2.5 drivers need to maintain a lateral distance

while overtaking a pedestrian, and this can mainly be influenced by the presence of other road users.

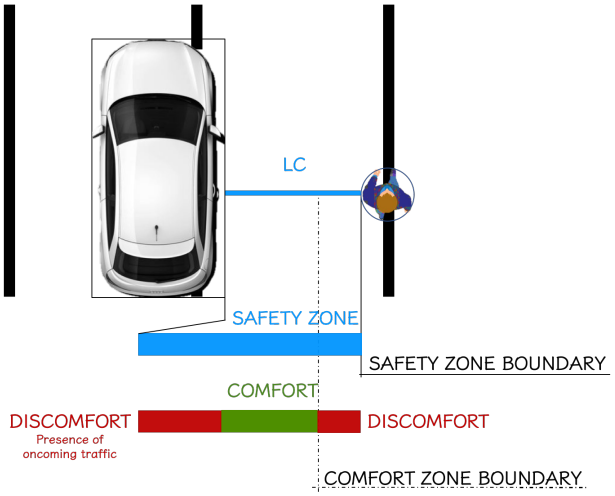

Figure 2.5: *Comfort and safety zone boundaries. LC represents the lateral clearance between the car and the pedestrian, who is represented as walking on the line*

2.3.6 Safety metrics

In order to quantify the specific driving scenario of pedestrian overtaking, with the purpose of devising an exploratory study for this driver-pedestrian interaction, it has to be outlined which are the main safety variables that have to be taken into account. Considering that in the literature no previous study has been carried out for this specific overtaking manoeuvre, in the following is outlined and presented the main metrics adopted in the context of overtaking of another vulnerable road user: the bicyclists. As described in previous studies [53] [19] [54] the main safety metrics adopted are the lateral clearance of the car to the cyclist and speed difference between car and cyclist. However, other variables could be considered to describe CZB during overtaking manoeuvres: lateral or longitudinal distances, velocities and accelerations maintained by the parties involved in the manoeuvre. Moreover, in more recent study related to naturalistic driving data three distance-metrics have been defined: minimum approaching gap (mAG), minimum distance steering (mDS) and minimum distance returning (mDR) [23].

From a driver perspective, the acceleration and the speed of the vehicle, together with the time at which a driver starts to brake when encountering the pedestrian, can be seen as an indicator of drivers' comfort before and during the overtaking maneuver. On the other hand, the lateral offset to the curb could be an indicator of the comfort zone boundary for the pedestrian during the overtaking maneuver. In this case, the pedestrian will try to maintain his/her position based on a trade-off between the assumed lateral clearance which might be given by the car and the practicability and surface condition of the curb. Also, from a pedestrian perspective, a component related to his/her level of comfort can be related to the direction of his/her walking. As a matter of fact, it usually recommended to walk on the opposite direction of overtaking vehicles (facing the traffic), so to directly perceive the presence of vehicles.

However, due to the large relative speed between the motorist and the pedestrian involved in the scenario, as well as the location of the pedestrian on the sidelines of the lane, it results to be difficult to adapt in whole the quantities of driver's decision to overtake mapped out for the event of a car overtaking another car [55]. Although the basic quantities of gap time (or distance) separating the overtaking and oncoming vehicle (when present) and driver's estimate, of this gap available, are crucial also in a pedestrian overtaking; the time (or distance) required by the driver-car combination to perform the maneuver, and driver's estimate of this time (or distance), expressed by Gordon for a car overtaking another car, are difficult to assess when a pedestrian is involved. Hence, a safety metric parameter adopted to combine together car's speed and driver's reaction distance, is the time in which the driver start to perform the overtaking manoeuvre [23]. This has been defined, in the following of this report, as time to collision (TTC), since refers to the time in which a driver deviates the vehicle from its collision path to the pedestrian.

It is worth mentioning that is an especially important aspect to single out which are the main safety metrics also for the purpose of designing proper ADAS, which could warn and alert a driver of an imminent collision, assumed that the driver had not detected the pedestrian. As expressed by [56] a high level of satisfaction and trust of alert and warning systems is reached whenever system's designers and driver's perception of the situation match, i.e. when a safety feature has been designed with the same definition of user's comfort zone boundaries. Hence, these boundaries define a zone beneath and above which drivers have a sense of discomfort. Whenever this is experienced a driver will take action to leave the situation perceived as risky (giving a larger distance or reducing speed) to return to normal driving [51]. However, risky situations for a VRU might not only be related to a misjudgment of the necessary-predicted lateral distance from a driver, but also to the drivers' intention to achieve a smooth ride, to comply with traffic rules and presence and other driving objectives.

To sum up, there are some research gaps regarding the comfort zone boundaries during the overtaking maneuver of a pedestrian as well as other safety metrics that can quantify the scenario. Previous study have considered mainly other VRUs, especially bicyclist. However, in this study a consistency with metrics adopted in investigations of interaction with other VRUs has been maintained. Hence, with the purpose of quantifying the metrics involved, the driver interaction with pedestrians has been considered from both drivers' perspective (equipping vehicles) and from a pedestrian perspective (equipping the VRU).

2.4 Advanced driver assistance systems

Considering that the main reason for the occurrence of crashes is the inability of road users to detect and perceive oncoming dangers before a sufficient amount of time [57], this does not mean it is obvious to design, develop and deploy an autonomous perception-control system that performs better than the average driver [58]. The main challenge, for the machine perception at the current state of technology, is related to the assignation of a correct semantic meaning to the sensed environment, which is a task that humans are able to fulfill very quickly and nearly without errors [59]. However, in recent years industry and academic projects have been evolved with the purpose of reaching a high level of accuracy and precision in the detection and tracking of moving objects (DATMO). In detail, ADAS and built-in safety systems are developed to detect, among other road users, pedestrians and predict the possibility of collision. This has been achieved mainly using computer vision together with sensor fusion techniques.

In the following of this section an introduction to pedestrian detection in broad terms will be presented. This is mainly useful, for the reader, to get acquainted with computer vision technology associated to "MobilEye" pedestrian detection system adopted in this study, by mean of the naturalistic driving study (NDS) data. Currently there are two main technology related to pedestrian detection from images: one based on images of the visible spectrum, and the second related to thermal infrared. Main pedestrian protection systems associated with these technologies usually follow a step-wise approach characterized by six different modules [60]:

1. Pre-processing
2. Foreground segmentation
3. Object classification and silhouette matching
4. Verification/Refinement
5. Tracking
6. Applications

According to the co-founder of MobilEye [61] the appearance of pedestrians in the scene can be divided into a number of categories:

- Pedestrian moving laterally
- Stationary pedestrian in primary host vehicle-path
- Pedestrian moving longitudinally
- Stationary pedestrian out-of-path.

It is worth mentioning that main computer vision techniques for object classification uses approach for fitting objects that are purely 2D, hence they only use the 2D information of the Region of Interest (ROI) given by the foreground segmentation.

Once a ROI has been classified (by mean of either holist or part based approaches) through different machine learning techniques, each labeled ROIs (with multiple defections on one single pedestrians actually present on the scene, and False Positives (FP) miss-classifications) needs to be approved by a proper algorithm. In [61], Shashua et al. propose a multi–frame approval process, which consists in validating the pedestrian–classified ROIs by collecting information from several frames: gait pattern, inward motion, confidence of the single–frame classification, etc. Moreover, between different frames each ROI classified as pedestrian needs to be tracked to reject bogus detection and with the purpose of estimating pedestrian trajectories. To accomplish this module, Kalman filters are used to maintain pedestrian estimates and Bayesian probability to provide an estimate of pedestrian classification certainty over time and a targets' trajectory and speed. However, the major challenge is the development of reliable on-line pedestrian detection systems. Due to the varying appearance of pedestrians (e.g., different clothes, changing size, aspect ratio, and dynamic shape) and the unstructured environment, it is very difficult to cope with the demanded robustness of this kind of system.

Hence, to put in a nutshell, the step-wise approach of computer vision approach adopted by MobilEye pedestrian detection system is the following:

1. Generation of candidate ROI

2. Single frame classification based on a two-stage classification algorithm

3. Multiframe approval process

4. Range measurement and pedestrian BoundingBoxes (BB) tracking

In addition, pedestrian detection from images is a high relevant area of research in which other techniques are applied further to the above. In [62] a cascade detection algorithm based on Harris corner detection algorithm [63] is applied for getting the features of pedestrian's contour. Moreover such a system implements optical flow algorithms to estimate motion vector of pedestrian and Grey theory [64] is used to predict the future driving path of vehicle. Based on estimated pedestrian and vehicle future paths the warning system represents an example of a complete ADAS based on camera images.

2.5 Naturalistic driving data

Naturalistic driving is a traffic research methods which refers to an unobtrusive observation when driving is performed in a natural and usual context. Expressed in other words, naturalistic data is a collection of big data, by mean of instrumented vehicles, which are driven in real traffic by users in their daily commuting activities. A relevant point to consider is that even if drivers are aware of the in-board presence of a data logger system, they become progressively unmindful of the observation system. This mainly because of the collection system being designed as discreet as possible. Each participants' vehicle is equipped with several sensors and small cameras, which continuously record vehicle state (e.g. speed, steering action and position), driver behaviour (e.g. eye gaze, distraction), environment and infrastructure conditions (e.g. weather characteristics, lane width). Capabilities related to these collections are manifold: from the study of human behaviour while driving to the test (a priori) of intelligent vehicle systems, from the understanding of accident causation to counter factual simulations (also know in literature as what-if analysis [65]), from analysis of traffic efficiency to the evaluation of eco-driving [66]. With the enabling greater number of naturalistic driving studies [67], it is possible to study in detail not only the behaviours of different drivers but also the conduct of VRUs. Moreover even the specific evolution of safety critical events (SCE) can be analyzed, with the goal of providing additional information for designers, for the development of safety systems to reduce traffic injuries and fatalities.

It is within this framework that the eUropean naturalistic Driving and Riding study on Infrastructure, Vehicle safety, and Environment (UDRIVE) has been performed over a time span of 4.5 year. Data collection took place between October 2015 and May 2017. In this period, well over 53,000 hours of vehicle data was collected on 192 cars drivers (total of 38,157 h and 152970 trips), 46 truck drivers (total of 14,503 h) and 39 scooters riders (total of 497 h) [68].

Limiting the focus on the car data, collected signals includes GPS , speed data and CAN data, as well as video data from a number of views including the driver's face, hands and feet, and covering both inside and outside the vehicle. Furthermore, as represented in figure 2.6, the data acquisition system (DAS) recorded continuous signals from a MobilEye smart camera, including the presence of vulnerable road users (cyclists and pedestrians) and the

distance between the car and the other road users. This camera offers the opportunity to find events wherein a pedestrian is present, as well partial measurements of pedestrian location within the scene. Furthermore, it is worth mentioning that the main challenge in naturalistic

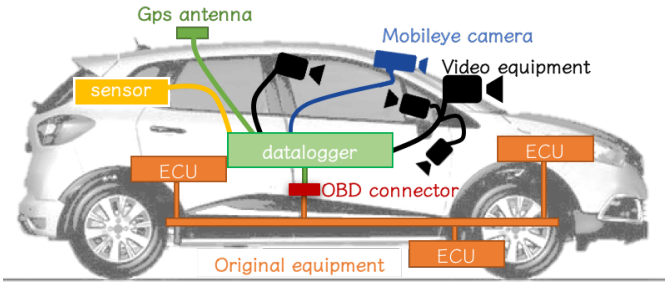

Figure 2.6: *Data acquisition system in UDRIVE*

studies, following data collection, is to inspect the data for meaningful events. This procedure is still far from automatic, although a lot of effort has been currently devoted to it and some operational and effective procedures have been developed and implemented [58]. Hence, with a view of detecting useful events, in which a pedestrian was overtaken, in this study it has been made reference to previous study performed and available within the database [25], [23]. These followed a common approach within ND data sets, that is to generate triggers that serve as indicators to detect the relevant information and then manually or automatically scan the data around the time-stamps suggested by the triggers. Those triggers are related to kinematic data representing the vehicle state.

With the intention of helping analysis in this study, the UDRIVE project encompassed the development of a dedicated software tool: Smart Automation for Large data Sets Analysis, SALSA, designed by non-profit organization Centre European studies safety and analysis des risques, CEESAR, based near Paris in France. Thus, SALSA has been mainly used in this project together with MATLAB in order to perform raw data enrichment. This imply: filter and query for data, visualize data, calculate new measures based on the acquired data, add annotations to data, missing data estimation and evaluation of performance indicators.

2.6 Euro NCAP

The European new car assessment program (NCAP) is a voluntary vehicle safety rating system, which publish safety reports on new cars, and confer "star ratings" based on the performance of the vehicles in a variety of crash tests, including front, side and pole impacts, and impacts with pedestrians. Moreover, due to the huge safety benefit of active safety features, since 2014 Euro NCAP added crash avoidance systems such as automated emergency braking (AEB) and lane keep assist/lane departure warning (LKA/LDW) tests to the overall star rating. As a side note, Euro NCAP requirements are not legislation, but they can highly influence customer demand and they are used as a decisive factor for fleet car selection. Furthermore, since one of the main goal of this independent assessment organization is to encourage significant safety improvements to new car design, they are emphasizing not only the car safety (strictly speaking with respect to the chassis) but also on "how it might assist other road users" [69]. Thence, since 2016 it has been introduced a scenario for the evaluation of AEB car-to-pedestrian, which was updated in 2018 considering also a longitudinal scenario. The latter is identified with the

acronym CPLA, which stands for car-to-pedestrian longitudinal adult. The testing scenario are based on the assessment methodologies for forward looking integrated pedestrian safety systems [70]. In detail, based on the pre-crash assessment performed within ASPECSS European projects [71] 3 accident scenarios were found as the most important for car-to-pedestrian crash configurations. These are in order of occurrence:

1. Crossing of straight road from near-side
2. Crossing of straight road from off-side
3. Along carriageway on a straight-road

Noteworthy, the scenario studied in this thesis project can be directly related to the third of the above-mentioned events, which accounts for 22.9 % of killed pedestrians [71]. In point of fact, if a driver goes wrong in the execution of a pedestrian overtaking manoeuvre (due to miss-detection, miss-perception or misjudgment of the scene) , he/she will run over a pedestrian if also the VRU cannot evade from a collision event. Thus the CPLA assumes that a pedestrian (represented with an adult dummy) is walking in the same direction of the vehicle with two different overlapping settings. These are 25 % and 50 % overlap, as depicted in the Figure 2.7, and are expected to be performed both with daylight and with no artificial light on the test track. The choice of the last setting is related to the casualty rate associated to this scenario, with 73.6% events happening in darkness. As expressed in the Euro NCAP VRU-AEB test

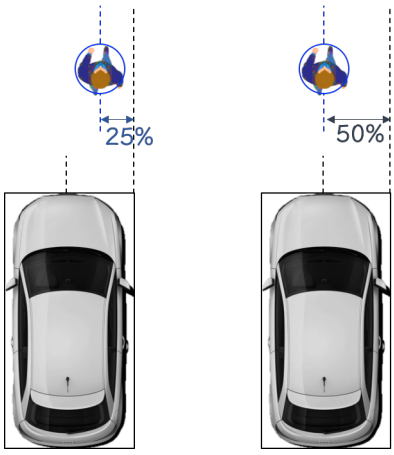

Figure 2.7: *Scenario representation of Euro NCAP CPLA safety feature assessment. Rating tests and assessment are described in the Vulnerable Road User Protection Protocol [72]*

protocol [73] the first scenario (CPLA-25) has to be used mainly for the evaluation of a Forward Collision Warning (FCW) system, with a car speed between 50 and 80 km/h, and a target speed of 5 km/h. The assessment criteria adopted for the FCW is the time to collision (TTC). Points are awarded when the warning is issued at $TTC \geq 1.7s$ [74]. As far as the assessment of the AEB system the criteria selected is the relative impact speed of the vehicle toward the pedestrian, if the vehicle was not able to avoid the collision; for CPLA-50 speeds of the vehicle under test are between 20 and 60 km/h, while the VRU is constantly walking at 5 km/h . Moreover to be eligible for scoring points an active safety systems has to be, by default, ON at the start of every journey and it has not to be possible to switch off the system with a simple push on a button. Also, a pedestrian-dummy has to be detected even if it is moving as low as 3 km/h and the system has to be active also when travelling at a higher speed than 80 km/h.

3 Approach and Methodology

Driver pedestrian interactions have been analyzed following two main approaches. The first is related to the understanding of driver behaviour considering data available within the database of the naturalistic driving project UDRIVE (see Section 2.5). On the other hand, the second method of study has been based on a data collection performed from a pedestrian in the suburban area of the city of Göteborg, Sweden. In the following the useful events extraction procedure from the naturalistic date sets has been described in Section 3.1. In Section 3.2 the procedure related to the field data experiments is described starting from equipment preparation until experimental protocol execution and sensor data processing. Lastly, the methodology to devise a driver model in the overtaking manoeuvre is presented in Section 3.3.

3.1 Naturalistic driving study

One of the main demanding effort related to a naturalist data collection is to detect and identify useful time stamps linked to a specific event under investigation. In UDRIVE data are collected based on trips; hence each trip associated to a car gives rise to a *Record*. To each record it is assigned an unique identification number, which allows the user to query for a specific trip, if needed. In the database, specific attributes are assigned to a record in addition to the unique ID. The *attributes* related to a "full record" can be the driver identification code, collection country, car identification number, date and time, to mention a few. Moreover, to each record it is associated a list of *signals* grouped in different *time series*, based on the frequency characteristics of sensor's message updating rate. To perform the above mentioned database querying process the tools employed have been SALSA (see Section 2.5) implemented in MATLAB.

With the purpose of tracking down specific events (like the overtaking manoeuvre), each record needs to be split in multiple "data-segments". Thus, a *Segment* refers to a fragment of a *Full record* and it comprehend a certain type of event within a begin and end time. For each scenario under investigation, a data analysts needs to design a proper segment generation script. Segments that are generated by the same code (in UDRIVE nomenclature *Node*) cannot overlap, and can be identified (within the same record) by an unique Subscript index, as well as by a begin and end time. Furthermore, within each segment new time series can be generated, containing post processing signals, like the TTC to a leading vehicle or a VRU location in the scene. Therefore a *Segment* is characterized by its own *Signals* (clustered in *Time series*) along with its own *Attributes*. The last-mentioned refer to user-defined properties of the segment itself, for example the weather condition, mean speed, minimum distance to a pedestrian.

In a nutshell:

- **Record** – recording session related to each driver trip, characterized by full-record properties, like attributes and CAN time series.
- **Segment** – portion of a record, categorized by segment properties, like scenario-specific attributes and post-processing signals. Segments differ from each other based on the scope of their generation, which in turn depends on the research topic under investigation.
- **Attribute** – either full-record or segment property specified by the user, expressed

by means of Boolean values, strings or numerical quantity, representing e.g. scenario performance indicators.

- **Time series** – grouping system composed by a time vector and signal values synchronized according to the mentioned time. Time vectors differ based on associated signals frequency.

- **Signal** – time dependent vector of data linked either to CAN-bus recorded information or to post-processing data augmentation process.

- **Node** – MATLAB script used to perform segment generation, as well as event post processing.

The graphical user interface available to the user is represented in Figure 3.1. However, for a detailed description about database architecture, along with SALSA tool description, the reader needs to relate to the EU project deliverable [75].

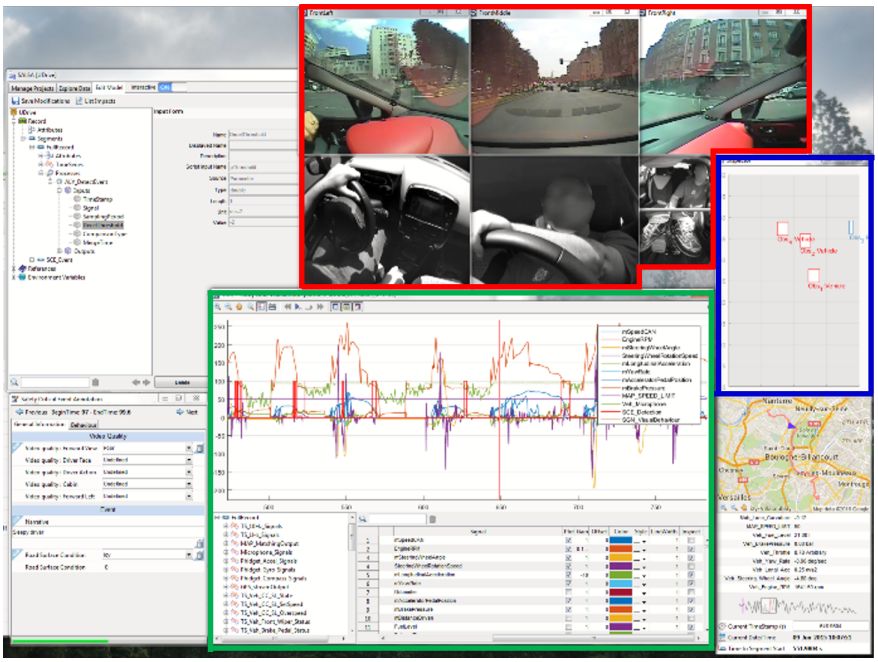

Figure 3.1: *SALSA visualization tool. Within the red border the video feed is represented. MobilEye object detection visualization panel is shown within the blue box. The green boundary includes multiple CAN signals' plots. Image credit to Clément Val, CEESAR [76]*

3.1.1 Raw data exploited

For each record a large amount of signals are available, these can be grouped in:

- **CAN-bus** data – signals recorded from the controller network in the vehicle, such as vehicle speed, vehicle inertial measurement unit (acceleration, gyro, magnetometer), turning indicator signal, to mention a few.

- **MobilEye** (ME) data – signals related to object location, object speed, width of the object detected by means of image processing technology (Section 2.4).

- **GPS** data – signals related not only to position (longitude, latitude), but also data associated to the map-matching process. This made available speed limit, road type (highway e.g.), road location (i.e. urban, rural).
- **Video** – video feed recorded by different cameras installed in the vehicles, which made it available the manual annotation process (see Figure 2.6).

3.1.2 Pedestrian overtaking identification

The pedestrian overtaking event identification process has been based on the approach adopted in previous study [25]. The method can be summarized in four main steps, as depicted in Figure 3.2:

1. Segment Generation - For each full-record segments have been generated based on specific criteria. These were related to events in which MobilEye sensor detected a VRU in the scene, the VRU was a pedestrian, the car kinematic behaviour showed a change in the lateral acceleration.
2. Data reduction and batch processing - Tuning and refinement of filtering variables, in order to avoid MobilEye sensor miss detection, by mean of batch processing on limited amount of records contained in the database.
3. Segment Annotation - Verification of pedestrian overtaking event by manual annotation.
4. Overtaking attribute definition - Annotation of overtaking specific characteristics, like phase definition based on steering signal, pedestrian direction or pedestrian location with respect to the lane.

Segment generation

The process of generating a segment associated to the specific event of "driver overtaking a pedestrian" has been based on previous segments presents in the database. For a detailed description refer to Nero's project [25]. First and foremost a segment characterized by the event "VRU disappear" was generated. The output was a Boolean signal (in the database it has was named "SC_VRUDisappear") directly dependent from MobilEye object detection sensor. Whenever the last detection of the VRU (i.e. it disappeared from the scene) took place within 50 m and the speed of the EGO vehicle was above 20 km/h, a state-change was created. The segment was therefore created with an offset of 10 s before the detection of the road user and 10 s after the last detection (the threshold of 10 s was set assuming the worst case event for which a car moving at 20 km/h would have at least reached the pedestrian located at 50 m in that time period). When multiple road users where detected the multiple segment generated were merged in a single one. These aforementioned thresholds allows to remove instances in which vehicles were travelling too slow or when the VRU was disappearing from the scene too far ahead compared to the car. The generated segment within the database was named "SEG_whenVRUDisappear", and the reference MATLAB script used was "ALY_SC_VRUDisappearATTRIBUTES". The latter was used to generate a Boolean signal "dVRU_OT_context" in the database, which was utilized as input in a new segment generation procedure. With the purpose of detecting the specific scenario analyzed in

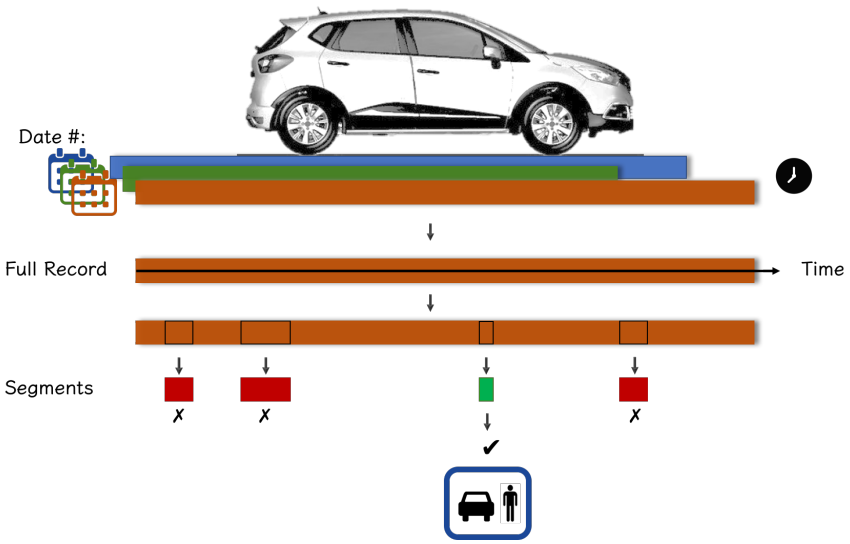

Figure 3.2: *Representation of overtaking manoeuvre segments detection, from full records to single event annotation. The process is performed for all different records corresponding to trips performed in different dates, with different duration (represented on the top of the image). In each event segments are generated and the manual annotation allows to discard (red crossed segment) or confirm (green segment) the overtaking event*

this project a new Segment has been generated. This has been used to perform a step wise action filtering process using kinematic characteristics of the vehicles within the begin-end time interval of the segment itself. The node, associated to the segment, allowed the user to manually query for specific attributes (generated as output from the node selfsame), like the last pedestrian detection distance for example.

It is worth mentioning that the ME system is providing information about four different obstacles that can be present in the scene and detected within the available FOV (approximately 50 degrees). Data that refer to the same obstacle-property (e.g. Obstacle longitudinal position) are available in four different signals, each one associated to the fours objects. Hence, a "by object" data storing system is adopted. When multiple obstacles are detected simultaneously, it occurs that an obstacle detected as "obstacle 1" in the previous time stamp is detected as "obstacle 2" in the following. Nonetheless, for each object detected the ME system is assigning a unique identifier number (ID).Therefore it has been of primary importance to keep track of the same road user detected over time, this by means of a matrix containing obstacle properties which refer to the same ID. Following the same nomenclature presented in [25], in each segment a mask object has been created. The term mask refers to a vector containing Boolean data, whose value were assigned, for each of the four objects, based on certain criteria. These criteria were dependent on the filtering action to be applied to the data. To clarify, whenever the detected road user was a pedestrian, and the road type was non urban the Boolean value was set to true. The exclusion of urban areas was necessary to avoid interaction between driver and pedestrian in the crossing scenario (very common in a city environment), which was out of the scope of this project. When multiple VRU appeared in the scene only data related to the closest VRU were considered to fulfill the previous criteria, for the mask generation. The masks generated for each of the four ME-detection obstacles were used to get the longitudinal and lateral positions in the car reference frame, limited to the scenario under investigation.

It is worth highlighting that due to the different collection sites involved in the UDRIVE project, differences were present between left-handed and right-handed countries. In order to develop an algorithm that could have been used for all Records, the same scenario definition was essential whatever collection site it was considered. Therefore a data adjustment was necessary since MobilEye was adopting the same reference frame without regard to the collection country. For the data collected in Great Britain (GB) ME was referring a pedestrian located next to the road shoulder, as it occurs for an overtaking manoeuvre, with a positive lateral distance. On the contrary, for a right-handed traffic country a pedestrian located next to the road curb was measured with a negative lateral distance. Therefore, as depicted in Figure 3.3 the sign of the lateral distance measurement has been corrected. The same process has been applied to the signal related to the ME detection of the lane edges. With reference to Figure 3.4 the "distance to lane" (continue line) and "distance to adjacent lane" (dashed line) signals for a left-handed traffic vehicle were characterized by an opposite sign when compared to a right-handed traffic vehicle. Therefore signals have been corrected in order keep consistency in the approach adopted in the event filtering process.

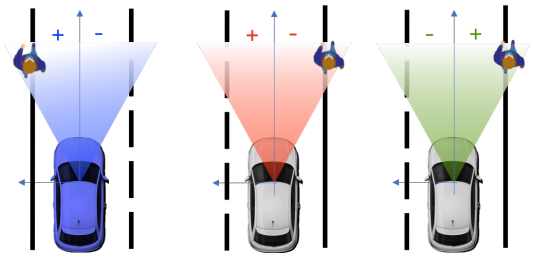

Figure 3.3: *Pedestrian lateral position sign correction. The obstacle lateral position has been adjusted keeping a positive value for the pedestrian located next to road curb. The blue vehicle represents the scenario of a left-handed traffic country, which has been used as reference. The grey vehicle refers to a right-handed traffic vehicle, for which the original ME detection sign (red representation) has been reverted and corrected (green representation), to keep a consistent approach*

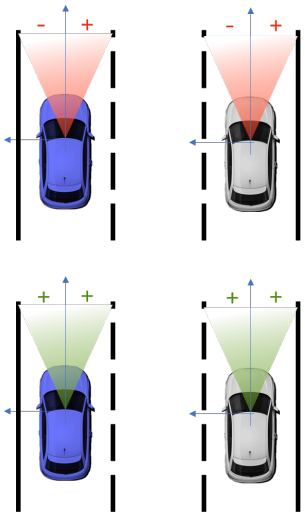

Figure 3.4: *Signal related to left and right lane edges. Original (red) sign and corrected (green) sign for left-handed traffic vehicle (blue) and right-handed traffic vehicle(grey)*

Data reduction and batch processing

Once all the signals showed consistent values independently from the record's collection site, the aforementioned mask has been used to find the pedestrian lateral position while the car was approaching the VRU. To promote events in which the pedestrian was present in the lane, a comparison between distance to the road shoulder and the pedestrian lateral position was performed. If the latter was lower than the former the pedestrian detection segment was flagged as "in lane". Moreover, due to limited ME sensor performances pedestrians were detected usually for a time period of one and a half seconds. In parallel ME sensor was prone to miss detection, i.e. traffic sign classified as pedestrians or bicyclist qualified as pedestrian at longer distances. Therefore, to reduce the amount of miss-detected events a threshold of 15 data points was defined, since wrong detection in the ME-data rarely lasted for longer then a dozen of time samples. At the same time, to cope with ME miss classification of bicyclist as pedestrians, the following approach was undertaken. Since the miss classification was prone to happen usually at a longer distance, if in the last ME detection (who resulted to be more accurate) the VRU was detected as bicyclist, the event was discarded, even if initially listed as "candidate" to the overtaking event identification. Furthermore, to tackle sensor miss detection that lasted for more than 15 time samples, it was observed that these happened at a significant longitudinal distance with respect to the car reference frame. Therefore, to be considered as overtaking-manoeuvre candidate a segment VRU detection had to show an average longitudinal distance, within the last two detection, lower than 10 m.
At the same time, a data quality check related to the amount of available data within each segment was performed. Only segments with a number of invalid data lower than 32% were considered for further filtering operation.
In the process of sorting out only segments containing an overtaking manoeuvre, a closer look was given to the transverse acceleration signal. The identification of peaks in the lateral acceleration was associated to the VRU lateral position. In detail, the mean lateral distance of the VRU over six time instances during the occurrence of the peak ($t_{peak} - 5 : 2 : t_{peak} + 5$) has been computed. This had to be greater than the lateral distance of the VRU during the whole event. The threshold of six time stamps was adopted according to the approach followed in previous study regarding bicycle overtaking events.
To be considered as an overtaking candidate, the absolute value of a steering wheel angle signal needed not to overcome a threshold of 200 deg. This because it was necessary to filter out events in which a pedestrian was standing at a traffic light and a car passed by him/her before turning at the intersection.
No filtering action was possible with respect to the ME signal of the relative speed between VRU and car, since the signal resulted to be unreliable and not accurate. Moreover, in order to be classified as event candidates for the manual annotation, segments needed to have a pedestrian detected within 4 meter (average of lateral distance).

The script (or Node) adopted for this segment generation was tested and tuned by means of a batch processing. This process allowed to test the script on a subset of the database (i.e. 1000 records) allowing to evaluate the performances of the code itself whenever a threshold was modified. This method was applied multiple times during the first part of the time allotted for this project.

Eventually, once the script proved to offer an accurate enough performance it was pushed into the UDRIVE database allowing it to be run over the complete data set.

Segment annotation

The output given from the overtaking segment querying process was giving to the user a list of overtaking manoeuvres, fulfilling the above mentioned filtering criteria. However, to address residual ME miss detection each segment needed to be verified. The verification process was enabled by video feed data. Watching front and front-right camera's images at each time stamp stated as "overtaking candidate", allowed to find out real overtaking events. By means of this activity it was possible to get a early estimate about the availability of pedestrian overtaking manoeuvres within the database and therefore the usability of data set.

Overtaking attribute definition

Once the segment verification process allowed to get a number of events which could allow a driver behaviour quantification, the last step of the event identification process was performed. An annotation panel has been designed, in order to help the annotators in the segment attributes definition. The factors considered in this process are summarized in the following:

- overtaking type (categorical: accelerative, flying, piggybacking)
- oncoming traffic presence in the scene (Boolean)
- leading vehicle presence in the scene (Boolean)
- event occurred in a straight road (Boolean)
- event took place in rural road (Boolean)
- pedestrian walking in the same direction of the EGO vehicle (Boolean)
- multiple people overtaken (Boolean)
- pedestrian action type (categorical: standing, walking, running)
- pedestrian position (categorical: in lane, walking above lane marking, walking in the curb)

Moreover, by mean of a joint analysis of video and signal data it was annotated also the begin and end time of each phase of the overtaking manoeuvre (for a detailed definition of each phase please refer to the following chapter).

It worth noting that annotators had to select every single one of the previous attributes in order to consider the annotation process as completed.

3.1.3 Overtaking phases definition

As remarked in the literature review (Section 2.2.2), researchers followed different approaches in order to classify and breaking down the overtaking event into multiple phases. The method presented hereafter has been founded on phases definition introduced by Dozza et al. [19][24] and adjusted by Jordanka et al. [23] [25] for a NDS data set (see Section 2.2.2. The main reason for this approach has been to get results that could allow a comparison between driver behaviour in the interaction with bicycles and with pedestrians. In order to relate the phase definition to the event annotation process, as described in [25] only the start of phase one

(when the VRU was visible in the video-feed) and the start of phase two (when the driver performs the steer-away input to the vehicle, in order to change vehicle heading angle) needed to be manually annotated.

However, the approach adopted in this study proposes a manual annotation of all the phases, according to driver's input to control the vehicle path. This because the motion is controlled through the actions of the driver who observes the vehicle's handling responses and carries out suitable steering to achieve the intended path. This annotation procedure has been possible since steering wheel angle signal, together with the video of the dashboard in the passenger compartment were available to the annotator. It is worth highlighting that when video and signal happened to be asynchronized, the annotation process relied only on the time stamp related to the steering wheel angle signal.

Therefore, during the annotation process the time stamp of the start of all phases, and the end of the overall manoeuvre has been manually annotated ensuing the following definition:

- **Phase One** - Approaching phase
  Begins when the VRU is visible in the video-feed and ends when phase two begins.

  As represented in Figure 3.5 the vehicle is approaching the pedestrian from behind. The main variables that may be used to describe this phase are the distance between the vehicle and the pedestrian (referred as minimum approaching gap mAG), and the TTC or the time headway (THW) in which the phases ends. The annotated time, however, is dependent mainly on the camera sensor performance and the annotator possibility of detection the pedestrian in the video feed.

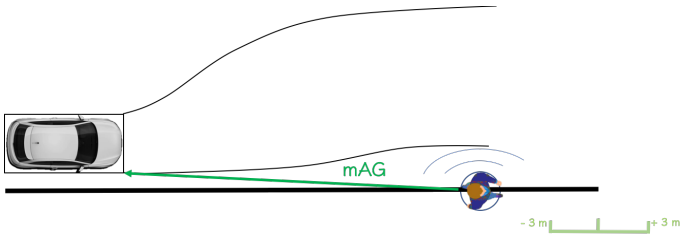

Figure 3.5: *Approaching phase*

- **Phase Two** - Steering Away/Pull Out phase
  Begins when the driver start to steer away from the collision path to the pedestrian and ends when phase three begins.

  As represented in Figure 3.6 the phase begins when the motorist inputs a steering control and the vehicle diverges from its possible collision course to the pedestrian. The variables describing this phase might adopt different values depending on the driver and the situation. The result of steering actions is represented by the increased lateral distance to the curb and for accelerative manoeuvre, the phase may be accompanied by an acceleration or deceleration of the vehicle. Also, the driver could use the indicator to show its intention to possible following vehicles.

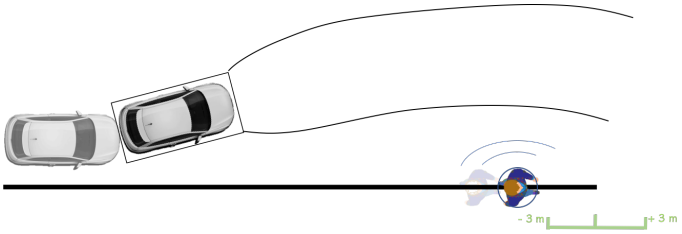

Figure 3.6: *Steering away*

- **Phase Three** - Course adjustment
  Begins when the driver performs a steering action in order to correct the path of the vehicle. This allows to prevent the vehicle from overrunning into the adjacent lane for example. The safety metrics that has been analyzed in this phase has been the minimum distance steering (mDS), which represent the end of the previous phase and the start of the third phase. The phase ends when the last phase begins. Figure 3.7

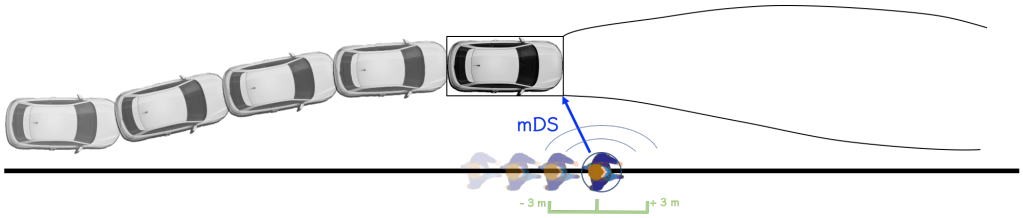

Figure 3.7: *Course adjustment*

- **Phase Four** - Returning phase
  Begins when driver performs a steering action in order to return back to the original position in the lane. This results to be one of the most important phases, since it includes the passing of the pedestrian, and therefore the lowest distance a car is keeping from the VRU during the manoeuvre ("mC" in Figure 3.8). The phase ends when the vehicle

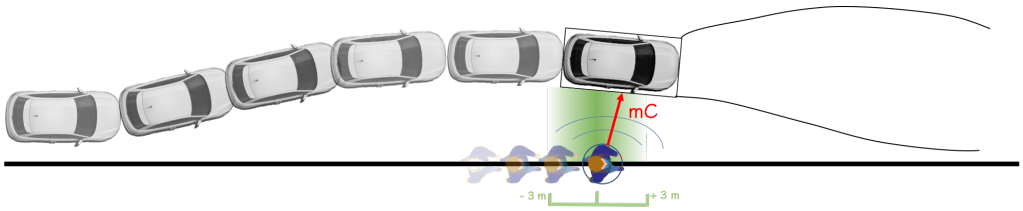

Figure 3.8: *Returning phase*

  return back in the original lane position, approximately keeping a lateral distance to the curb similar to the one in the approaching phase. The leeway that the drivers leave for the pedestrian when returning in the lane can be characterized by the minimum returning gap (mRG in Figure 3.9). In this phase the indicators could be used by the drivers to inform other users about their intention.

3.1.4 Extrapolation of position and velocity of the VRU

Since the pedestrian location was dependent on the possibility of ME sensor to detect obstacle located only in front of the vehicle, it has been necessary to extrapolate the pedestrian position

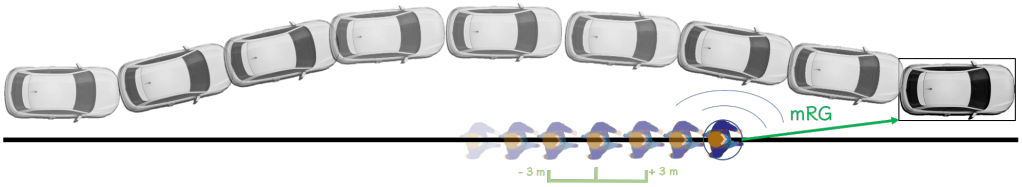

Figure 3.9: *Manoeuvre completed*

during the whole duration of the overtaking. As can be depicted in Figure 3.10 the detection of the pedestrian was highly dependent by the change of vehicle heading angle ψ during the second and third phases.

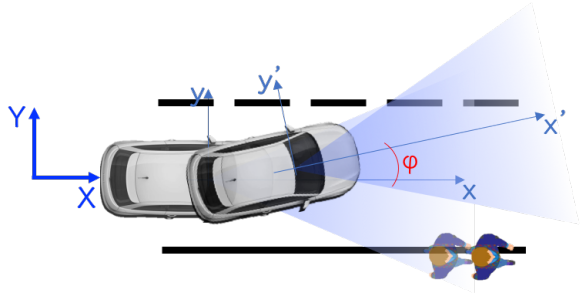

Figure 3.10: *Representation of the scene in which the pedestrian gets out of the FOV of MobilEye sensor. Inertial reference frame is represented with blue X-Y, while the car-fixed frame is represented with x-y*

Hence, the extrapolation process has been necessary for all events, since once the pedestrian was out of the field of view of ME (represented by the blue triangular area) no information were provided about pedestrian position in the scene.

In order to reconstruct pedestrian's position it has been necessary to find a proper measure available for the entire duration of the scenario under investigation. In a previous study [25] the signal provided by ME of the distance to the road edges and or line markings have been used to perform the extrapolation. However the signal has noted to be unreliable: " the raw ME signal [...]seemed to function a bit unreliable, namely that the lateral distance to VRU was greater than the lateral distance to the lane edge, effectively placing the VRU outside of the lane for instances despite the video-feed showing the VRU being located in the middle of the lane." [25] Furthermore since the overtaking event identified in the querying process were mainly occurring in secondary roads, without central and side lane markings, the signal of the lane boundaries was affected by missing or default data. Therefore, a new approach had to be adopted.

Car trajectory

In the attempt of retracing the car path from the begin time until the end time of the segment the kinematic model of the vehicle has been adopted. In the kinematic bicycle model, the two front wheels (respectively the two rear wheels) are lumped into a unique wheel located at the center of the front axle (resp. of the rear axle) such as illustrated on Figure 3.11

In [77] the kinematic equations are expressed by:

$$\dot{X} = V\cos(\psi + \beta(\delta)) \tag{3.1}$$

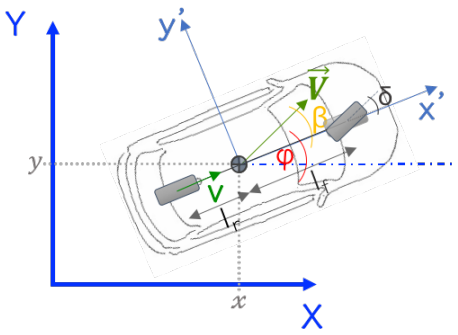

Figure 3.11: *Kinematic model adopted in order to convert car trajectory in the inertial reference frame X-Y*

$$\dot{Y} = V \sin(\psi + \beta(\delta)) \tag{3.2}$$

$$\dot{\psi} = \frac{V}{l_r} \sin(\beta(\delta)) \tag{3.3}$$

where $\beta(\delta)$ is the vehicle slip angle in the center of gravity, δ is the front wheel steering angle, $\vec{V}$ is the vehicle speed in the center of gravity, while ψ is the yaw angle (also known as heading of the vehicle).

From the database it has been considered both the signal related to the "yaw rate" as well as the raw signal of the IMU. Moreover, it has been neglected the vehicle side-slip angle (β) since the speed available (v) was considered recorded by the rear-wheel odometer. Thus the vehicle position (x,y coordinates) was computed in the global reference frame as:

$$x = \int_s^e v \cos(\psi)\, dt$$
$$y = \int_s^e v \sin(\psi)\, dt$$

being "s" and "e" the start and end time stamp of the segment.

It is worth highlighting that in the attempt to get a good result in the trajectory estimation a Kalman filter characterized by state vector [GPS latitude, GPS longitude, GPS heading, vehicle speed, yaw rate, longitudinal acceleration] has been set up.

However, since the kinematic model was giving results (when the trajectory was superimposed to the actual map of the road) as reliable as the Kalman filter trajectory estimation, the bicycle model has been adopted. A reason for this choice was also based on the difficulty in the definition of a general setting for the Kalman filter for the multiple car models present in the data set.

Once the trajectory have been computed a representation panel of the 2D scene was designed to provide to the annotator a direct result of the trajectory. Hence, in the overtaking attribute definition process each trajectory has also been verified by the annotator.

Pedestrian path

Pedestrian position was evaluated starting from the data points given by ME sensor and therefore expressed in the car reference frame. Once the car trajectory (in the global frame) was available, also the pedestrian position was converted into a fixed/inertial reference frame. The transformation matrix (${}^{global}R_{local}$) between the reference frames can be expressed by a rotation matrix, in which the angle ψ corresponds to the vehicle yaw angle.

$$ {}^{global}R_{local} = \begin{bmatrix} \cos(\psi) & -\sin(\psi) \\ \sin(\psi) & \cos(\psi) \end{bmatrix} \tag{3.4} $$

With the assumption that during the manoeuvre the pedestrian was walking along a straight path, it has been necessary to detect which was the direction and position of this assumed path. It has to be considered that the average detection time was roughly 2.0 seconds (20 data points at 10 Hz), while the total time over which the position needed to be extrapolated was roughly 10 seconds. Therefore, in order to get accurate results for the overall path it was crucial to detect outliers within the 20 ME detection.
To perform this operation a specific algorithm has been used: RANSAC. The acronym stands for RANdom SAmple Consensus. This is considered as the state of the art for the detection of outliers and it offers an high degree of reliability also with noisy measurements. The main assumption at the root of RANSAC is that, given a set of inliers, there exists always a model that optimally explains or fits this data [78]. The key reason for the adoption of this method is that it has an higher level of performance when compared to a simple least squared method. This is related to RANSAC's attempt to exclude outliers (during an iterative process) before the evaluation of the model fitting to the data. This is done by fitting lines to several random subsets of the data; consequently a random subset consisting entirely of inliers will have the best model fit. The larger the number of iteration, the higher the possibility of correct inlier identification. An important input parameter to the model is the threshold distance, which represent the maximum value of the norm between the line (that needs to be fitted to the data) and a point to be considered as inlier. Furthermore it is relevant the threshold of the number of inliers. This needs to be tuned adaptively to get the best line fit.

The output first-order model given by RANSAC has been represented by the variable , also referred as pedestrian trajectory slope with respect to the inertial frame, as depicted in Figure 3.12.

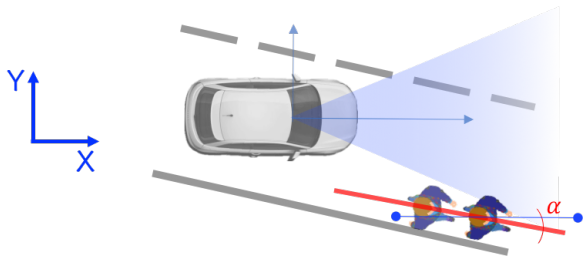

Figure 3.12: *Representation of the RANSAC fit (red line) of the pedestrian detection*

Once the pedestrian walking direction has been evaluated, it has been assigned a pedestrian position (along the path mentioned above) at each time stamp.

To perform this operation the pedestrian motion was firstly evaluated in pedestrian's reference frame and eventually converted to an global reference frame. It has to be noted that

the pedestrian was assumed to walk at a constant speed and without any lateral movement while the overtaking was occurring. Therefore the position of the VRU at the time instant $t_k$has been set equal to:

$$x_{VRUt_k} = x_{VRUt_{k-1}} + V_{VRU}(t_{k-1} - t_k) \tag{3.5}$$

A first evaluation of V_{VRU} has been based on ME signal of the relative speed between vehicle and pedestrian:

$$\pm V_{VRU} = V_{CAR} + \Delta V \tag{3.6}$$

Where $\pm$ is related to the walking direction of the pedestrian, being the same direction of the vehicle or the opposite. However, since ME signal related to the relative speed between the vehicle and the VRU has been proven to provide often unreasonable results (speed higher than common walking/running speed: eg. above 15-20 km/h), the speed of the pedestrian has been evaluated using a second approach. This was relying on the signal given by ME of the longitudinal distance between the VRU and the vehicle. The first degree term of the polynomial fit to this signal (over time) was considered to give the relative velocity, RV with dimension-unit meters per second. The velocity of the pedestrian was thus derived in kilometers in the form of:

$$\pm V_{VRU} = RV3.6 + V_{CAR} \tag{3.7}$$

However, as it has already been noted in previous study following this approach [25], the speed of the VRU resulted to be sometimes overestimated.

Therefore, based on the annotation process, a third method was adopted when previous results revealed to be inaccurate. The annotator had to choose between three pedestrians motion based on available information of the VRU from the video-feed. $V_{VRU} = 0km/h$, when the pedestrian was standing during the event, $V_{VRU} = 5km/h$ for a walking pedestrian, $V_{VRU} = 9km/h$ in the condition in which the VRU was running.

For those event in which the speed evaluation from ME differed of $\pm$ 2km/h from the annotated speed, the latter has been assumed as the actual pedestrian speed, and therefore it has been used for pedestrian position extrapolation.

Eventually, pedestrian's displacement has been extrapolated starting from the mean position of the inliers (from RANSAC) within the last five detection of ME (considered to be the more accurate). Thus at each time stamp, following the equation 3.5, the position was updated backward in time and forward in time. The former refer to pedestrian position during the annotated phase one, two and three, while the latter refer to the VRU position when the car is in the returning phase. The process was performed considering the direction of the pedestrian as described in the annotation process.

The last step has been the transformation of the VRU positions from the pedestrian reference frame to the global reference frame, which served as link between the car motion and the pedestrian motion over time. This has been done by mean of a rotation matrix, as expressed in equation 3.4, with angle .

3.1.5 Comfort zone boundaries

The minimum approaching gap (mAG), minimum distance steering (mDS) and minimum returning gap (mRG), where computed as actual distance in the global reference frame between vehicle's closest corner to the VRU and the pedestrian side. To perform this operation each

vehicle model present in the data set was considered as a rectangular shape from a bird-eye view of the scene. Therefore before having passed the pedestrian it has been considered the front-right corner, while in the returning phase it has been considered the rear corner of the vehicle. It has also to be considered that a specific metric was computed while the vehicle was passing the pedestrian. This metric has been defined as minimum clearance (mC), being the minimum distance of the right-side of the car and the pedestrian. In a nutshell: $mC = min(Dist_{Front}, Dist_{Rear})$.

The time headway (THW) has been derived using the safety metric minimum approaching gap (mAG between the car position and the pedestrian) and the vehicle speed via

$$THW = \frac{mAG}{V_{CAR}} \tag{3.8}$$

while the TTC was evaluated in the form:

$$TTC = \frac{mAG}{\Delta V} \tag{3.9}$$

Moreover, a reference time was defined in order to compare different manoeuvres performed by different drivers. This has been named time to pedestrian, and it has a value $T2P = 0$ in the time stamp in which the car and the pedestrian were aligned orthogonally with respect to the road, as represented in Figure 3.13. This time stamp was identified when the front of the vehicle was reaching the minimum distance to the pedestrian, while passing. Therefore this parameter has been considered to evaluate the time history within and between overtaking manoeuvres, for example: the time in which the phase four was starting has been reported with respect to the T2P described above.

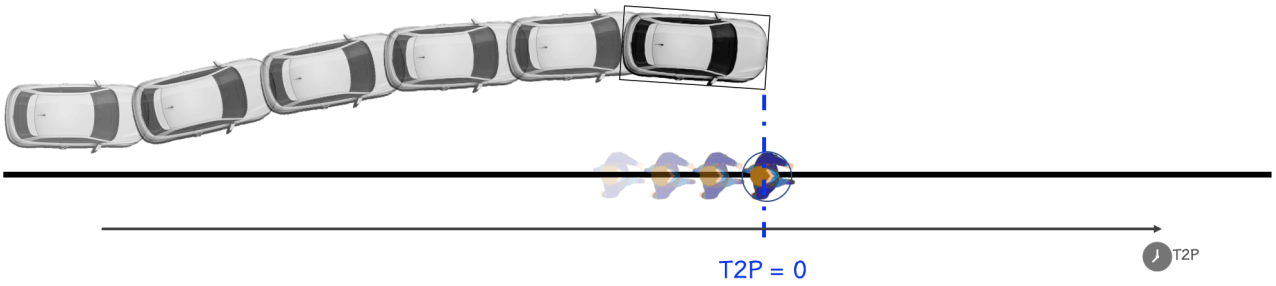

Figure 3.13: *Visualization of the variable time to pedestrian. T2P=0 when the front of the vehicle reaches the lower distance to the pedestrian*

3.2 Field data collection

Within this project a parallel activity to the NDS analysis has been carried out. If the UDRIVE data allowed to have an understanding of the driver behaviour, the field data collection has made it possible to evaluate safety metrics from a pedestrian point of observation. In the following it will be described the hardware adopted together with the software platform. The experimental protocol adopted in the real traffic data collection and the data post processing will be presented subsequently.

3.2.1 Tools

The main requisites for the data logger were related to its wearability as well as to the availability of electronic systems within the department of Mechanical and Maritime science. Specifically, a LiDAR sensor, together with a 9 degree of freedom (DOF) inertial measurement unit (IMU), a web-cam (720 pixels) and a GPS receiver have been adopted in the set up of the data logger system. A description in broad terms related to the working principle of the main adopted sensors will be presented in the next sections.

LiDAR

The name LiDAR is used as acronym of light detection and ranging, sometimes such a sensor is also referred to laser range-finder. As the acronym suggests, this sensor allows users to get distance measurement of objects present within the field of view of the sensor. Hence a LiDAR sensor continuously fires off beams of laser light, and then measures how long it takes for the light to return to the sensor. This is based on the principle of the time of flight of the light beam, which gives the actual distance of a detected target. It is worth highlighting that no direct speed measurement is possible from this sensor as opposed to the available Doppler effect in radio assisted detection and ranging (RADAR) systems. However, speed computation is possible in LiDAR with point to point derivative measurement. Different types of this sensor exist in the market, and their performances in terms of post processing possibilities are mainly related to the number of light-beams which characterize the sensor itself. Nowadays it is possible to find not only static single beam LiDAR sensor with a limited field of view (FOV), but also 360 deg multiple beams sensors. Moreover, it is right for the reader to bear in mind that such devices only gives to the user a point-cloud measurement of the surrounding scene, that is a set of data points at a certain distance with respect to the reference frame of the sensor itself. However to properly understand the environment from the raw sensor information (like the point cloud) it is necessary to extract and classify that information in order to portray what the device is seeing and which kind of objects are present in the scene. Therefore a necessary step presented in the data analysis (see Section 3.2.3) is the classification and clustering of the point clouds measured by the sensor. The laser rangefinder adopted in this project has been the single beam Hokuyo UXM-30LAH-EWA.

IMU

An inertial measurement unit is an electronic device designed to measure accelerations, angular rates, and the magnetic field surrounding the body equipped with the sensor itself. This is achieved using a combination of 3 DOF accelerometers, gyroscopes and magnetometers. Its potentials are related to possible sensor fusion together with a GPS receiver, as well as the calculation of attitude (i.e. body's orientation in 3D space), velocity and position of a given object in space. Typical implementations of IMU occurs by mean of Strapdown inertial system approach, which integrates angular rate from the gyroscope to calculate angular position. The attitude estimate is used to transform acceleration measurements into an inertial reference frame (hence the term inertial navigation) where they are integrated once to get linear velocity, and twice to get linear position [79]. The same evaluation of attitude and heading reference systems (AHRS) has been shared as open source Madgwick filter [80], which has also been adopted in this study. This allows the user to get reliable estimation of the three Euler angles

(roll, pitch and yaw). The Madgwick filter is considered an accurate ARHS algorithms since it is integrating both the approach of computation of the orientation from gyroscopes as well as the estimation of the orientation from accelerometer and magnetometer into a fused solution taking into account the benefits of each source of information. Within this project the 9 DOF PhidgetSpatial Precision 3/3/3 High Resolution has been adopted.

ROS

The Robot Operative System (ROS) is defined as "an open-source, meta-operating system for your robot. It provides the services you would expect from an operating system, including hardware abstraction, low-level device control, implementation of commonly-used functionality, message-passing between processes, and package management. It also provides tools and libraries for obtaining, building, writing, and running code across multiple computers"[81]. Being classified as meta-operating system means that ROS shares characteristics with some middleware systems and frameworks (message callback), but it also has features that are typical of OS systems, like hardware abstraction, package management, developer toolchain. It is worth to give details about a conceivable definition of middleware system. Within a distributed network the middleware is a software layer that stands between the operating system and the application side [82]. Hence, as a middleware, ROS allows the user to integrate different systems and let them work together in an homogeneous environment . Furthermore, ROS has some specific attributes [83]:

- plumbing: ROS is characterized by a dedicated publish-subscribe messaging infrastructure, which allows to support a quick and easy distributed computing systems.

- tools: ROS provides a widespread set of tools for configuring, debugging, visualizing, logging, testing, and stopping distributed computing systems.

- capabilities: ROS run a broad collection of libraries that implement useful robot functionality, with emphasis on manipulation, mobility and perception.

- ecosystem: ROS is maintained, sustained and improved by a large community, with a strong focus on integration and documentation. Online blogs and forums, as well as shared projects (on github) allow the user in finding and learning about the ROS packages, which are made accessible from developers around the world.

In the next sections of this report it will be used a specific terminology associated to ROS, therefore a concise description of the vocabulary used there is assumed to be useful for the reader.

- **Nodes**: a node is process that perform computation; it is an executable. Each node performs a specific processing part, usually a part of the algorithm. Thus, each node has a specific script associated to it. In other words, a node is a process that executes a ROS program. For the sake of clarity, considering an unmanned ground vehicle, each sensor has an associated control node, another node may be used to regulate vehicle wheels, one dedicated node may perform the localization and a further node could combine all these information to run a path planning algorithm.

- **Messages**: nodes communicate with each other by passing messages. A message is nothing but a data structure, characterized by specific fields. Each message description can be found in the msg/ sub-directory of each ROS package.

- **Topics**: each message in ROS is routed via a transport system that has a publish/subscribe semantic. A node sends out a message by publishing it to a given topic. Therefore, each topic has to be associated to a specific "name" that is used to identify the content of the specific message. Specifically, a node that is interested in a certain kind of data will subscribe to the appropriate topic. A topic can be associated to a message bus, this has a name, and anyone can connect to it with the purpose of sending or receiving messages [84].

- **Services**: a service allow to perform a request / reply interaction, which is needed is such a distribution system. There are two sets of services: one for the request and one for the reply. A specific node, that is making available a certain message, provides a service under a dedicated name; at the same time, a client is sending a request message and it is waiting for the reply in order to use the node content.

- **Bags**: *.bag is a format for saving and playing back ROS message data. Bags are an important mechanism for storing data, such as sensor data, allowing a synchronization of measurements.

Embedded system

The device adopted in order to merge together different sensors has been the Raspberry Pi 3 model B. On this single board computer it has been installed the Ubuntu 16.04.4 operative system (OS). As well the version "kinetic" of ROS has been implemented. Metaphorically speaking the Raspberry Pi (RPi) has allowed to get an "intersection" point between different sensors, allowing to perform visualization, management and recording from the same device.

Within the project it has been developed an open source package (available on github) by which the drivers related to each sensor has been grouped together. It has to be considered that each driver acts as translator between a sensor and the data logger that is using this sensor. To accomplish this goal a specific node (see terminology in subsection 3.2.1) has been implemented. The script associated to this node is allowing the user to request for three data logger status: idle (only visualization of data), rec (recording), shtdn (shutdown of the system). As soon as the data logger is booted up, a launch file is run by the Raspberry Pi, allowing the system to receive information from each sensor. Launch files provide a convenient way to start up multiple sensor-nodes as well as initialization of specific requirements (e.g. frame rate) associated to the system.

As previously described the way in which sensors communicate with the master is through messages grouped in topics. The Table 3.1 summarizes each sensor characteristics and associated topics for each sensor message, also a list of the associated connection type to the Raspberry Pi is presented.

A specific node has been developed also for the flag button listed above. The purpose of such a device is to allow the user to flag, by mean of a Boolean signal, some interesting events. In other words, looking at the system usage, as soon as the scene (observed by the sensors) represents an overtaking manoeuvre, this can be highlighted by mean of a click. The button has been connected by mean of the General Input General Output port available in the Raspberry

Table 3.1: Sensor typology and connection type

Sensor	Model	ROS Topic	Message content	Update rate [Hz]	Connection Type
LiDAR	Hokuyo UXM-30LAH-EWA	\scan	Range and Angle for 1520 points	20	Ethernet
IMU	PhidgetSpatial 1044_0	\imu\data_imu	acceleration-x-y-z,yaw-pitch-roll,magnetic field	250	USB
Camera	Creative Live! Cam Sync HD	\cv_camera\image_raw	rgb images	25	USB
GPS	Globalsat BU-353S4	\vel \fix	position and speed	1	USB
Flag Button	-	\flagbutton_pressed	Boolean	10	GPIO

computer board. From a software perspective, the node is adopting the "wiringpi" library and it is started up as soon as the RPi is booted. A specific message "div_datalogger.msg" is published with an update rate of 10 Hz. The default value (false) is upgraded to a "true" value whenever the button is pressed.

In order to control the data logger status a web app has been adopted. In detail, the Raspberry Pi has been set as an access point, allowing to have a wireless network accessible to whichever client connected to it. The browser user interface has been based on a previous activity performed by the supervisor of this project, allowing the user to have two possible selections: data visualization and data management. In the visualization mode real time sensor measurement are displayed to the user. LiDAR data, IMU orientation and camera images are showed in three different web pages. Considering the data management mode, the user can benefit of a window showing terminal logged messages (information messages, warning messages and error messages). Moreover, from this interface the user can start and stop the recording of all sensor messages storing them in a bag file. Furthermore a "shutdown" button allows to close down the complete system. It is worth mentioning that the computer communication protocol adopted for the graphical user interface is the websocket, which provides full duplex real-time data transfer between a "client" (whichever browser connected to the wireless network) and the Raspberry Pi "server".

Figure 3.14 represents how the graphical user interface has allowed sensor measurement visualization and management.

Necessary step for a proper event recording has been the "zeroing" of the gyroscope, associated to the IMU. This activity needs to be performed every time the system is restarted, keeping the sensor static for a couple of seconds.

To allow data synchronization while recording, it has been necessary to provide a time clock to the system. Considering that no internet connection where available (the wi-fi has been used as access point) the Raspberry Pi has been equipped by a real time clock (RTC) Adafruit DS1307 RTC [85].

All the data have been stored on a standard USB pen drive (64GB), which was always connected to the logger. A Yuasa NP7-12 (12 V, 7000 mAh) battery has been used for the LiDAR system power management; while the RPi has been powered by a standard portable charger (5 V, 6000 mA) via micro-USB.

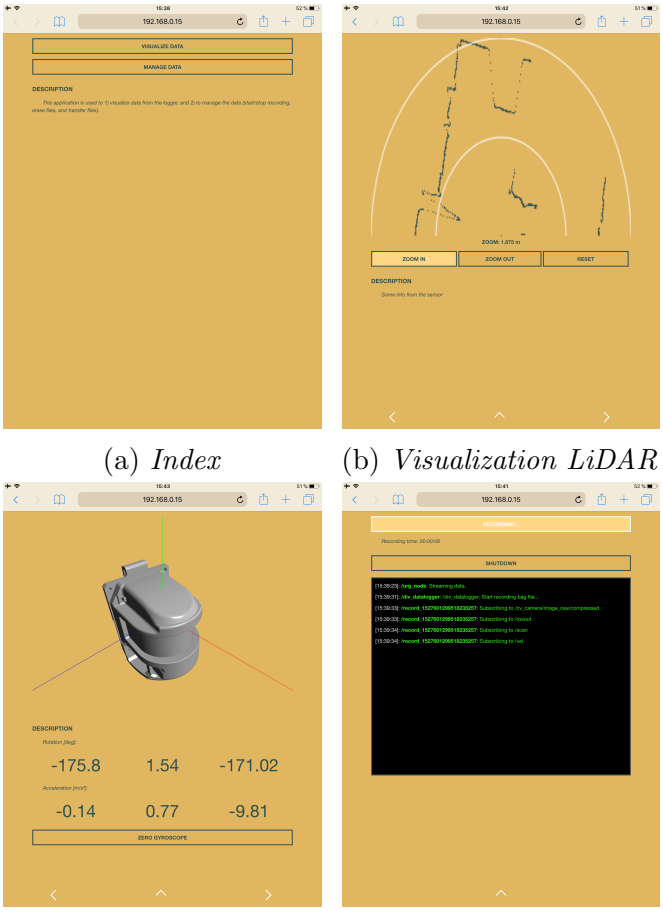

(a) *Index* (b) *Visualization LiDAR*

(c) *Visualization IMU* (d) *Manager page*

Figure 3.14: *Web interface for sensor equipment visualization*

Hardware assembly: 3D printing

The measurement sensors needed to be arranged in a specific way that allowed the logger to be wearable. To achieve this goal the hardware has been designed and manufactured using a 3D printer. On account of completeness, a general overview of the working principle of this additive manufacturing technique would be delineated in the following.

The making of a 3D printed entity is achieved using additive processes. In this process an object is created by laying down successive layers of material until the object is completed. Each of these slabs can be seen as a thinly sliced horizontal cross-section of the ultimate object. This printing method is known as fused deposition modelling (FDM) [86] also known as fused filament fabrication (FFF). The 3D printer used in this project (Dagoma discoeasy 200) is based on robotized Cartesian structure characterized by three prismatic joints, which allow a complete motion of the printer extruder-head in the 3D space. The material which is extruded is PLA (polylactic acid), while the extrusion process encompass a cold end and a hot end. The former is composed by a gear- or roller-based system, which pulls and feed the material towards the hot end. The latter hosts the liquefier of the 3D printer that melts the filament. It allows the molten plastic to exit from a small nozzle to form a thin and tacky bead of plastic that will adhere to the material it is laid on [87].

The work flow necessary to print an object is the following:

1. design of the object model by mean of a computed aided design (CAD) software

2. conversion of the CAD file into *.stl file

3. preparation of the g-code, which sets all necessary slices of the model

4. loading of the coil of plastic material

5. uploading of the proper 3D file in the printer control system

The software tools adopted for this process have been: Autodesk Inventor 2018 for the design of digital element; Cura by Dagoma for the g-code generation.

In Figure 3.15 the step-wise approach mentioned above is represented, from digital 3D model to final printed device.

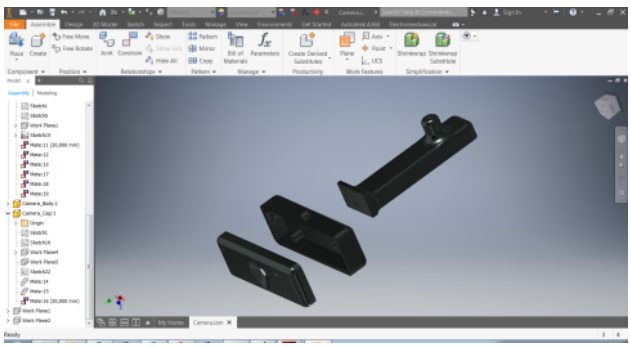

(a) *CAD model*

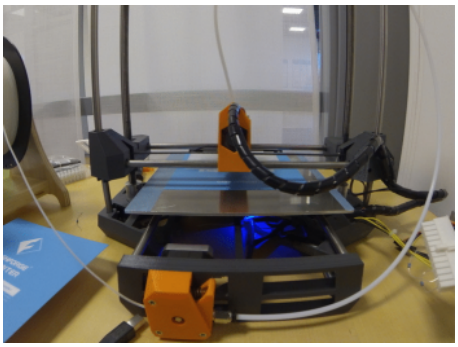

(b) *Printing*

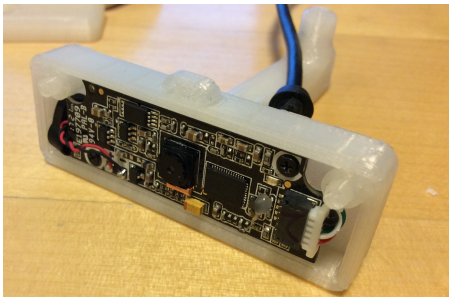

(c) *Final object*

Figure 3.15: *Web interface for sensor equipment visualization*

In detail, the 3D parts designed for this activity have been:

- Camera case
- IMU case
- Raspberry Pi case
- Battery pack case
- Overall sensor equipment holder

The camera case was designed to have a pivoting point which allows angle adjustment. The IMU case is taking advantages of the specific shape of the LiDAR in order to place the IMU sensor just under the LiDAR axis (the LiDAR is sweeping the scene with respect to a fixed axis). As well, the LiDAR shape has been considered for the holder. The latter has been split in two elements which can be used to adjust sensor's location with respect to user's waist. Thus, the holder allows the user to wear the equipment as if it was a strapdown device. For a closer look to CAD files please refer to the online github repository.

3.2.2 Experimental protocol

The experiment was conducted on two different days in a collection site located in Tuve area in Göteborg. The road choice was based on previous collection for driver-bicyclist interaction studies. It was necessary to avoid roads with pavement or dedicated pedestrian lanes on the road or close to it. The road had to have a single lane per each direction, since the overtaking manoeuvres may different on roads significantly when multiple lanes.

It has to be considered that the protocol was designed in order to answer to the five research questions at the root of this thesis activity (see Section 1.1.1). Thus, the protocol was implemented in such a way to get two main factor under analysis. These were:

- pedestrian walking direction
- pedestrian lateral position

The former has allowed to investigate possible difference in road users interaction when the pedestrian was either walking in the same direction of the traffic or facing the traffic. The experimental question related to this factor was: "does the eye-contact influence human behaviour in the execution of the manoeuvre?". The second factor was associated to the pedestrian location on the road, being he walking either on the line marking at the edges of the road or on the curb (namely with a shift of 40-50 cm away from the lane center).

It is worth highlighting that a single pedestrian was wearing the data logger for the complete duration of the collection. Having a single person walking along the street has allowed to avoid the introduction of a potential factor related to pedestrian appearance in driver's perception of the scene. The reader has to consider that to increase safety the pedestrian was wearing a reflective vest, however this outfit was not deemed to be abnormal for drivers in Sweden.

During the experiment a round trip path was followed by the pedestrian starting from the scenario in which he was walking on the line markings and in the same direction of the traffic. Once the scenario in which he was walking on the curb was performed, the planned protocol was completed repeating the previously mentioned settings walking in the opposite direction of the traffic.

The selected area is represented in Figure 3.16, where the extremity points of the walking path are delimited with red markers. While recording data, the pedestrian was expected to reach again the starting position in order to consider the scenario as completed.

Figure 3.17 depicts the equipment worn during the field data collection, a representation of the field test scene is given as well. It has to be noticed that the batteries for the power management of the embedded system were fitted into a backpack carried by the pedestrian. During the collection an equipped vehicle (LiDAR, GPS, IMU, Figure3.17b) was available on the granting of Autoliv AB. However, data of the equipped car have not been analyzed within this thesis work.

Figure 3.16: *Aerial view of the scene. Credits to google.com*

(a) *Equipment*

(b) *Pedestrian observed from car's perspective*

(c) *Pedestrian walking on line marking*

Figure 3.17: *Experimental data collection*

3.2.3 Experimental data – post processing

In order to answer to the research questions associated to the field experiment, measured data needed to be post processed. The reader has to keep in mind that, while walking, the data logger (which was strapped to the pedestrian waist) was affected by a motion in the 3D space. In detail the roll and pitch rotations caused the detection of the ground every step of the pedestrian's way. In order to detect the CZB for different overtaking vehicles from the complete (190 degrees) LiDAR scanned area three main steps have been necessary:

- equipment 3D motion estimation
- road extraction and ground detections removal
- car clusters detection, extraction and tracking

The overall process from 2D raw data to car tracking is summarized in the Figure 3.18.

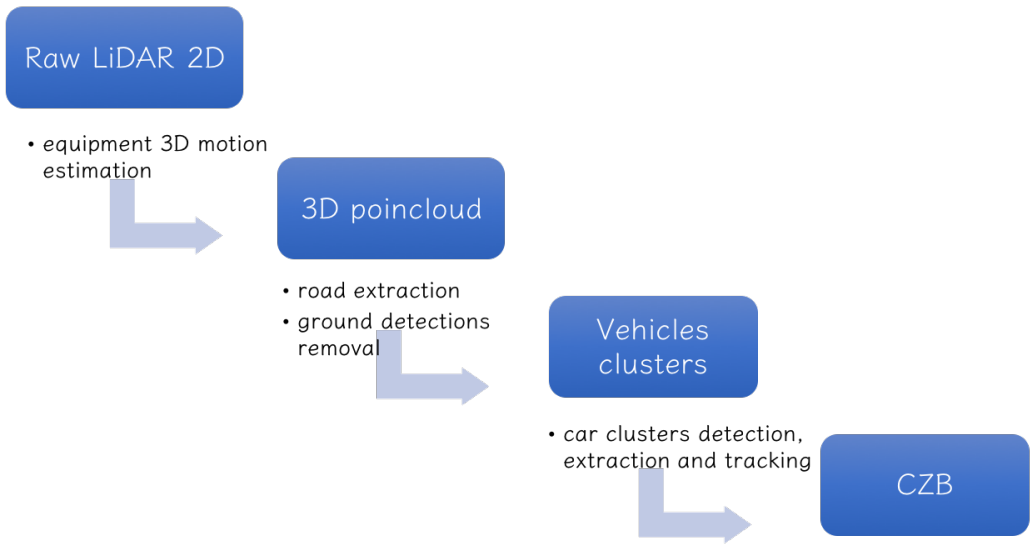

Figure 3.18: *Step-wise approach followed for field experiment data*

Equipment 3D motion estimation

The first data post processing activity has been devoted to get a 3D pointclod from the available 2D LiDAR data fused together with the IMU data. The application of the Madgwick filter has allowed to get a direct information about the orientation of the sensors equipment assembly in 3D space. By mean of a chain of reference frames transformation it has been possible to apply the IMU orientation at each time stamp of the LiDAR data.
Ideally speaking, while walking the waist was following a sinusoidal motion (due to step by step movement in the walk) and the 2D LiDAR scan plane was tangent to this harmonic pattern. Hence at each time stamp the LiDAR was detecting different zones in the environment, due to

the variation of its location. From an optimal position in which the scan plane was parallel to the ground (e.g. while standing) the 2D scan beams were either detecting the ground in front of the pedestrian, or due to this tilt the LiDAR was detecting the ground behind the pedestrian. These front-rear ground detections were thus repeated in a periodic way for the whole duration of the record. The IMU data have been used in order to evaluate the aforementioned 3D motion allowing to get information in a 3D space. Thus, the LiDAR data was enriched and converted into a 3D pointcloud.

Road extraction and ground detection removal

The second main step in the field test data analysis has been related to a pointclod filtering action. In other words, the detected area outside the road boundary as well as the aforementioned ground lines have been removed. The goal of this process has been to include in the final pointclouds only data related to vehicles travelling on the road. A 3D box with dimensions ([-100,+100],[-0.5,9],[-0.4,2]) in the Cartesian ([x],[y],[z]) space has been determined, being x aligned along the road, y perpendicular to the road and z up with center in pedestrian waist. Thus laser points outside of this box were discarded.
Since some ground detections were still present it has been adopted the "RANSAC" algorithm in order to detect such lines outliers. This algorithm was adopted to fit lines through points in the 3D space. Given that the ground appeared as a straight line in each LiDAR frame, every point that was inlier in the line fit was assumed as outlier of the overall pointcloud and therefore these points have been removed. In detail only lines with a slope within the interval 15 - 75 deg were considered as ground, to avoid the removal of front car bumper points, who appeared also in the form of line at a long distance from the pedestrian.

Car cluster detection, extraction and tracking

After the pointcloud filtering process, mainly car detection datapoints were present in the pointcloud. In the following step, laser points that were related to the same vehicle have been detected and differentiated from noise datapoints (still present in the scene) or from other vehicles sensed by the LiDAR in the same time instant. Thus, if multiple vehicles (e.g an overtaking vehicle and an oncoming vehicle) were simultaneously present in the scene, each vehicle was clustered as a standalone object and the process was repeated for the whole duration of the field test data. To accomplish this task the "Euclidean cluster extraction" class available in the Point Cloud Library (pcl) has been implemented. In the literature this approach is defined as "Graph based methods", which consider the pointcloud as if it was a graph. Therefore each point is considered as an edge connected to a pair of neighboring points. The algorithm is creating a graph of the minimum spanning tree, where weights are based on distances between points. In other words, all points that are present in the scene within a defined radial distance are grouped in a single common cluster.

It is worth mentioning that the cluster shape detected by the LiDAR was changing over time. With reference to the Figure 3.19 from left to right (positive x-axis direction) it is represented the overall vehicle cluster shape at different time instants. In the first detection the front of the car appears as a straight line, secondly the vehicle front-right corner is also detected; while passing the pedestrian (located in the origin of the reference frame) only the side of the vehicle is sensed by the LiDAR. The second to last cluster refers to the rear corner of the vehicle, and eventually the rear bumper of the car is detected.

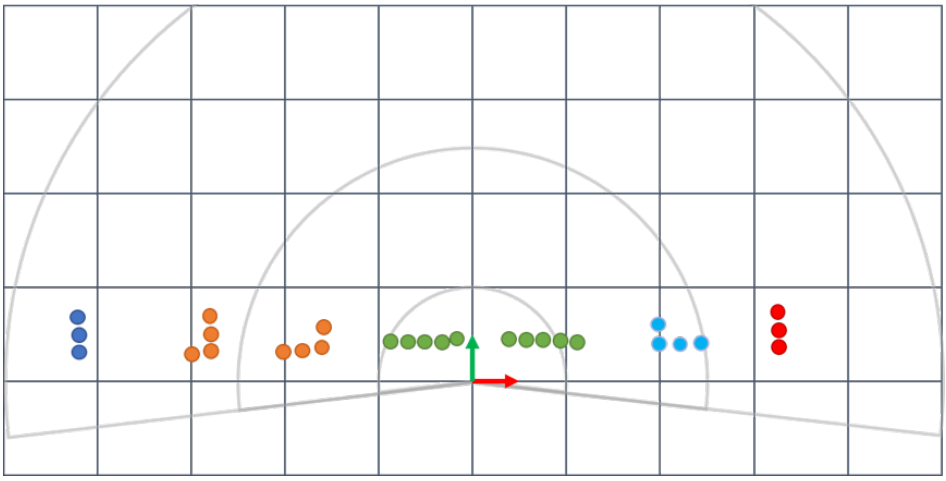

Figure 3.19: *Bird-eye view of the cluster shape time-evolution during the manoeuvre. Observation are represented in the LiDAR reference frame, with associated field of view. From the left side, blue points represent the vehicle's front, orange points are related to the simultaneous front-side detection of the vehicle (with their intersection corner available), green dots represent the unique detection of vehicle side, light-blue colors represent rear-side of the vehicle, and the red points are related to rear bumper detection at larger distances*

Since the output of the previous process had been related to the vehicle shape detection at each time stamp, the subsequent step, in the post process activity, has been the car tracking over multiple time stamps. To each vehicle present in each frame it was assigned an Identifier number (ID) that was either a new ID or the ID of the previous vehicle depending on some tracking criteria. These criteria were the vehicle position in the lane, and the vehicle speed computed between the cluster position in the previous frame and the position in the actual frame.

Thus, each frame belonging to the same vehicle has been grouped allowing to get a time series of vehicle position and speed over the whole duration of the manoeuvre.

As well an automatic annotation algorithm was implemented so to assign some attributes to the grouped vehicle-ID. First of all a vehicle was annotated either as overtaking vehicle or oncoming vehicle depending on its travelling direction.

Moreover, to each overtaking event the vehicle was characterized either as overtaking with oncoming traffic or without oncoming traffic. Following previous studies [19], the oncoming traffic was considered as "present" whenever a vehicle was detected in the scene in the opposite lane, travelling with opposite direction of the overtaking vehicle, within -20 – +120 m along the road direction. It is worth highlighting that the first detection occurred usually at a lower distance, therefore it has been necessary to extrapolate the time in which each vehicle was entering and exiting the zone of -20 – +120 m. The extrapolation process assumed a vehicle speed constant over time, starting from the mean vehicle speed evaluated for both overtaking and oncoming vehicles.

The vehicle speed evaluation was computed starting from the relative speed (ΔV_{V-p}) between vehicle and pedestrian evaluated from the LiDAR position data. Thus, ΔV_{V-p} was considered equal to the rate of change of the longitudinal position of the front of the car (for detections before it had passed the pedestrian) and the rear of the car (for detections after it had passed the pedestrian). Since the LiDAR data were affected by some noise in the measurements, some

position outliers needed to be detected. In detail in each frame the maximum longitudinal point (red axis in Figure 3.18) of the cluster was considered for the front of the vehicle (negative dimension), while the minimum longitudinal point was considered to be related to the rear of the car, once the car had overcome the pedestrian (returning phase). Since it was assumed a constant car speed over the passing phase, the RANSAC algorithm was adopted to detect outliers. It was necessary to get rid of maximum (minimum) points when they were considered not to be related to the front (rear) of the overtaking vehicle.

With reference to Figure 3.20 a representation of the process associated to the vehicle speed estimation is given. The relative speed was computed for both the front and rear points of the car as the slope of the first order model fitted through the inliers. Eventually the ΔV_{V-p} was computed as a weighted average between speed of front/rear and number of inliers in the front/rear data points.

To evaluate the absolute speed of the vehicle the GPS data related to the pedestrian walking speed (V_{ped}) has been taken into account. Therefore, assuming a constant speed of the pedestrian over the duration of each scenario, the overtaking vehicle speed as been computed as $V = \Delta V_{V-p} \pm V_{ped}$, where $\pm$ refers to pedestrian walking direction with respect to the traffic.

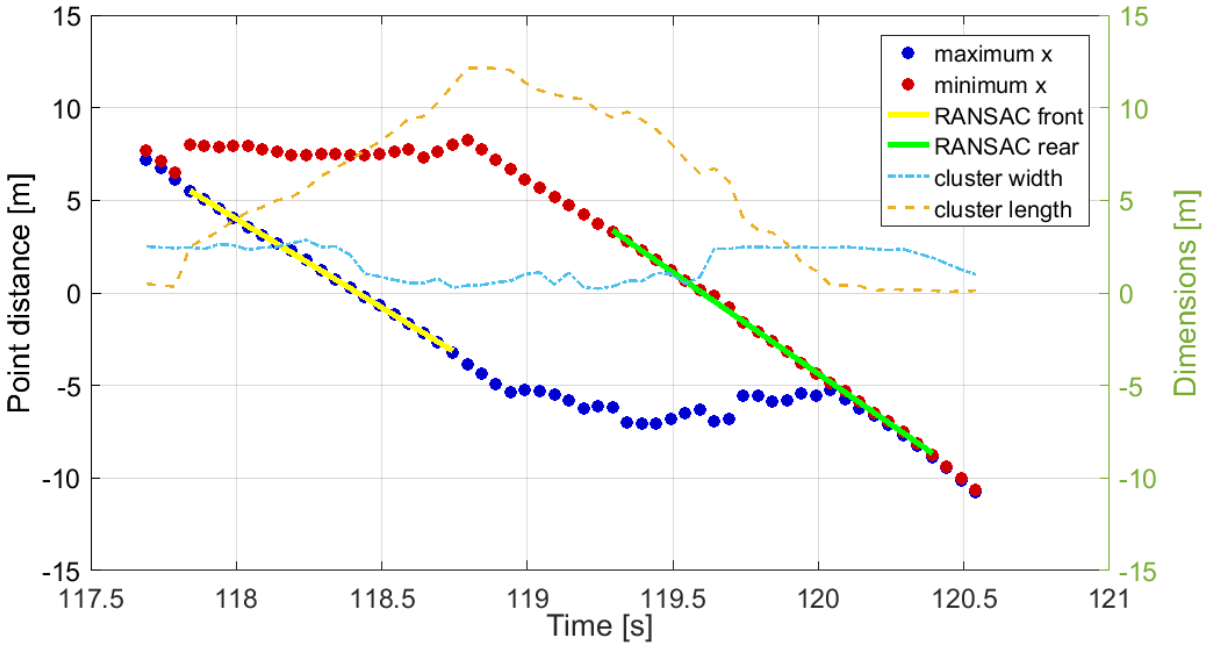

Figure 3.20: *Cluster min-max points, length-width over time. The yellow and green lines refer to the RANSAC inliers detection for the front and rear of the vehicle respectively. The slope of the line fitted through the inliers represents the relative speed between vehicle and pedestrian (ΔV_{V-p})*
The time evolution of the cluster shape in terms of length and width is also represented

Furthermore, whenever the overtaking vehicle was following a leading vehicle during the overtaking manoeuvre with a time headway of less than 3 s, it was classified by the algorithm as piggy backer (Section2.2.1).

It has to be considered that the cluster dimension was different for different vehicle types. Within the overall overtaking duration, for each vehicle the length and width has been observed

allowing to automatically categorize vehicles typology based on the cluster length. Three categories have been selected, with specific cluster length each:

- small vehicle type – cluster length $\leq 5m$ (namely a car)
- medium vehicle type – $5m <$ cluster length $\leq 10m$ (namely a Light Duty Vehicle)
- long vehicle type – cluster length $> 10m$ (namely a bus/truck)

In Figure3.20 an example of how the cluster shape is changing over time (in terms of length and width) is represented for the specific scenario of Truck overtaking.

3.2.4 Comfort Zone Boundaries

The detection tool described in the previous section allowed to detect two main safety indicator variables: the minimum clearance at which a car driver performs the manoeuvre and the associated speed during the event.

The minimum clearance was evaluated as the minimum distance between the car clustered points and the pedestrian, during the full duration of each event.

No other safety metrics were possible to be evaluated from the collected data.

3.3 Driver model

With the objective to understand which factors are influencing drivers' choice of the CZB, a driver model has been devised. This model has direct implications on which variables a vehicle safety system should consider and how tests in assessment protocols could be designed. To achieve these objectives a Bayesian linear regression model has been implemented. The Bayesian linear modelling attempts to apply Bayesian inference instead of the frequentist approach. For the sake of completeness a broad introduction to regression models is presented. In linear regression modelling it is assumed that a response variable (y) is combination of weights (β) multiplied by each predictor variable (x), with the inclusion of an error term which accounts for random sampling noise (ϵ). Assuming three predictors the model equation is:

$$y = \beta_0 + \beta_1 x + \beta_2 x_2 + \beta_3 x_3 + \epsilon \tag{3.10}$$

β_n is also defined as model parameter, with β_0 known as model intercept, while $\beta_{1...3}$ are the regression coefficients and represent the influence of each variable to the response. The output of a linear regression is a single estimate for each model parameter, based on the collected data. This single parameter is evaluated through the maximum likelihood estimation. On the other hand, in the Bayesian viewpoint the linear regression is expressed in terms of probability distribution instead of punctual estimates. Hence the output (estimate) is not a single value but a distribution characterized by a mean and variance. As well, the Bayesian regression model (BRM) approach allows to have not only responses generated from a probability distribution but also the model parameters. Thus, the main reason behind the adoption of a BRM, in this project, has been the possibility of getting a posterior distribution of the model parameters. Applying the Bayes theorem [88], it stands out that:

$$Posterior = \frac{Likelihood \cdot Prior}{Normalization} \tag{3.11}$$

The Prior P(β) represents previous knowledge of the model, or a guess associated to how the model parameters should be. This differs to the frequentist approach, which assumes that the model is only related to the data.

The likelihood function P($y|\beta$) represents the observed evidence, by means of the data.

The Posterior distribution P($\beta|y$) uses the data (likelihood) to weight the previous knowledge (prior): this allows to obtain the distribution representing the parameter values. Since the posterior is expressed in form of distribution, to approximate the posterior the sampling method is adopted in order to draw samples from the posterior. This is performed by means of a Markov Chain Monte Carlo (MCMC) method.

The normalization parameter represents the marginal distribution of the data. However, since the main interest is related to the parameter values, the normalization ($P(y)$) does not have any reference to them. In fact, it is just a number which makes sure that the resulting posterior distribution is a true probability distribution.
Usually the normalization parameter is not considered and and the model for is expressed by

$$P(\beta|y) \propto P(y|\beta) \cdot P(\beta) \tag{3.12}$$

The model is fitted to the actual data (y) considering the Bayesian approach of improving the initial estimate as more data are gathered in the BRM.
Hence the overall work flow for the model fitting has been:

- Specification of the prior model parameters, if known.
- State the formula mapping inputs and output
- Perform MCMC to draw samples from the posterior distribution for the model parameters

In the formula definition many factor (or predictor variables of the regression model) have been considered, trying to understand the effect of each one of them on drivers' manoeuvre execution.

Moreover, three models have been implemented to evaluate three different response variable (y). One has been related to the NDS data analysis, for which the TTC has been considered as response of the model. Instead, the second model has been related to the lateral clearance (mC) between vehicle and pedestrian, and the third model has been related to the vehicle passing speed.

A dedicated consideration about the family distribution of the data has been made. It has to be considered that both the variable time to collision and mC could never reach a negative value. The former because no negative or null TTC has been expected from the NDS data since no crash occurred; the latter because cars where always passing the pedestrian with a certain margin. Hence the family of both the TTC and mC responses has been set equal to a lognormal distribution. This resulted also as the best distribution fitting the actual data.

In the model defined in this project, any estimates ahead of time are assumed for the UDRIVE collection , hence a non-informative prior has been adopted.
However, for the data collected with the LiDAR equipment, the lateral clearance model has been set adopting as prior distribution the distribution of the UDRIVE data set.

The software package adopted for this analysis has been brms, which provides an interface to fit Bayesian generalized linear models using Stan, which is a C++ package for performing full Bayesian inference in R.

It has to be considered that the core of the brms package is the brm function, for which a dedicated formula needs to be specified: it contains information on the response variable as well as on predictors at different levels of the model.

The formula is usually expressed as $response \sim predictors$. In order to separate each predictor effect from each other the + is used, while group levels are defined by mean of $(coef|group)$. The main formula that have been considered are:

NDS

$$TTC \sim oncomingTraffic + pedestrianDirection + (1|DriverID) \tag{3.13}$$

$$TTC \sim oncomingTraffic + pedestrianDirection + vehicleSpeed + (1|DriverID) \tag{3.14}$$

FT

$$mC \sim oncomingTraffic + pedestrianDirection \tag{3.15}$$

$$mC \sim oncomingTraffic + pedestrianDirection + vehicleSpeed \tag{3.16}$$

$$vehicleSpeed \sim oncomingTraffic + pedestrianDirection \tag{3.17}$$

In the NDS data it was possible to keep track of the participants, hence data have been grouped by driver ID, to take into account the disparity (in the number of events) between different drivers.

Different model formula have been evaluated considering the leave one out (LOO) information criterion (lower LOOs indicate better model fit).

Furthermore, the brm package allowed to perform inference about the predicted values. This process has been achieved simulating the posterior predictive distribution of an hypothetical replication of the experiment. The stimulated hypothetical data set has been defined with $y^{rep} = (y_1^{rep}, ..., y_j^{rep})$, where each y_j^{rep} is drawn from a distribution with mean and standard deviation expressed by the model.

The evaluation of a model has been based also on posterior predictive checks (ppc). These allow to compare the replicated data under the fitted model (y^{rep}) to the observed data (y). These posterior predictive analyses allow to "look for discrepancies between real and simulated data" [89]. In other words, the ppc have been considered to assess whether the model gives valid predictions about the reality.

Moreover, to show and test how the model was fitting the data, the posterior predictive distributions (y^{rep}) were examined for four test statistics [89]: the largest of the observed outcomes ($max(y_j)$), the smallest ($min(y_j)$), the average ($mean(y_j)$) and the sample standard deviation ($sd(y_j)$). Each of the four test statistic is represented by the histograms of the posterior predictive distributions, which are compared to the observed data. For a proper model, the predicted data distribution has to contain the actual data elements.

Eventually, to assess if a factor is providing effective influence on the driver choice of the CZB, the difference (or "delta") between distributions (with and without a specific factor) has been evaluated. Hence, in the result chapter a dedicated Section will be given to highlight the contrast between factor in the scene (i.e. oncoming traffic present vs absent).

3.4 Comparative analysis

The two data sets analyzed in this activity (NDS and FT) have been compared. The statistical test has been implemented in order to evaluate possible differences between the data gathered in terms of leeway and vehicle speed. Adopting the frequentist inference a two-sample t-test has been run in order to compute the p-values.

In the t-test the null hypothesis considers that, for each respective data set, the mean of the measures have the same average value and equal but unknown variances. Conversely, the alternative hypothesis states that populations have unequal means.

The t-test has the purpose of accepting or rejecting the null hypothesis for the scenario of the overtaking manoeuvre performed in the naturalistic or in the field test data. Furthermore, the p-values represent at which significance level the rejection of the null hypothesis still holds. The significance level (alpha) was set to 5% based on previous study approach [25].

4 Results

This chapter presents the results associated to both the NDS data analysis and the FT experiment. Moreover, general observations about driver behaviour as well as an analysis of the sensor performance will be outlined. Finally a driver model will be presented.

4.1 Naturalistic driving study

From a data set of 300'000 full-record trips, available for the analysis in the UDRIVE database 6842 segments approximately were appointed as events for a longitudinal driver-pedestrian interaction. Of these, 1362 events were listed as possible pedestrian overtaking . These refers to the number of events in which a pedestrian was identified under the (right) conditions by the "segment generation" and "data reduction" processes (Section 3.1.2). Since by definition, a segment refers only to a section of a complete record, one car record could be responsible for more than one segment listed as possible overtaking event. Out of the 6000 segments roughly 400 have been annotated during this project. Within these, 138 have been considered as overtaking manoeuvre events, while 42 have been grouped under as "passing" events, being the pedestrian located either on a dedicated pavement or far away from the lane edge. For those events, no manoeuvre was identifiable; in other words, no steering wheel action (or other change in the vehicle control) was applied by the driver. The overall number of overtaking manoeuvres available grouped by country is represented in Table 4.1.

Table 4.1: Summary of the event identification process

Country	**N. total events**	**N. useful events**	**percentage**
France	84	68	63%
United Kingdom	34	27	25%
Germany	9	5	5%
Poland	6	4	3.5%
Netherlands	4	4	3.5%

Of the 140 overtaking manoeuvres annotated 14 were related to scenario in which the road was curved, or there were other factor in the scene (15 events). Hence, these were excluded from analysis. As well a couple of records needed to be excluded due to missing data from the CAN bus, for example the steering-wheel angle being set at a constant default value for the whole duration of the record.

Due to the limited amount of time allotted for this project, a subset of the 68 events belonging to France have been chosen for a detailed phase and event annotation process.

4.1.1 Qualitative results

From a general point of view, some qualitative observations can be made regarding the analyzed overtaking maneuvers.

It has to be considered that 17 different participants were driving the vehicles during the detected overtaking manoeuvres, with a non equal partitioning between the number of events per driver ID. Also it has to be highlighted that a single driver was responsible for 25% of the

events.

In Figure 4.1 a general picture of "where" the detected events took place is given.

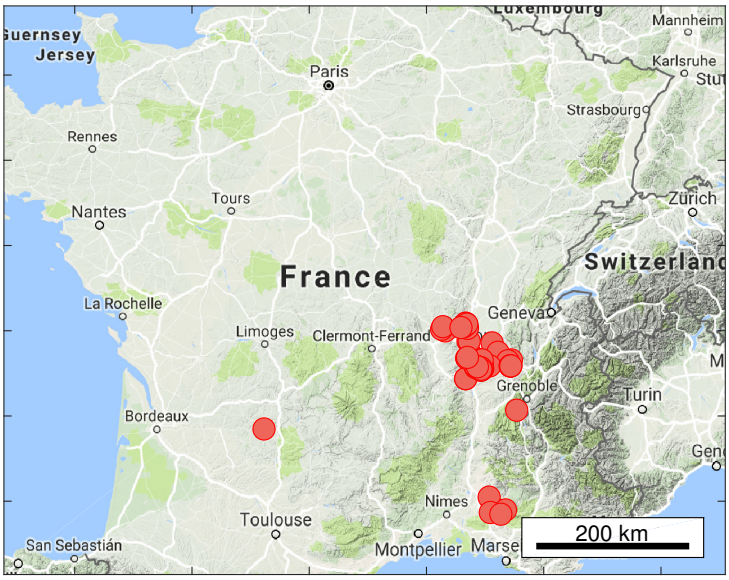

Figure 4.1: *Map distribution of overtaking events in France*

Considering the closest lateral clearance between the car and the pedestrian, its value is highly influenced by multiple factors, like the road characteristics which are however difficult to assess. As a matter of fact, it has to be considered that only a smaller subset of events had a ME signal associated to road edges that was not showing default or NaN (not a number) data.

Furthermore, in order to relate the results to the research questions of this project, the main effects of each factor will be compared by mean of box plots. Box and whisker plots —also called a box plots—displays the five-number summary of a set of data. The five-number summary is the minimum, first quartile, median, third quartile, and maximum.

Results will be presented considering two main factors: the pedestrian walking direction and the presence of oncoming traffic. Table 4.2 summarizes the number of events available in each scenario.

Table 4.2: Number of events available, grouped by pedestrian walking direction and oncoming traffic presence

Oncoming traffic	**Pedestrian walking direction**	**Events available**
present	same	N = 19
	opposite	N = 10
absent	same	N = 23
	opposite	N = 16

Also, it has to considered that the overtaking strategy, namely accelerative and flying, will be considered as grouping factor in the following.

4.1.2 Time related results

First and foremost an evaluation of the overall event duration is displayed in Figure 4.2. A detailed representation of the duration of each phase is depicted in Figure 4.3. Each phase duration is listed in Table 4.3. It represents results in the form of mean and standard deviation, with data grouped based on the typology of overtaking manoeuvre, and by presence of single or multiple pedestrians in the scene. A detailed description of the safety metric TTC is

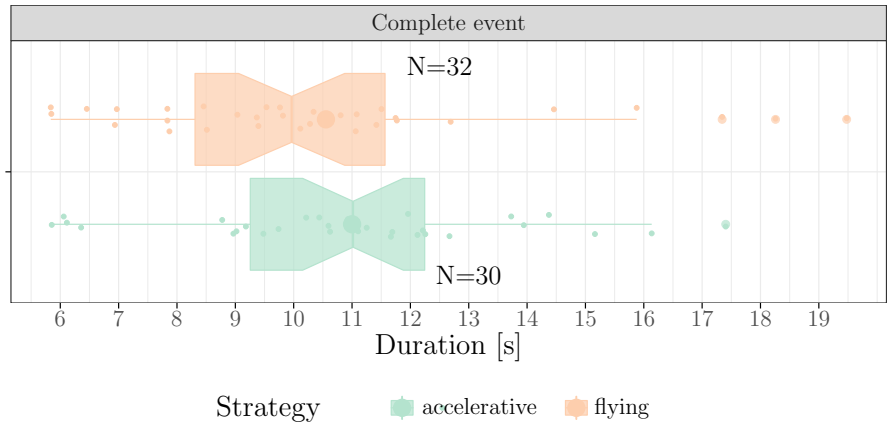

Figure 4.2: *Duration of the complete overtaking manoeuvre. Data are grouped by manoeuvre strategy, which is named overtaking strategy*

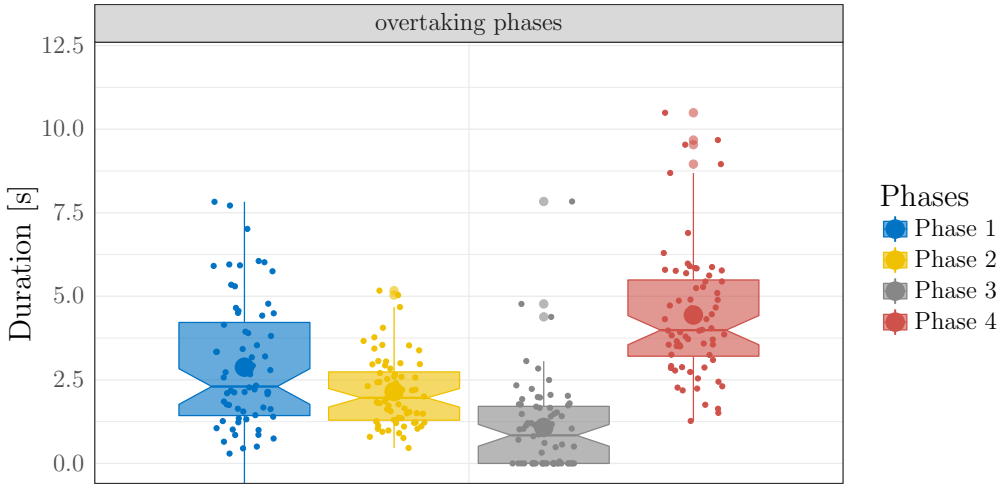

Figure 4.3: *Duration of each overtaking phase. Data refer to the complete data set with no grouping factor adopted*

summarized in Table 4.4 and Table 4.5 in which results of the THW are also reported. A representation of the results is given in Figure 4.4a. Data are grouped by oncoming traffic factor ("present","absent"), with dedicated consideration about the pedestrian walking direction. A cumulative distribution is presented in Figure 4.4b, where the oncoming traffic factor has been considered for each pedestrian walking direction. The reader has to consider the test protocol for active safety system (Euro NCAP CPLA, see Section 2.7) which suggest a $TTC \geq 1.7s$.

Table 4.3: Manoeuvre duration grouped by strategy (Top) and by number of VRU (bottom)

		Phase 1	**Phase 2**	**Phase 3**	**Phase 4**	**Total**
Accelerative	Mean [s]	3.6	2	1.1	4.4	11
N = 30	std	± 2	± 0.9	± 1.8	± 1.3	± 2.9
Flying	Mean [s]	2.5	2.3	1.1	4.6	10.6
N = 32	std	± 1.4	± 1.2	± 0.8	± 2.2	± 3.4
Single VRU	Mean [s]	2.9	2.2	1	4.5	10.6
N = 55	std	± 2	± 1.1	± 1.4	± 2.0	± 3.3
Multiple VRU	Mean [s]	2.6	2.1	1.3	4.2	10.2
N = 13	std	± 1.9	± 1	± 1.3	± 1.9	± 2.9

Table 4.4: Time to collision and time headway grouped by strategy and oncoming traffic factor

			TTC	**THW**
Accelerative	**Oncoming traffic present**	Mean [s]	2.8	2.6
	N =17	std	± 1.4	± 1.4
	Oncoming traffic absent	Mean [s]	3.7	3.5
	N =13	std	± 1.7	± 1.8
Flying	**Oncoming traffic present**	Mean [s]	3.5	3.3
	N =20	std	± 1.4	± 1.3
	Oncoming traffic absent	Mean [s]	4.2	4.3
	N =12	std	± 2.0	± 2.3

Table 4.5: Time to collision and time headway grouped by strategy and pedestrian walking direction

			TTC	**THW**
Accelerative	**Same walking direction**	Mean [s]	3.3	3
	N =23	std	±1.5	±1.4
	Opposite walking direction	Mean [s]	3.5	3.8
	N =7	std	±2.2	±2.3
Flying	**Same walking direction**	Mean [s]	3.5	3.1
	N =18	std	±1.4	±1.3
	Opposite walking direction	Mean [s]	4.5	4.9
	N =14	std	2.2	±2.4

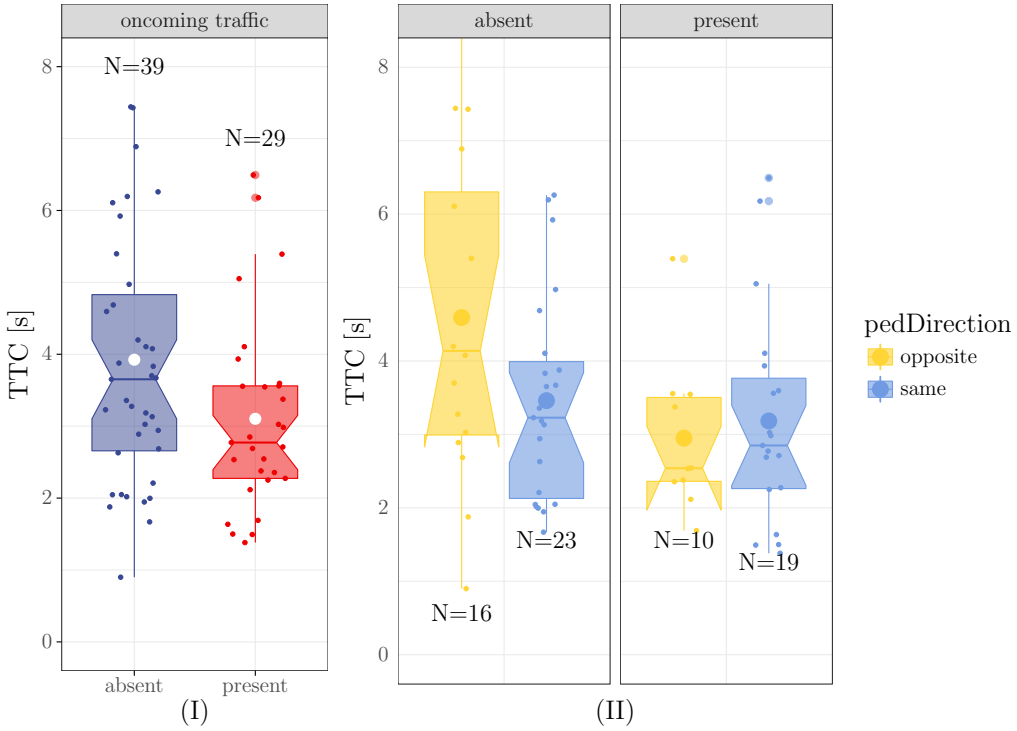

(a) *TTC at start of steering away (Phase two). (I): TTC grouped by oncoming traffic presence (II): TTC grouped by pedestrian walking direction within the oncoming traffic factor. White dot refer to mean value*

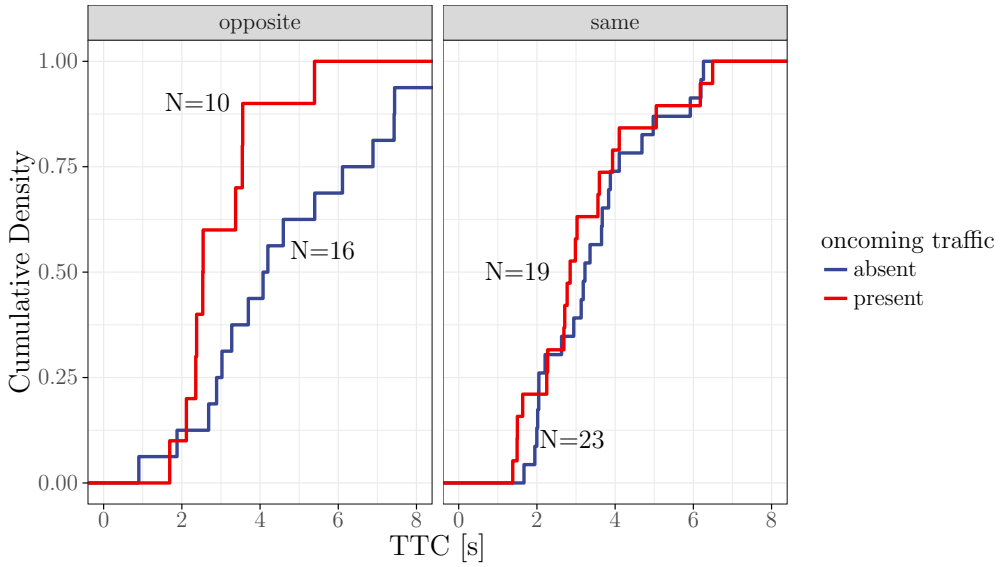

(b) *Cumulative density function of the TTC at start of steering away (Phase two), data are grouped by pedestrian walking direction and oncoming traffic presence*

Figure 4.4: *Time to collision*

The start of the returning phase has been noticed to be performed before the vehicle has actually passed the pedestrian. Referring to the defined variable of time to pedestrian (T2P), Figure 4.5 represents the time at which drivers performed the steering input for the start of phase four.

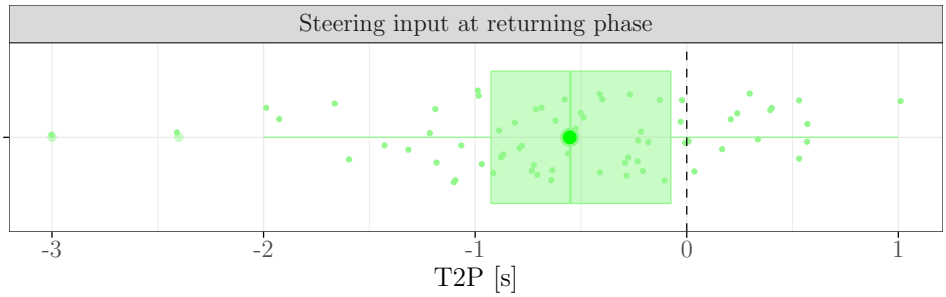

Figure 4.5: *Start of returning phase in term of T2P. Time instant in which the front of the car is closer to the pedestrian is represented by the dashed line*

4.1.3 Distance related results

In the following it will be given a general presentation of the CZB in terms of distances. Each phase has been characterized by specific metrics as described in 3.1.3.
Table 4.6 contains information about the comfort zone boundaries with data expressed in form of mean and standard deviation.

Table 4.6: Summary of CZB[m] grouped by overtaking strategy and oncoming traffic presence

			mAG	**mDS**	**mC**	**mRG**
Accelerative	**Oncoming Traffic Present N =17**	Mean [m]	32.9	15.3	0.9	45.5
		std	±22.6	±15.2	±0.34	±34.0
	Oncoming Traffic Absent N =13	Mean [s]	49.5	21.4	1.2	42.3
		std	±31.0	±17.9	±0.54	±24.3
Flying	**Oncoming Traffic Present N =20**	Mean [s]	50.0	22.2	1.00	55.0
		std	±22.6	±18.7	±0.53	±30.3
	Oncoming Traffic Absent N =12	Mean [s]	74.7	31.1	0.96	58.8
		std	±49.5	±19.9	±0.32	±39.5

The metric mAG has been described in Figure 4.6a, which depicts the CZB considering the oncoming traffic, with the pedestrian walking direction as nested factor. The cumulative distribution of this comfort metric is represented in Figure 4.6b, in which the oncoming traffic presence is evaluated for each pedestrian walking direction. Another comfort-safety metric of relevance is the leeway (mC) adopted by different drivers while passing the pedestrian.

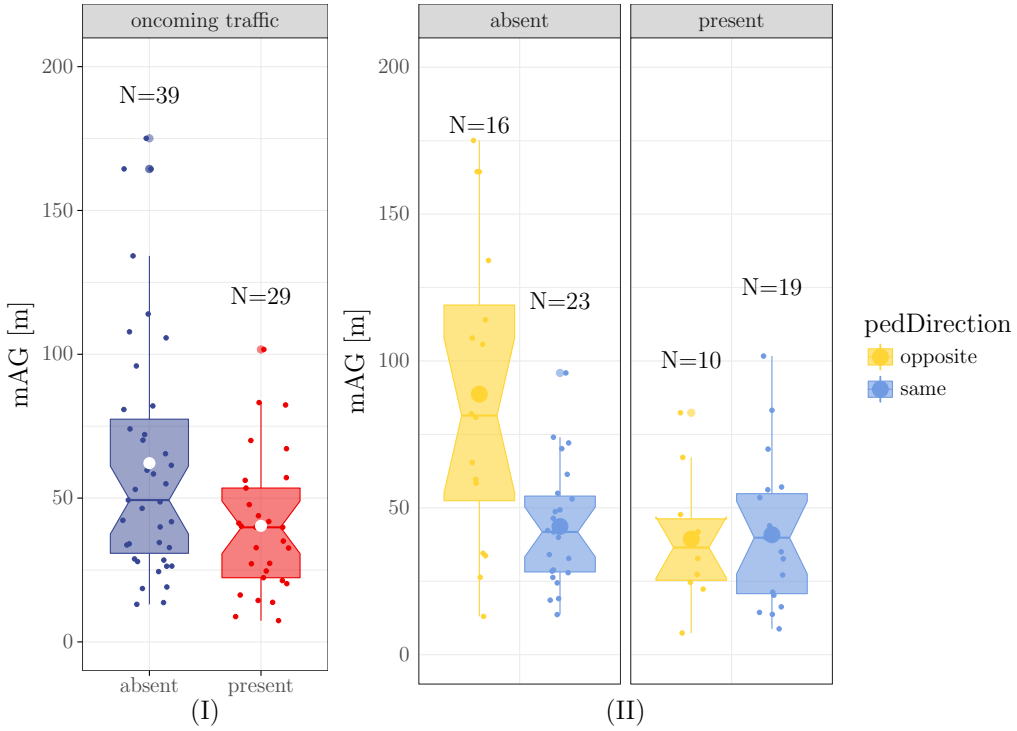

(a) *Distance between car and pedestrian at start of steering away: minimum approaching gap (mAG). (I): mAG grouped by oncoming traffic presence (II): mAG grouped by pedestrian walking direction within the oncoming traffic factor. Colored circles refer to mean value*

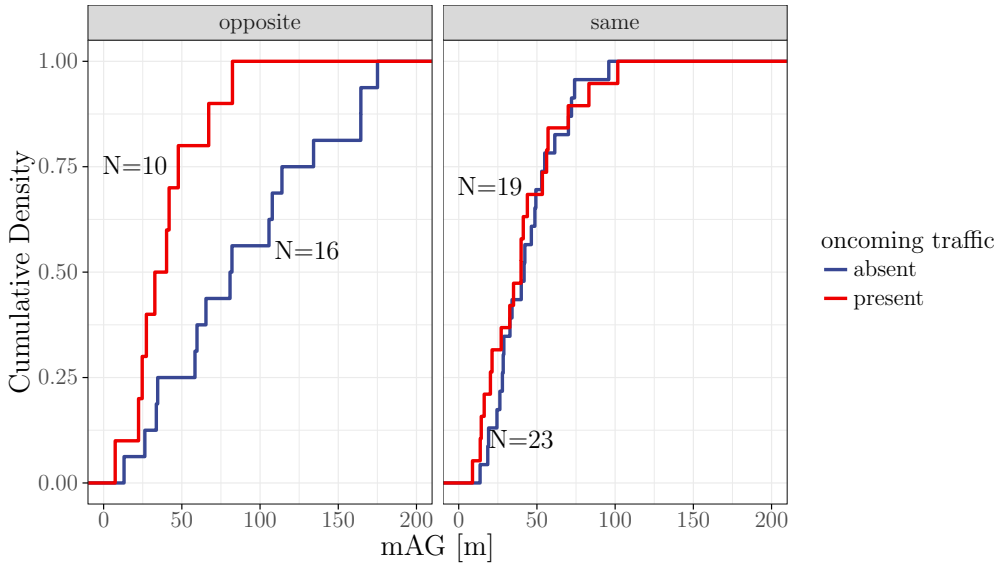

(b) *Cumulative density function of the minimum approaching gap (mAG) at start of steering away (Phase two), data are grouped by pedestrian walking direction and oncoming traffic presence*

Figure 4.6: *minimum approaching gap*

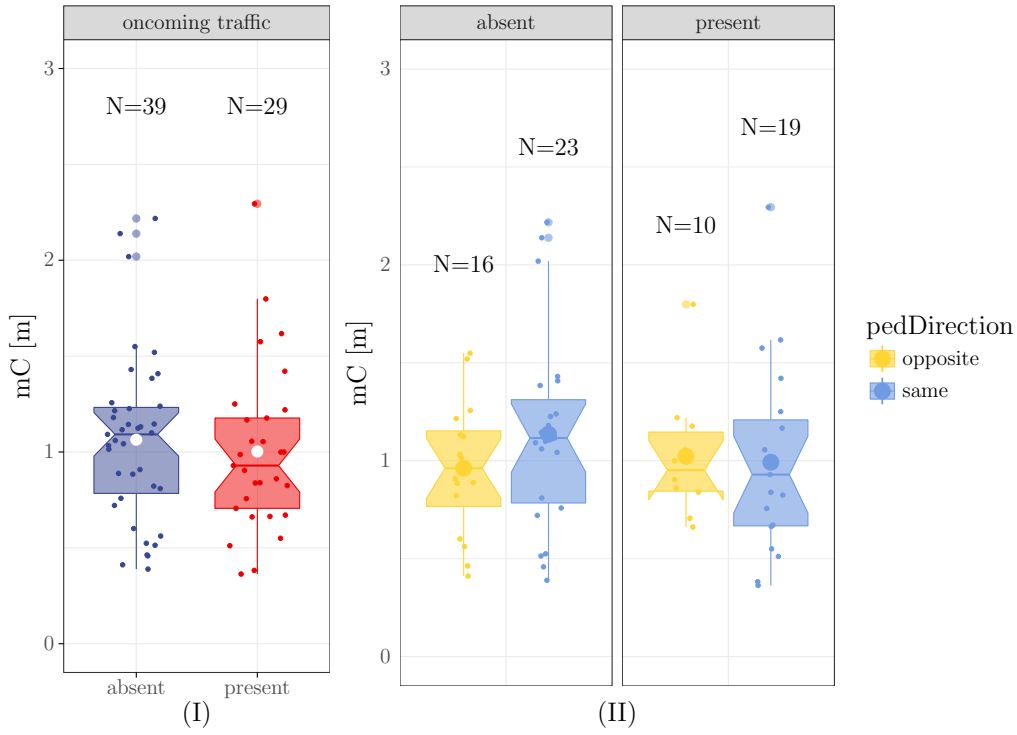

(a) *Distance between car and pedestrian while passing: minimum clearance (mC). (I): mC grouped by oncoming traffic presence (II): mAG grouped by pedestrian walking direction within the oncoming traffic factor. White dot refer to mean value*

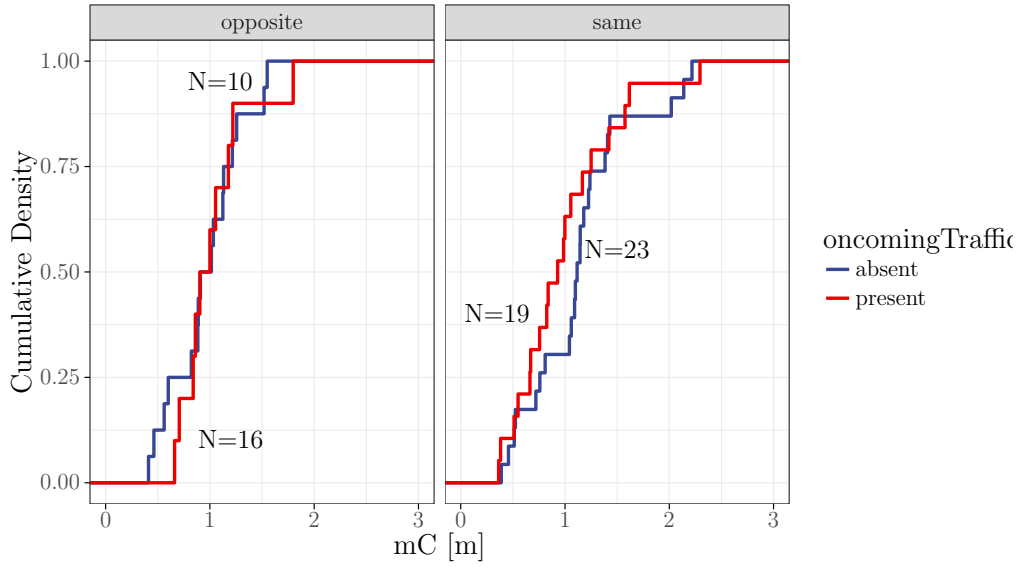

(b) *Cumulative density function of the minimum clearance (mC) while passing, data are grouped by pedestrian walking direction and oncoming traffic presence*

Figure 4.7: *minimum clearance*

Data are graphically displayed following the aforementioned approach.
Box-plots in Figure 4.7a consider the oncoming traffic influence and the pedestrian walking

direction as nested factor. The cumulative density in Figure 4.7b allows to understand which is the leeway between car and pedestrian for each walking direction.

Another variable considered important to have a complete picture of the manoeuvre is the minimum returning distance (mRG) at which the event has been annotated as complete. Data are represented by mean of box plots in Figure 4.8, following the same grouping factors and color scheme previously adopted.

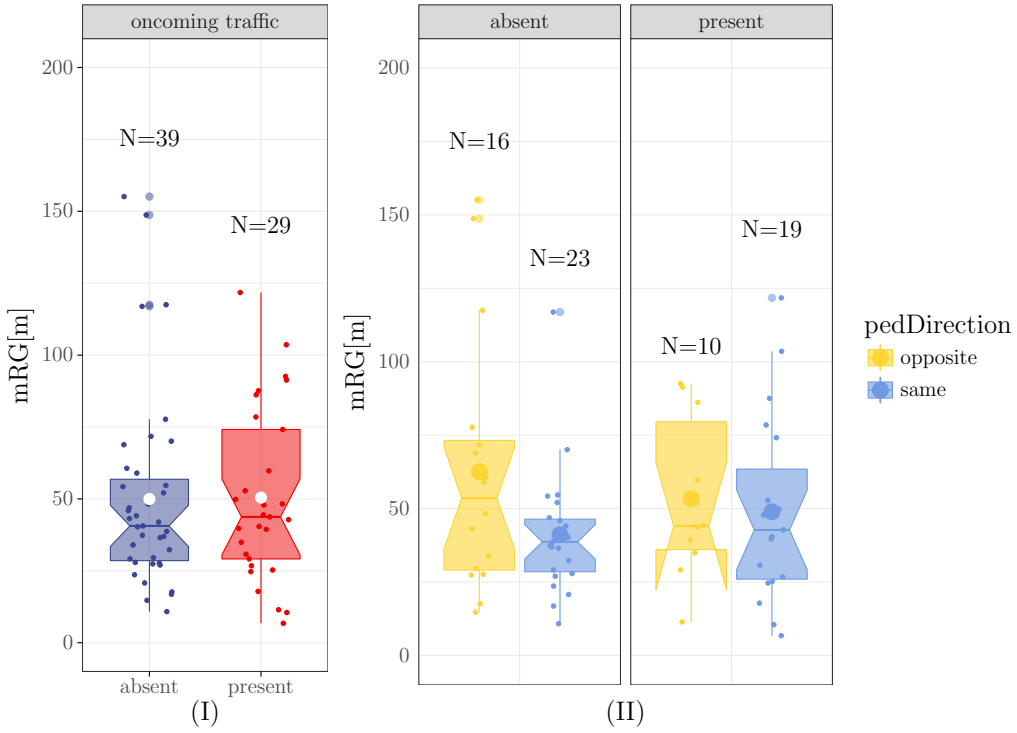

Figure 4.8: *Distance between car and pedestrian at the end of the manoeuvre, in the returning phase (mRG). (I): mRG grouped by oncoming traffic presence (II): mRG grouped by pedestrian walking direction within the oncoming traffic factor. White dot refer to mean value*

4.1.4 Speed related results

The vehicle speed plays an important role in driver's interaction with other users. It essential to evaluate both driver comfort and safety. Thus, the vehicle speed is paramount in the driver decision about manoeuvre phases, and distance to other road users. Since the speed is uncommonly constant for the whole duration of the event, in Table 4.7 data are listed considering the speed reduction performed by the driver during the approaching phase ΔV_{ph1}, the vehicle speed at the steer-away V_{ph2}, the average speed of the car within $\pm 3m$ from the VRU position, while passing the pedestrian $V_{passing}$. Eventually the speed increase during the returning phase ΔV_{ph4} is also given. Table 4.8 represents the same variables but considering the pedestrian walking direction instead of the oncoming traffic presence.

The vehicle speed while passing the pedestrian is strongly related by the overtaking strategy, as represented in Figure 4.9.

A closer look to the vehicle speed before having passed the pedestrian (phases 1-2) allows to estimate driver speed reduction, especially in accelerative events. Since in Euro NCAP safety systems are rated based on vehicle speed reduction, the average driver behaviour to perform

Table 4.7: Summary of Speed reduction during approaching phase (ΔV_{ph1}) and returning phase (ΔV_{ph4}), Vehicle speed at steering away-start of phase two (V_{ph2}), vehicle speed while passing the pedestrian ($V_{passing}$)average value within $\pm 3m$ from the pedestrian position. Data are grouped by overtaking strategy and oncoming traffic presence

			ΔV_{ph1}	V_{ph2}	$V_{passing}$	ΔV_{ph4}
Accelerative	**Oncoming Traffic Present N =17**	Mean [km/h]	*-14.2*	43.1	42.9	*11.1*
		std	*±17.3*	±15.9	±14.0	*±9.9*
	Oncoming Traffic Absent N =13	Mean [km/h]	*-8.4*	48.3	43.7	*8.3*
		std	*±8.8*	±13.4	±10.7	*±4.4*
Flying	**Oncoming Traffic Present N =20**	Mean [km/h]	*1.1*	54.0	51.8	*0.5*
		std	*±6.4*	±14.9	±15.1	*±5.0*
	Oncoming Traffic Absent N =12	Mean [km/h]	*0.4*	60.6	59.9	*-1.3*
		std	*±4.0*	±15.0	±16.2	*±7.6*

Table 4.8: Summary of Speed reduction during approaching phase (ΔV_{ph1}) and returning phase (ΔV_{ph4}), Vehicle speed at steering away-start of phase two (V_{ph2}), vehicle speed while passing the pedestrian ($V_{passing}$)average value within $\pm 3m$ from the pedestrian position. Data are grouped by overtaking strategy and pedestrian walking direction

			ΔV_{ph1}	V_{ph2}	$V_{passing}$	ΔV_{ph4}
Accelerative	**Same walking direction N =23**	Mean [km/h]	*-11.6*	46.7	44.6	*9.7*
		std	*±14.2*	±13.5	±11.6	*±8.3*
	Opposite walking direction N =7	Mean [km/h]	*-8.6*	44.0	39.4	*8.8*
		std	*±10.0*	±18.4	±13.4	*±2.6*
Flying	**Same walking direction N =18**	Mean [km/h]	*-1.4*	54.3	52.6	*0.5*
		std	*±5.5*	±13.5	±14.2	*±7.4*
	Opposite walking direction N =4	Mean [km/h]	*1.4*	63.0	62.4	*-2.1*
		std	*±3.8*	±16.1	±17.1	*±5.7*

this task is represented in Figure 4.10. In detail the speed change is evaluated in each phase, showing a null speed variation as average, for flying manoeuvres.

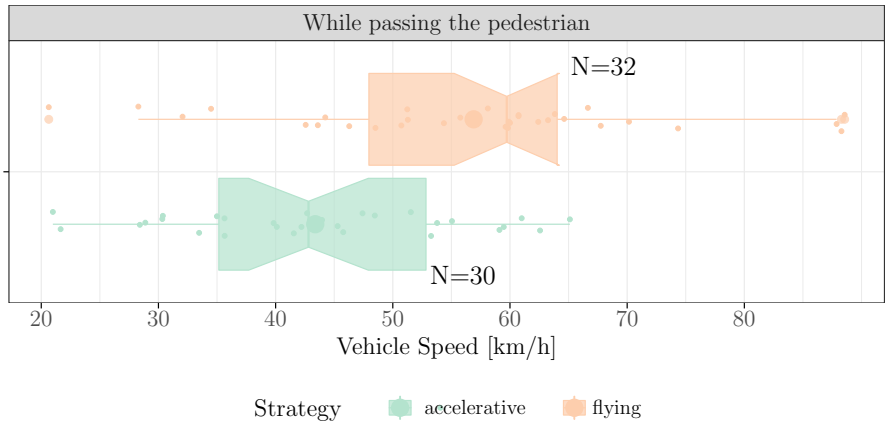

Figure 4.9: *Vehicle speed while passing the pedestrian, average value within ±3m from the pedestrian position. Speed grouped by overtaking manoeuvre*

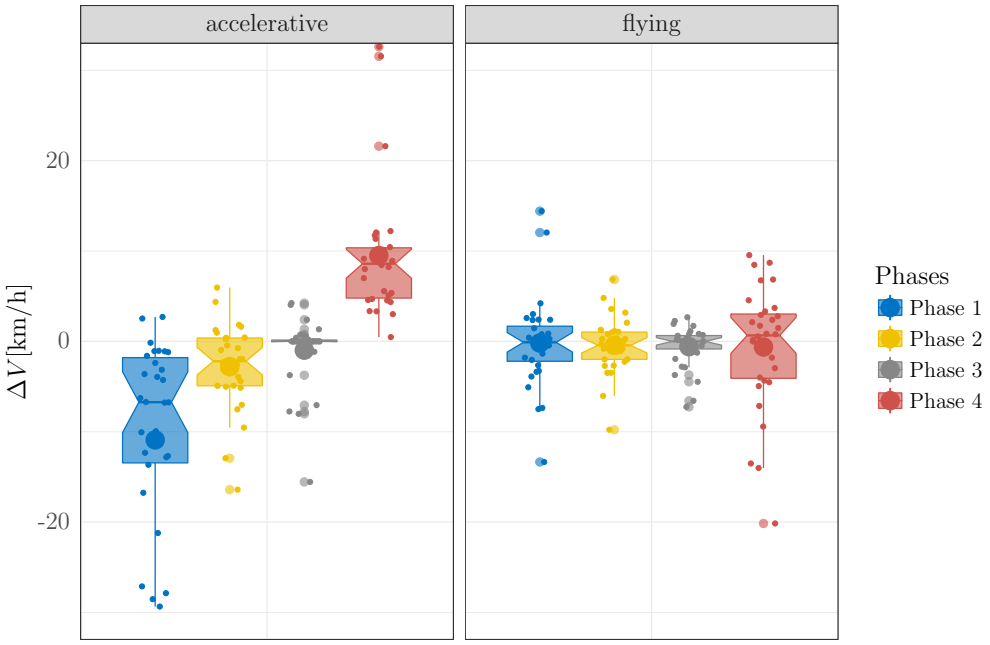

Figure 4.10: *Speed reduction in each phase, grouped by overtaking manoeuvre strategy*

Considering exclusively the accelerative events, the speed reduction in the main phases is evaluated giving particular attention to the pedestrian walking direction. Data are represented in Figure 4.11.

Moreover, it has been evaluated a possible relationship between vehicle speed and different metrics, being those related to safety or to driving comfort.

Figure 4.12 represent data distribution of the TTC and the corresponding vehicle speed at the steer away. At higher speed drivers are willing to anticipate the manoeuvre. Data are

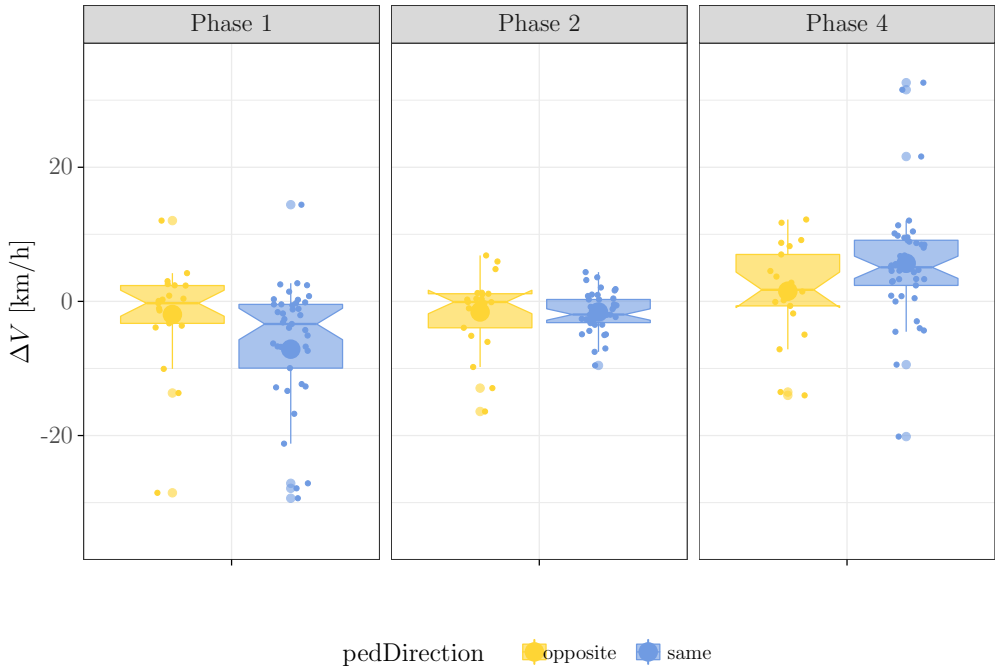

Figure 4.11: *Speed reduction in Approaching (phase 1), steering away (phase 2), returning (phase 4). Data, related to the accelerative events, are grouped based on pedestrian walking direction (pedDirection)*

grouped by overtaking strategy, while in Figure 4.13 the grouping factor considered is related to the presence of oncoming traffic.

Figure 4.12: *Time to collision and corresponding vehicle speed at the steering away. Data are grouped by overtaking manoeuvre strategy. Box plots refer to the TTC (on the side) and to the vehicle speed (on top). Scattered point shapes are associated to the oncoming traffic presence*

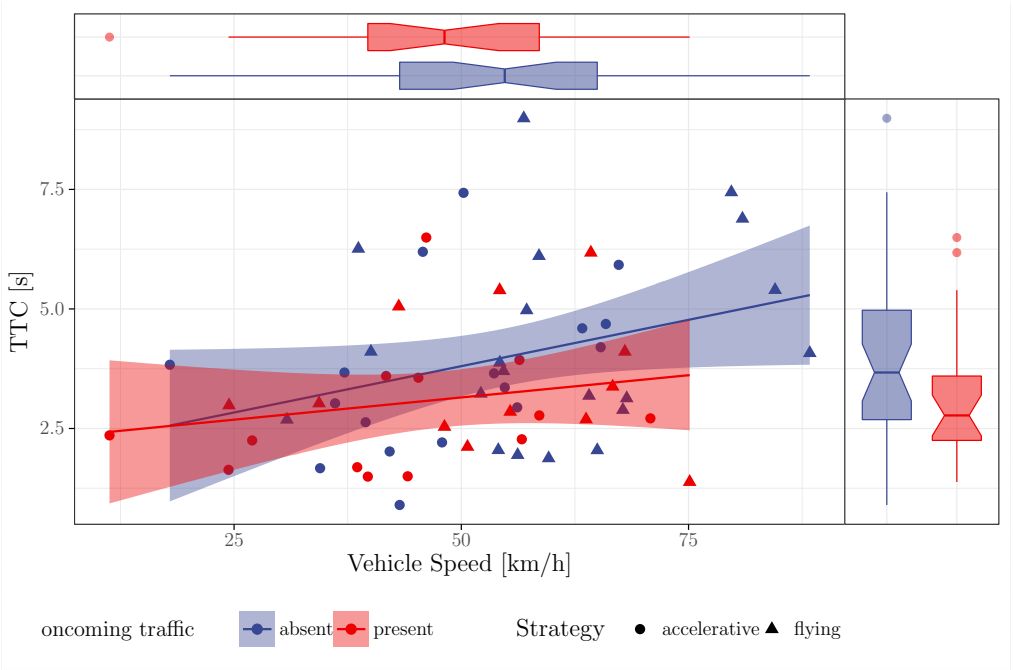

Figure 4.13: *Time to collision (TTC) and corresponding vehicle speed at the steering away. Data are grouped by the oncoming traffic factor. Box plots refer to the mC (on the side) and to the vehicle speed (on top). Scattered point shapes are associated to the overtaking strategy*

A relationship between the vehicle speed and the phase two duration is depicted in Figure 4.14. Grouping the data by the oncoming traffic factor allows to highlight that an high speed not only influences the steer away in terms of TTC (Figure 4.13) but also the complete phase duration.

A relationship between the minimum lateral clearance and the corresponding vehicle speed while passing the pedestrian is represented in Figure 4.15. Due to lower vehicle speed in accelerative events, no clear trend can be noticed between speed and clearance for such events. However, for flying events a trend can be appreciated: the higher the speed, the higher appear to be the leeway to the VRU. The same interrelation is represented in Figure 4.16, with grouping factor the oncoming traffic presence.

4.1.5 Vehicle trajectories

In Figure 4.17 it is represented the vehicle trajectory during the overtaking manoeuvre for multiple events, which are normalized with a T2P = 0 s. Hence, the reference frame represents the position of the pedestrian when the front of the car reaches the lowest distance to the pedestrian. The mean vehicle trajectory is represented with the corresponding vehicle's left and right side (black dotted lines), evaluated for the data acquisition vehicles in UDRIVE. The vehicle position is shown within one standard deviation in the highlighted blue area. Focus is given to a distance of 60 m, being 30 m before the vehicles reached the pedestrian and 30 m after the vehicle passed the pedestrian longitudinally. Lateral distance to the pedestrian is represented along the vertical-green axis, which has a different axis scale compared to the horizontal-red axis.

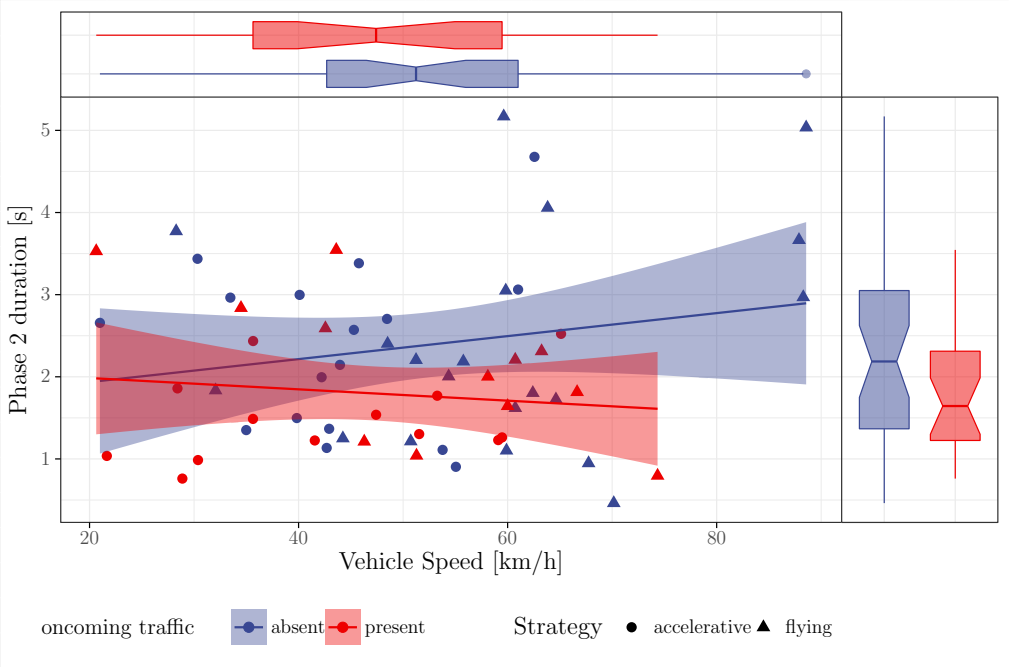

Figure 4.14: *Phase two duration and corresponding vehicle speed. Data are grouped by the oncoming traffic factor. Box plots refer to the duration (on the side) and to the vehicle speed (on top). Scattered point shapes are associated to the overtaking strategy*

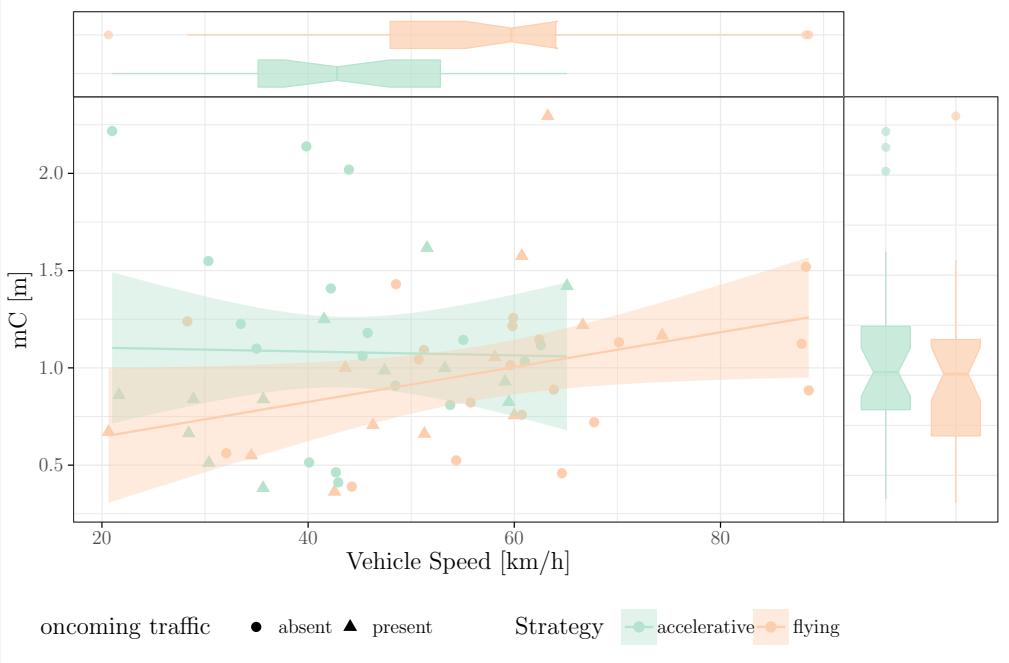

Figure 4.15: *Minimum clearance (mC) and corresponding vehicle speed. Data are grouped by the overtaking strategy. Box plots refer to leeway mC (on the side) and to the vehicle speed (on top). Scattered point shapes are associated to the oncoming traffic factor*

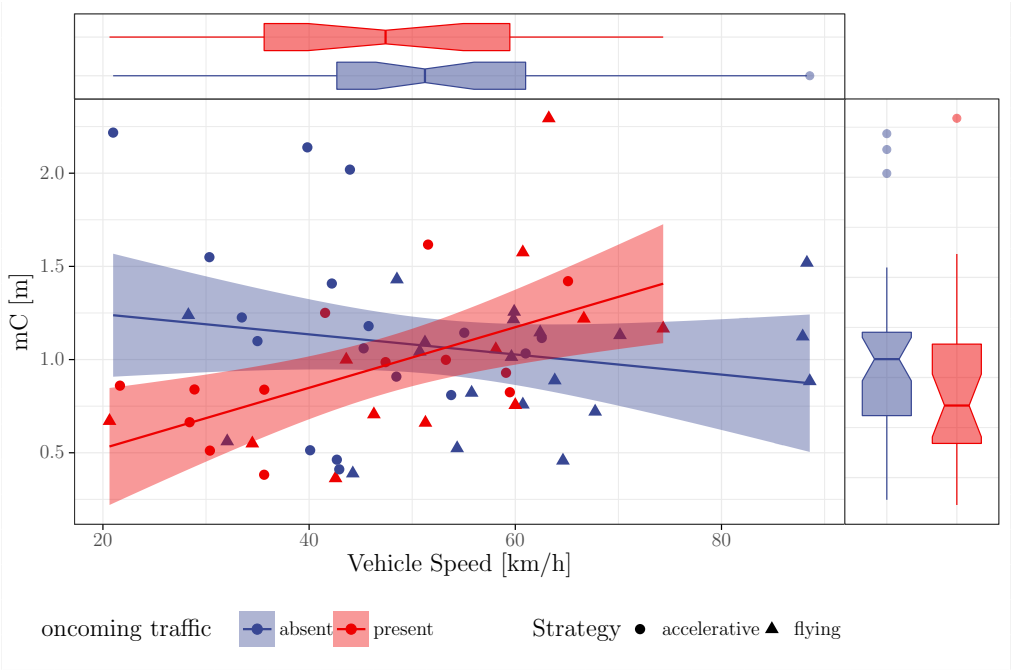

Figure 4.16: *Minimum clearance (mC) and corresponding vehicle speed. Data are grouped by the oncoming traffic factor. Box plots refer to leeway mC (on the side) and to the vehicle speed (on top). Scattered point shapes are associated to the overtaking strategy*

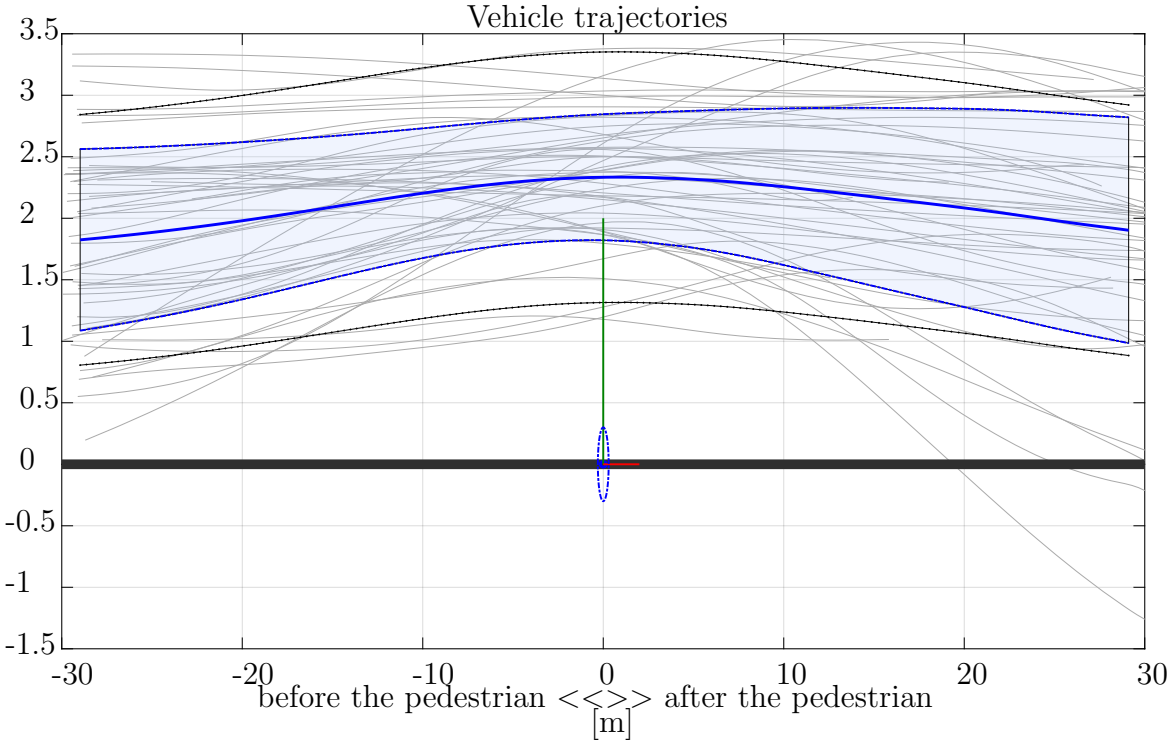

Figure 4.17: *Vehicle trajectories for multiple overtaking events. The black dotted lines represent the vehicle side in the condition of mean trajectory (represented in blue). The light blue area represents the 68% (1σ) of values related to the mean vehicle trajectory. The red and green segments represent the x and y axis respectively. The dashed blue shape, centered in the reference frame origin, represents the pedestrian in the scene. Aspect ration between axis is not equal, to emphasize the vehicle's lateral displacement*

4.1.6 ADAS pedestrian detection

The ADAS system providing information about pedestrian position in the longitudinal scenario has been considered in terms of operation. The system has never triggered a warning signal during the events analyzed. This warning signal is associated to the system capability of pedestrian collision warning (PCW). MobilEye detection of the pedestrian in the scene occurred with an average duration of 2.3 s (std 1 s). The detailed duration of the detection is represented in Figure 4.18, in which data are grouped with respect to the pedestrian position. Moreover,

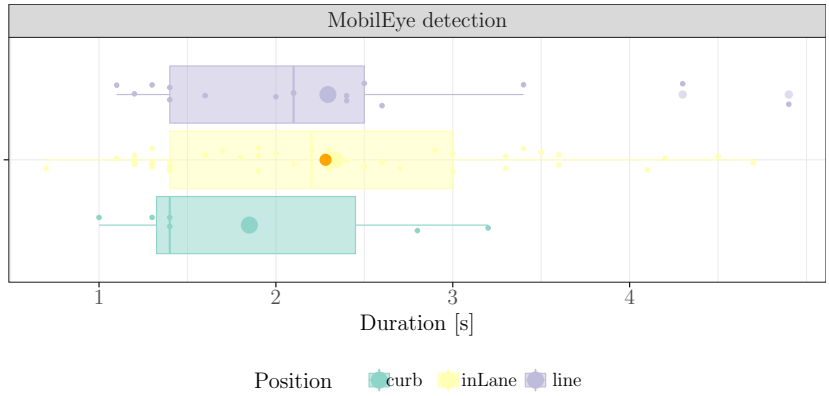

Figure 4.18: *MobilEye pedestrian detection duration for different VRU positions*

it has been noticed a significant dependency between the detection duration and the vehicle speed. The higher the vehicle speed was, the lower the detection duration, as represented in Figure 4.19. Results are not directly related to driver behaviour, however they emphasize the challenges that the driver assistance systems need to overcome.

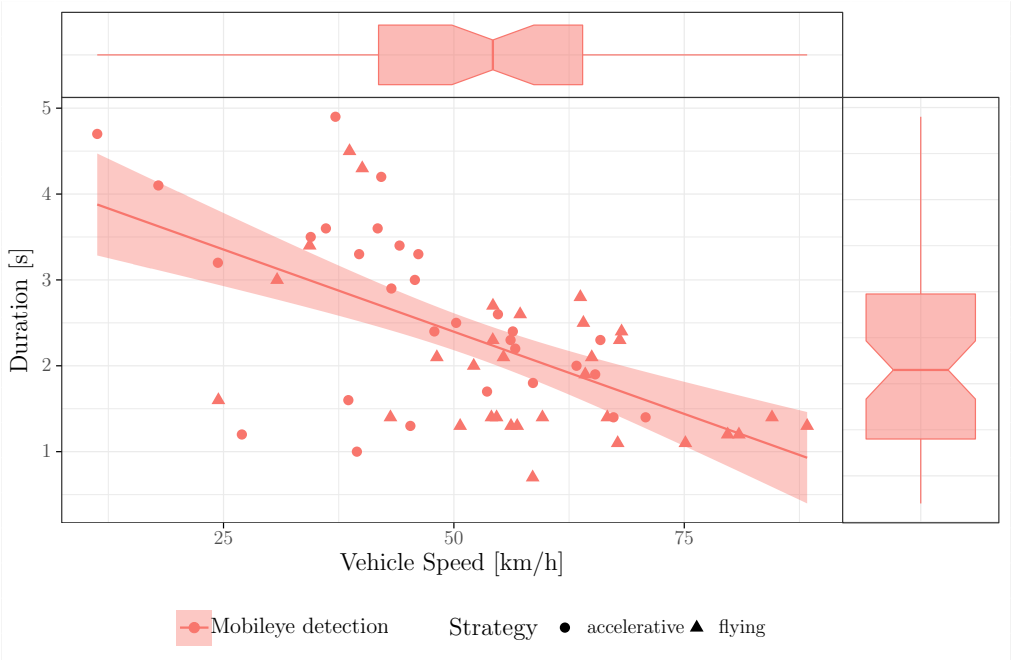

Figure 4.19: *ADAS system measurements in terms of detection duration and vehicle speed. Box plot refer to the detection duration (on the side) and to the vehicle speed (on the top)*

4.2 Field data collection

The data collection has been performed in two different dates, for a time duration of approximately 2 hours, which have been needed to set up and follow the experimental protocol. The effective recording time has been roughly 3.5 hours overall. Over this data recording time, 630 overtaking events have been manually annotated, however the automatic annotation tool has provided results related to 481 events. Thus in the following results will be presented with respect to this overall amount of manoeuvres.

4.2.1 Qualitative results

One of the main findings related to the field test has been the performance of the data collection platform implemented during this project. This suggests a reliability of the embedded system implemented for the specific use of data collection. However, results have been affected by the limited LiDAR possibilities in the detection of vehicles at long distances, due to the significant motion of the sensor equipment while walking.

In general terms, some observations could be made regarding the analysis "on the road". A large number of drivers seem to feel comfortable and safe enough overtaking the pedestrian also with oncoming traffic. This was expected and comprehensible since the pedestrian was not located in the lane. Therefore his presence on the road was rarely perceived as a threat, leading to events that were always classified as flying, when the manoeuvre strategy is taken into account.

However, drivers left more lateral clearance than the generally recommended 1.5 m only for 44% of events when the pedestrian was walking on the line, while the rate increases to 75% when the VRU was walking on the curb. Especially in maneuvers with oncoming traffic, many violations of this recommendation were observed. Those situations were very uncomfortable for the pedestrian, as vehicles passed very close to the VRU, often less than a meter away. The closest maneuver was at a distance of 28 cm.

4.2.2 Vehicle type related results

Different vehicles types have been observed during the data collection. Figure 4.20 represents the distribution of data with respect to the two different experimental settings (pedestrian walking on line line marking or curb). Data are represented also considering the factor of the oncoming vehicle present in the scene.

It has to be considered that the "long" vehicle types refers to both bus-drivers and truck drivers. These two categories are usually behaving in a different way (after a manual annotation of the events), thus the clearance's value should be considered keeping in mind such possible nested difference in drivers behaviour.

It is worth highlighting that, in the following, the results will be related solely to the small vehicle category, being this the larger subset available.

4.2.3 Distance related results

The safety metric that has been analyzed is the minimum clearance (leeway) at which a car is passing the pedestrian during the overtaking manoeuvre. Two main factor has been proved to

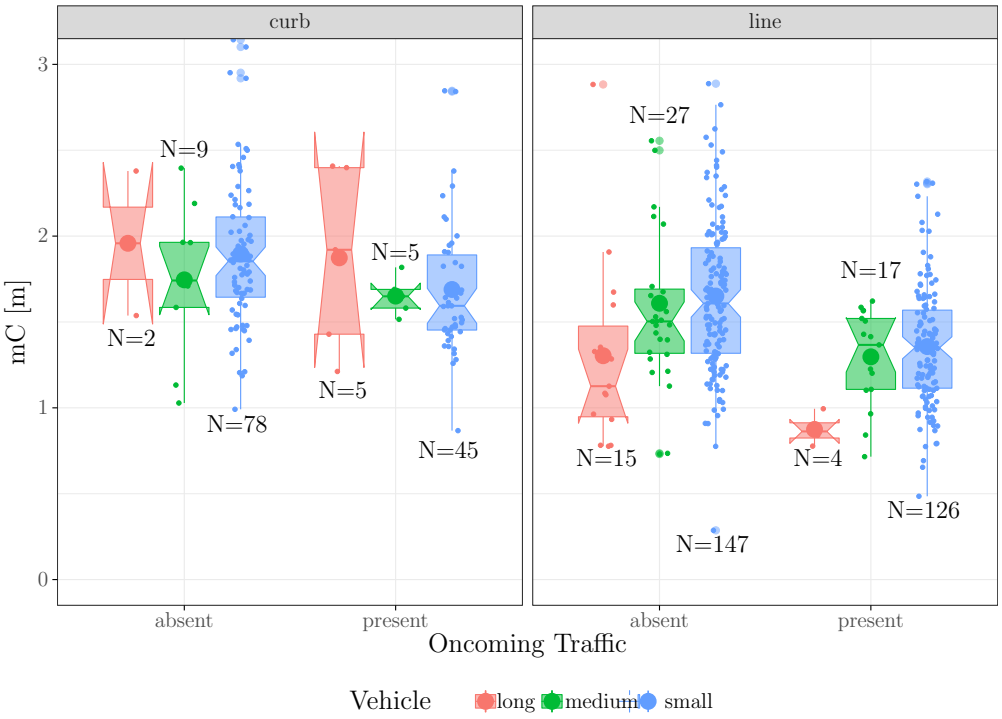

Figure 4.20: *Field test data grouped by pedestrian walking position, representing the minimum lateral clearance (mC) between vehicle and pedestrian. The factor related to the oncoming traffic is also considered.*
Boxplots represent also the mean values with a colored dot sign. The total number of events in each scenario is also reported

influence the driver behaviour, with a confidence interval (C.I.) of 95%.
These are:

- oncoming traffic presence
- pedestrian walking direction

Whenever an oncoming vehicle is present in the scene, drivers need to squeeze the comfort boundary with the pedestrian, keeping a distance, within a comfortable level, also with respect to the oncoming vehicle. Conversely drivers are willing to increase the lateral distance to the pedestrian. Data are displayed in Figure 4.21.

In Figure 4.22 data are factorized based on the pedestrian walking direction. Distinction is given for the pedestrian walking position.

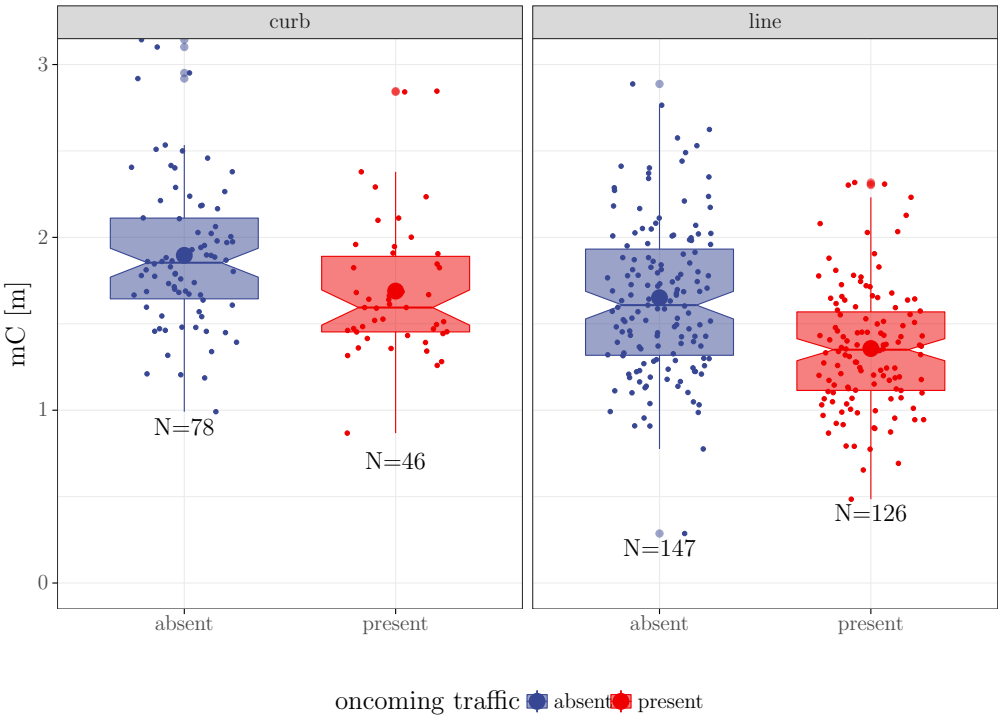

Figure 4.21: *Minimum lateral distance between car and pedestrian while passing (mC). Data refers to "small" overtaking vehicles, showing the influence of the oncoming traffic factor. Data are split up based on the pedestrian walking position. The mean value is represented by a circle shape*

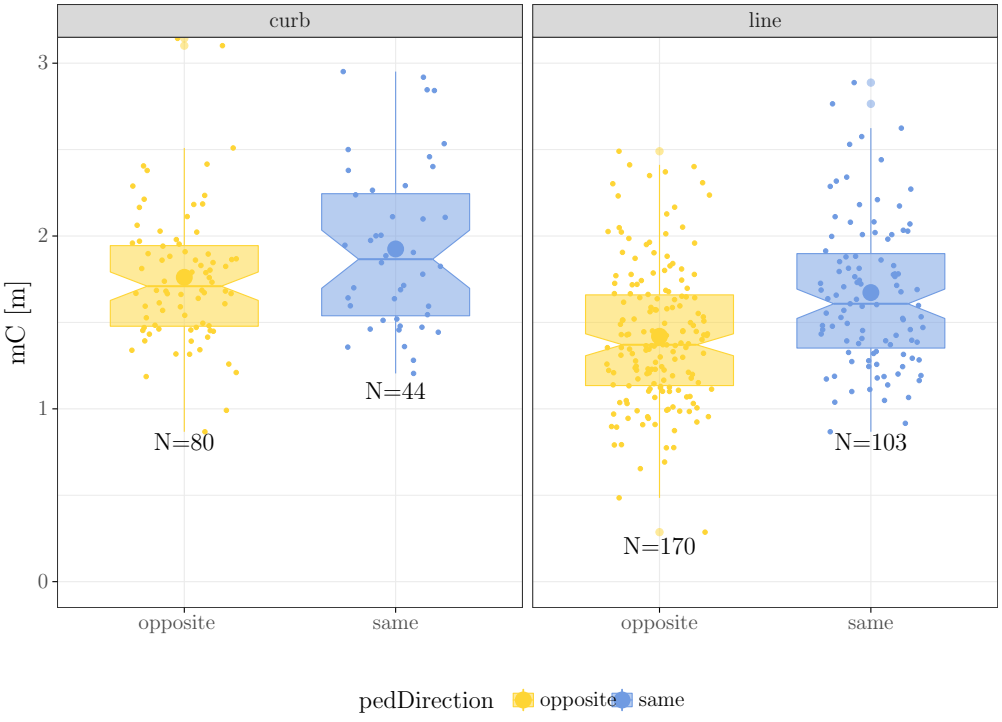

Figure 4.22: *Minimum lateral distance between car and pedestrian while passing (mC). Data refers to "small" overtaking vehicles, showing the influence of the pedestrian walking direction factor. Data are split up based on the pedestrian walking position. The mean value is represented by a larger circle shape*

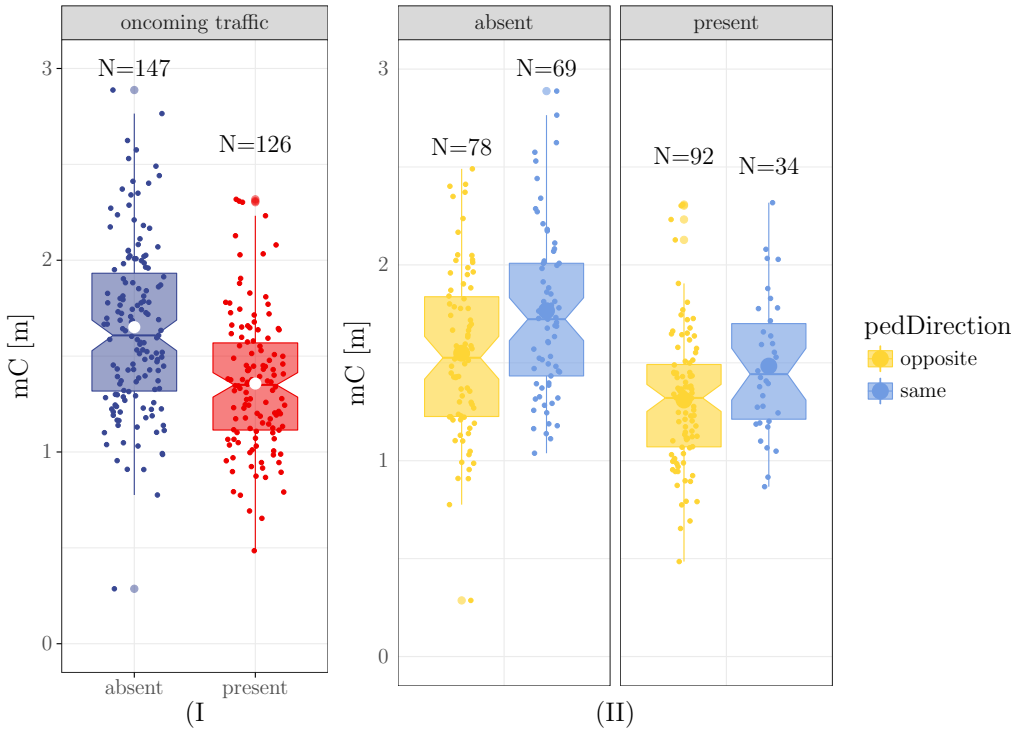

Figure 4.23: *Minimum lateral distance between car and pedestrian while passing (mC). Data refers to "small" overtaking vehicles with the VRU walking on the painted road markings. (I) Data are grouped based on the factor of the oncoming traffic. (II) The influence of the pedestrian walking direction given the oncoming traffic presence or absence is displayed. The mean value is represented by a larger circle*

It stands out that drivers are used to reduce the comfort zones if an oncoming vehicle is present in the scene and if a pedestrian is walking in the opposite direction of the car, facing the traffic.

Since the scenario in which the pedestrian was walking on the line markings highlights a lower comfort boundary (mC) kept by the car while passing, a closer look to this subset of data is provided.

In Figure 4.23 boxplots represents mC for drivers when overtaking a VRU walking on the lane edge (painted line). The oncoming factor and the nested factor of the pedestrian walking direction are considered.

A cumulative distribution of the minimum clearance (mC) for the small vehicle type and for the pedestrian walking closer to the road center are represented in Figure 4.24 and Figure 4.25.

Thus far, CZB has been reported mainly related to the scenario in which the pedestrian was walking on the "line" considering "small" vehicles. However, in order to understand whether the perceived pedestrian position (line or curb) could influence driver's decision about the lateral distance with respect to the road edge, in Figure 4.26 it is displayed at which distance different vehicles were located during the manoeuvre. Being the lane width 3.5 m and the pedestrian shift (out of the lane when walking on the curb) of 0.5 m, all measurement have been normalized with respect to the road line marking. Hence, given the vehicle width it has been possible to evaluate which vehicles were reaching and overstepping the road center line during the event.

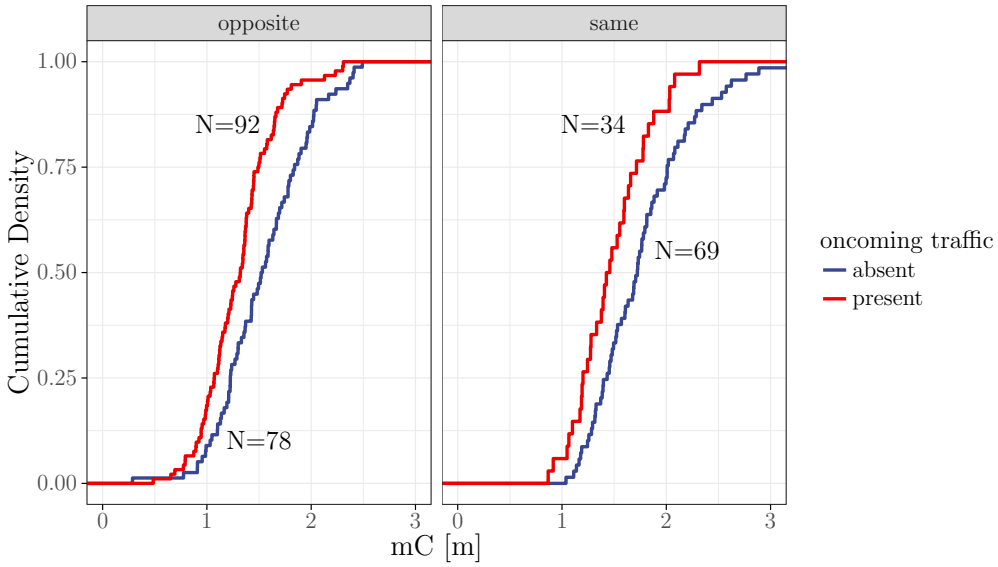

Figure 4.24: *Cumulative density function of the minimum clearance (mC) while passing the pedestrian, data are grouped by pedestrian walking direction and oncoming traffic presence in each direction. Data refer to "small" vehicle type and "on line" pedestrian position*

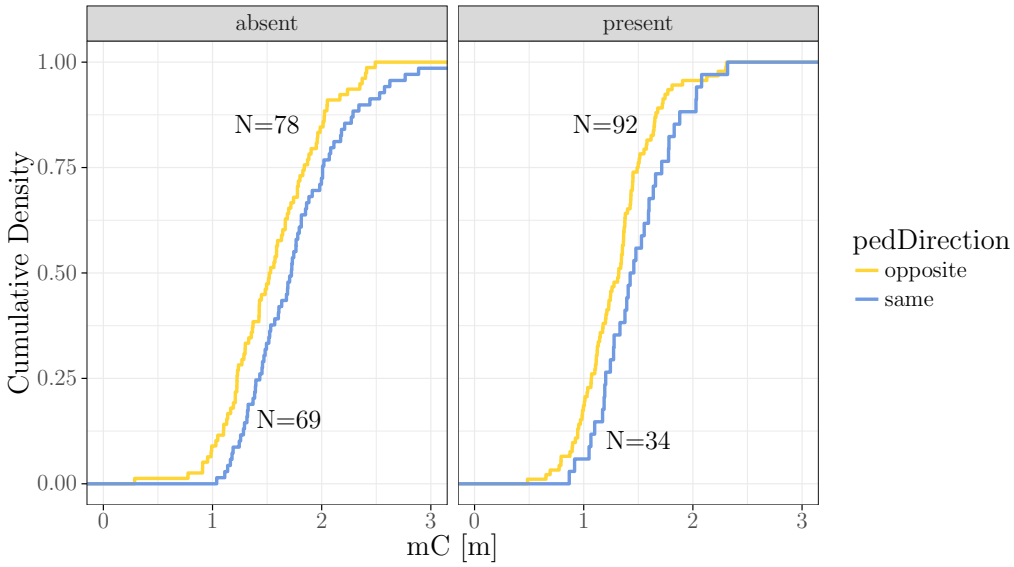

Figure 4.25: *Cumulative density function of the minimum clearance (mC) while passing the pedestrian, data are grouped by oncoming traffic presence and pedestrian walking direction being the oncoming traffic "present" or "absent". Data refer to "small" vehicle type and "on line" pedestrian position*

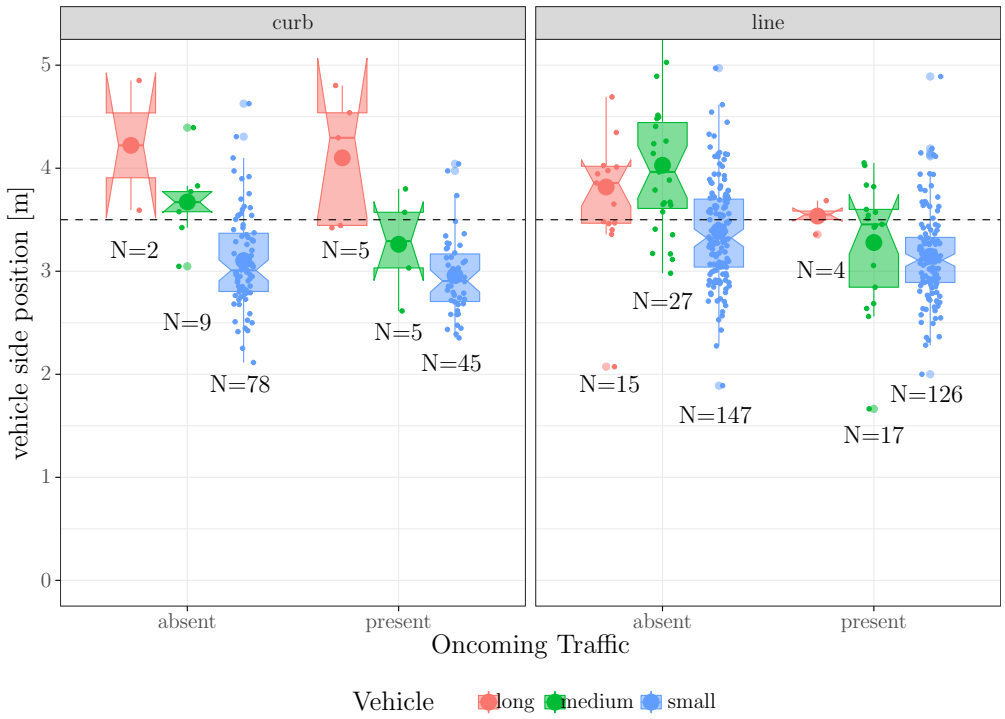

Figure 4.26: *Representation of the distance of the vehicle side (next to the driver) with respect to the road line marking. Dashed line represents the lane width.A distance below the lane width threshold represents a vehicle that performed the manoeuvre remaining in the lane. Conversely distances represents vehicles that overcome the center line during the event. Data are referred to all vehicle types and all measures are expressed in a reference frame fixed to the road painted markings*

4.2.4 Speed related results

In Table 4.9 "small" vehicle type data are summarized for both vehicle passing speed and lateral clearance.

Table 4.9: Minimum clearance (mC) and passing speed $V_{passing}$, data are grouped by oncoming traffic and pedestrian walking direction factors

			mC	$V_{passing}$
Oncoming traffic present	**Same walking direction N =34**	Mean [m-km/h]	1.48	57.66
		std	±0.35	±9.53
	Opposite walking direction N =92	Mean [m-km/h]	1.31	55.96
		std	±0.35	±7.47
Oncoming traffic absent	**Same walking direction N =69**	Mean [m-km/h]	1.77	60.11
		std	±0.46	±8.92
	Opposite walking direction N =78	Mean [m-km/h]	1.55	58.19
		std	0.43	±8.90

Following the same factorization approach of the safety metric "mC" the vehicles speed distribution are represented hereafter. However data are displayed in order to highlight possible relationships between the vehicle speed and the clearance while passing the pedestrian.

In Figure 4.27 data are grouped considering the oncoming traffic presence, while in Figure 4.28 the grouping factor is the pedestrian walking direction. Data refer to events in which the pedestrian was walking on the line markings. While Figure 4.29 and 4.30 refer to VRU walking on the curb.

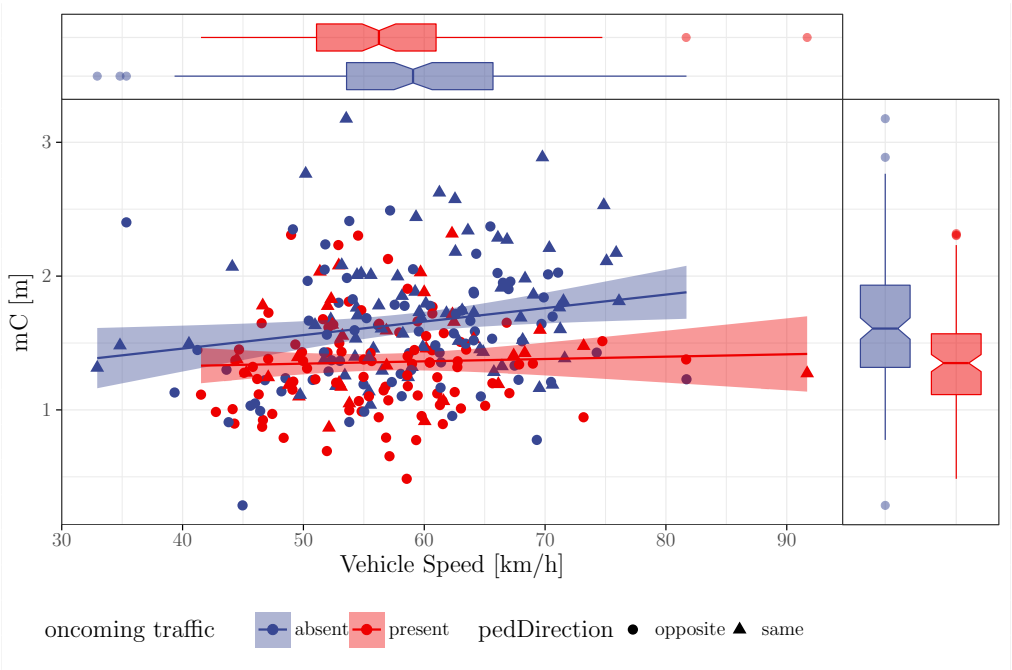

Figure 4.27: *Minimum clearance (mC) related to the vehicle speed while passing. Data are grouped by the oncoming traffic factor. Box plots refer to the mC (on the side) and to the vehicle speed (on top). Scattered point shapes are associated to the pedestrian walking direction. The event represented related to the pedestrian walking on the "line"*

Figure 4.28: *Minimum clearance (mC) related to the vehicle speed while passing. Data are grouped by the pedestrian walking direction factor. Box plots refer to the mC (on the side) and to the vehicle speed (on top). Scattered point shapes are associated to the oncoming traffic presence. The event represented related to the pedestrian walking on the "line"*

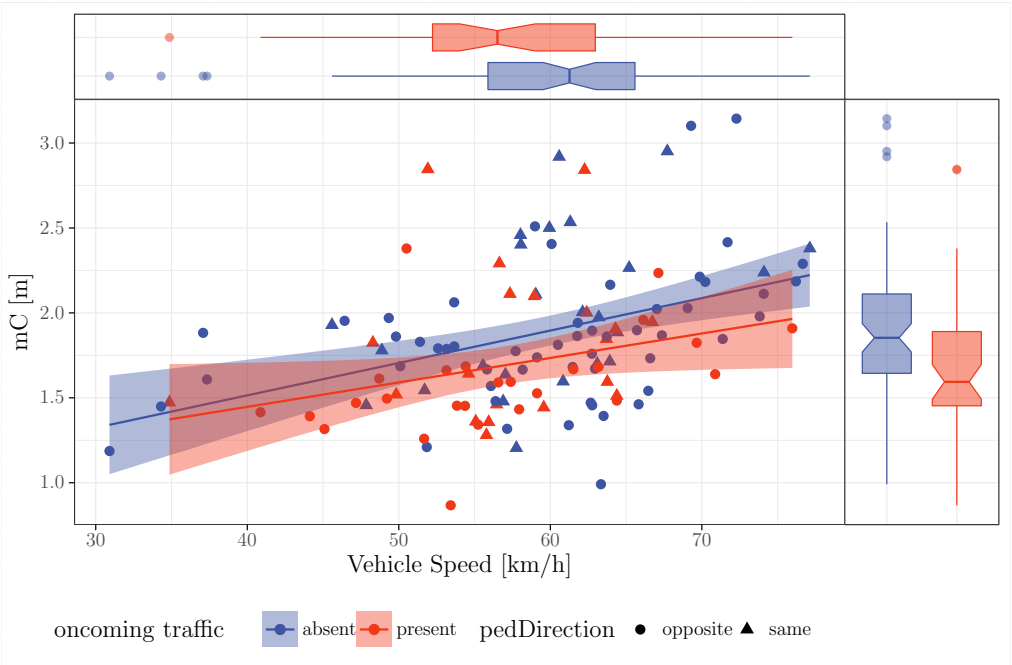

Figure 4.29: *Minimum clearance (mC) related to the vehicle speed while passing. Data are grouped by the oncoming traffic factor. Box plots refer to the mC (on the side) and to the vehicle speed (on top). Scattered point shapes are associated to the pedestrian walking direction. The event represented related to the pedestrian walking on the "curb"*

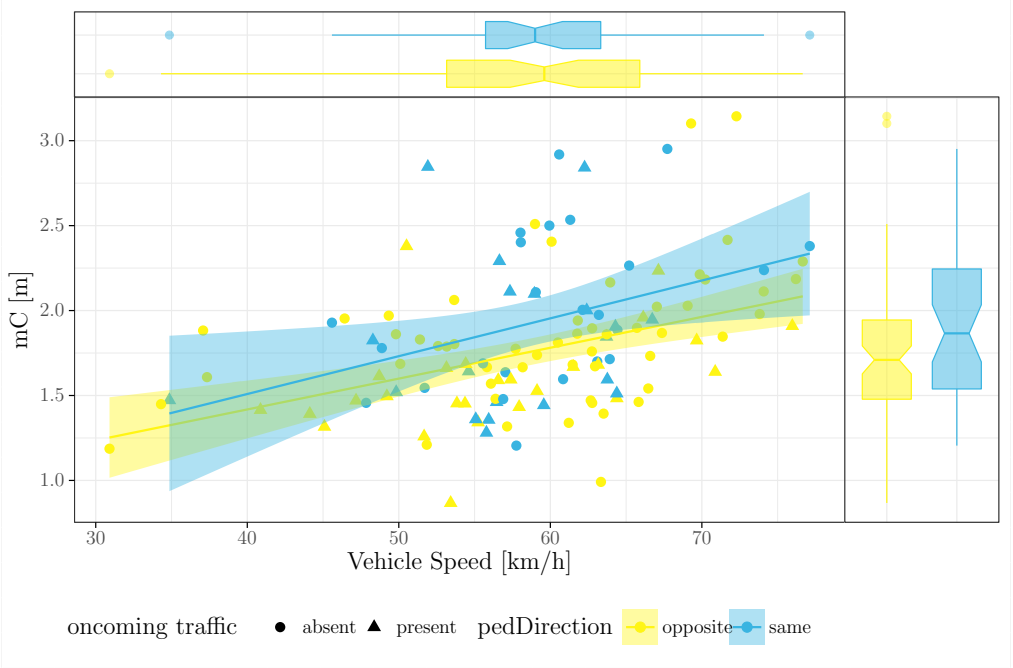

Figure 4.30: *Minimum clearance (mC) related to the vehicle speed while passing. Data are grouped by the pedestrian walking direction factor. Box plots refer to the mC (on the side) and to the vehicle speed (on top). Scattered point shapes are associated to the oncoming traffic presence. The event represented related to the pedestrian walking on the "curb"*

4.3 Driver model

The application of the Bayesian regression theory has allowed to get three main driver models. Results are presented in the following subsections, considering that the naturalistic driving study provides a model for TTC and the field test collection has been adopted to evaluate a model of the mC and the vehicle passing speed.

4.3.1 Time to collision

The results will be presented by mean of a predictive check of the model fit to the data, and through a four test statistic approach. The best formula to fit the model has been:

$$TTC \sim oncomingTraffic + pedestrianDirection + vehicleSpeed + (1|DriverID) \quad (4.1)$$

The representation of the actual data and the posterior distribution are presented in Figure 4.31. It has to be considered that the adopted data refer only to the "flying" strategy, in which driver react solely by steering control (for data visualization refer to Figure 4.12). Accelerative manoeuvres are not considered since drivers are adjusting the vehicle speed during the phase one; thus reacting to the pedestrian presence before the steer-away is performed.

In order to show how the model is actually fitting the data, four test statistics (min, max, mean and standard deviation) are analyzed for the posterior predictive distribution and the observed data gathered from the UDRIVE database, as represented in Figure 4.32.

In detail, the model has been utilized in order to perform a comparison between corpora, to evaluate which factor could influence the driver behaviour. It has to be considered that the

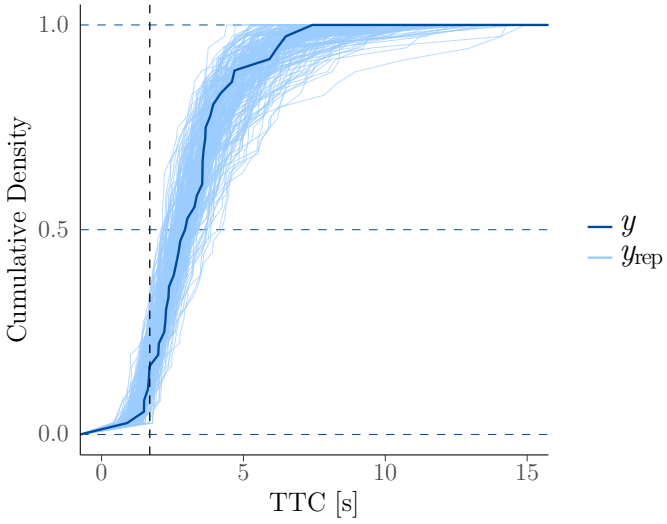

Figure 4.31: *Cumulative density of the actual data (y) together with 200 samples of the posterior predictive distribution (y_{rep}). The vertical dashed-line represents the vale TTC=1.7 adopted by Euro NCAP CPLA 25 test*

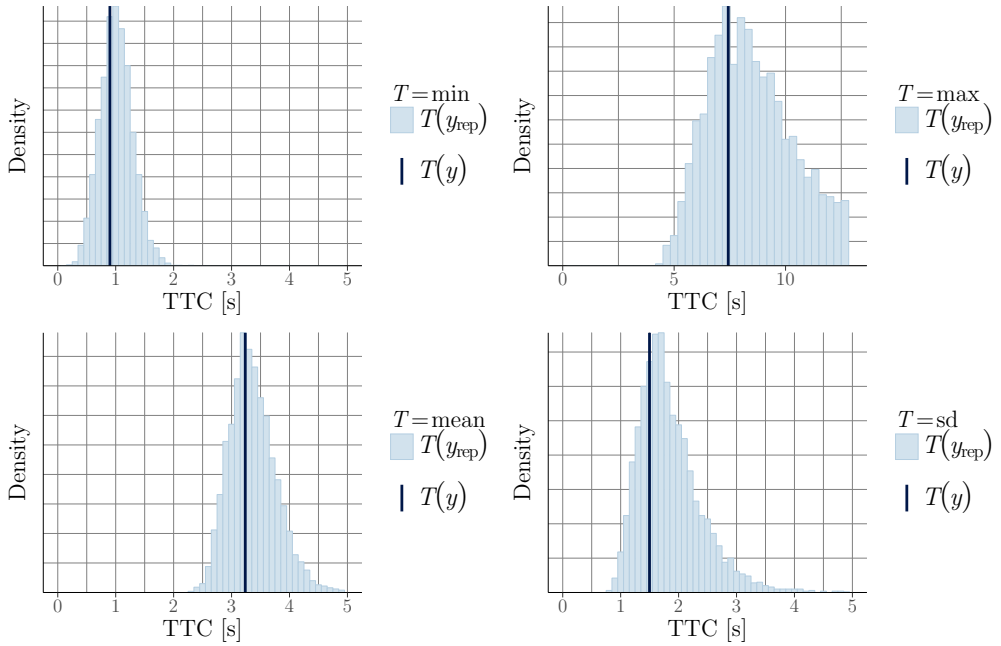

Figure 4.32: *Statistical test of min (top left), max (top right), average (bottom left) and s (bottom right). The observed data are represented by the dark blue bin (T_y) and the distribution of the predicted values from the model are represented by light blue bins ($T(y_{rep})$)*

factor “oncoming traffic” was showing a relevant effect in the time at which driver are used to start the steering manoeuvre, as represented in the distribution of median in Figure 4.33.

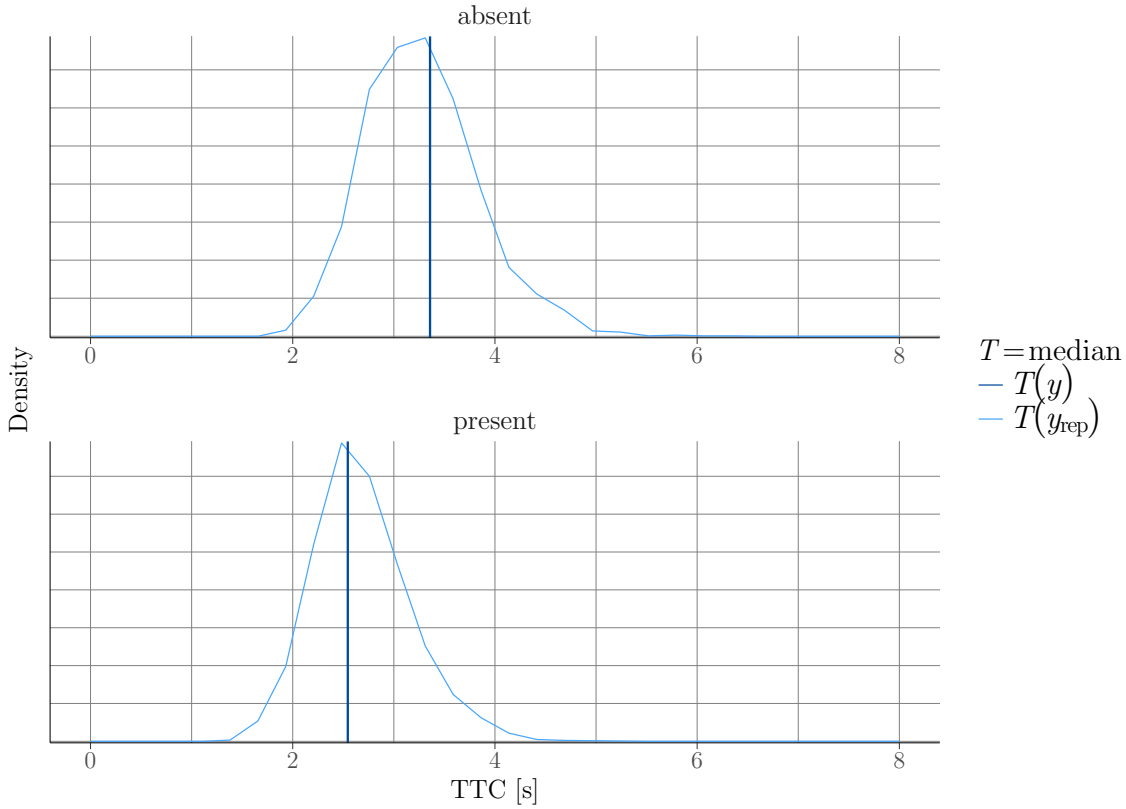

Figure 4.33: *Grouped distributions by oncoming traffic. Statistical test of the median value of the observed data (T_y) and posterior predictive distribution of the media value ($T(y_{rep})$)*

Hence a specific comparison of this effect in the data distribution has been evaluated. This has been done looking at the difference between distributions in which the oncoming traffic was present or absent. The histogram representation of the difference between oncoming_present and oncoming_absent is depicted in Figure 4.34a. Hence the model allows to state that the most credible time delay at which driver are starting the manoeuvre when an oncoming vehicle is present in the scene is -0.61 s 95% CI [-2.14,0.80], compared to the condition in which no oncoming vehicle is present in the scene. In other words: it is likely for drivers to anticipate the start of the steer away when no oncoming is present in the scene.

As well the pedestrian walking direction has been evaluated; the difference between distribution of the median value associated to the posterior is represented in Figure 4.34b. It is displayed that the time at which driver perform the steer away (to avoid a possible collision) is not actually influenced by the pedestrian walking direction. In other words, the Bayesian model allows to state that no change in behaviour is shown based on walking direction (0.04 s[-1.63 1.43]).

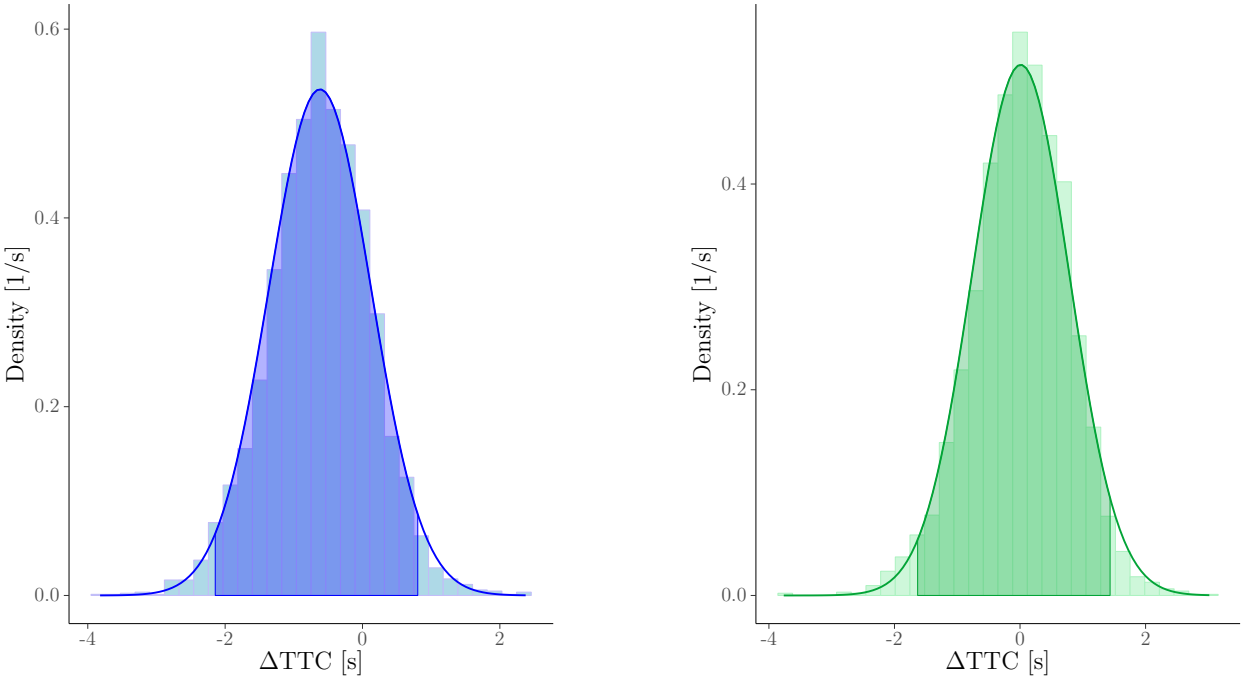

(a) *Difference of median distribution between TTC with oncoming traffic, in the adjacent lane, absent VS oncoming traffic present*($y_{rep\_present} - y_{rep\_absent}$)

(b) *Difference of median distribution between TTC with pedestrian going in the same VS opposite direction of the traffic* ($y_{rep\_same} - y_{rep\_opposite}$)

Figure 4.34: *Factor influence on driver behaviour CZB [s]. The highlighted area represents the 95% credible interval*

4.3.2 Minimum lateral clearance

Considering the data collected on the Swedish road, in order to compute the driver model of the lateral clearance, the scenario has been limited to the condition in which the vehicle was a car and the pedestrian was walking on the road line.

The model that resulted to give the best fit has been characterized by the equation:

$$mC \sim oncomingTraffic + pedestrianDirection + vehicleSpeed \tag{4.2}$$

In order to exploit the benefit of the adoption of the Bayesian approach, it has been possible to adopt as prior distribution the model fitted to the mC values related to the NDS data. Hence, this is used to suggest to the model the prior knowledge related to the driver CZB while passing.

The fit of the model to the actual data is represented by a cumulative distribution in Figure 4.35a. In the figure it is possible to appreciate which is the distribution with marked the 90^{th} and 10^{th} percentile.

The model fit has been evaluated following the same approach presented in the Figure 4.32 for the TTC variable, and it has been proved to be suitable in representing the actual observations.

Moreover the influence of the oncoming traffic factor and pedestrian direction are evaluated, following the same approach presented for the NDS model.

The analysis shows that compared to the scenario in which no oncoming is detected in the scene, drivers are more likely to stay closer to the pedestrian of about -0.285 m (95% CI

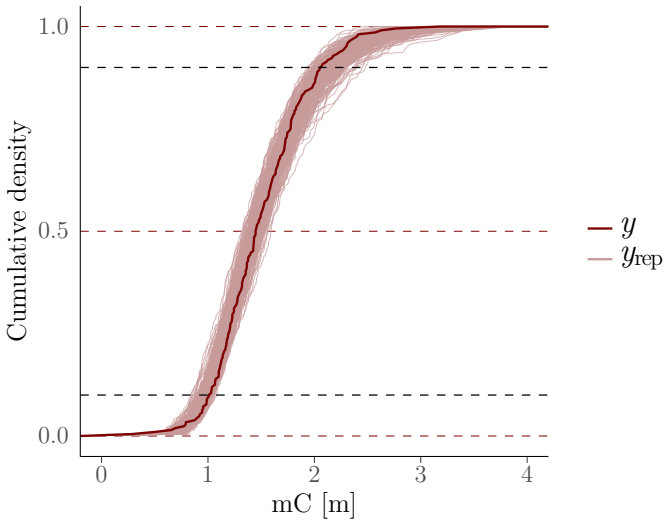

(a) *Cumulative density of the actual data (y) together with 200 samples of the posterior predictive distribution (y_{rep}). Observation refer to small vehicle type, with a pedestrian walking on the line marking*

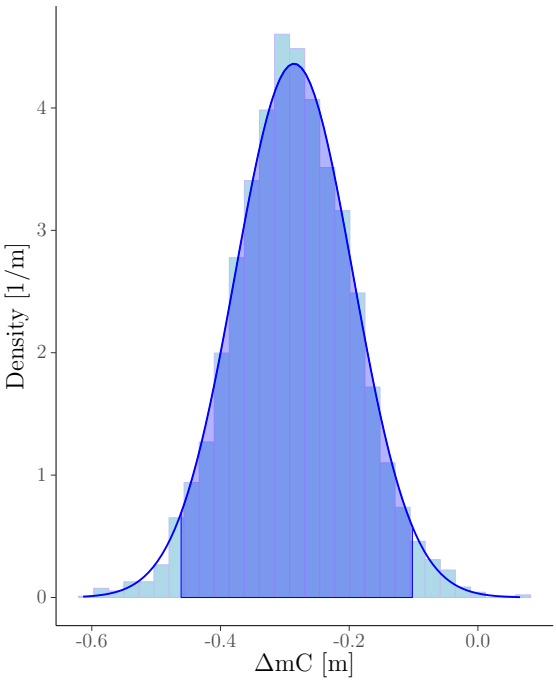

(b) *Difference of median distribution between mC with oncoming traffic present VS oncoming traffic absent ($y_{rep\_present} - y_{rep\_absent}$)*

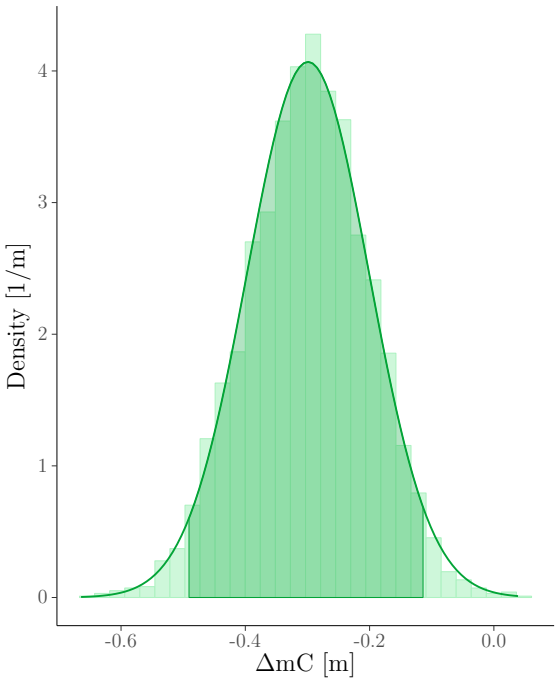

(c) *Difference of median distribution between mC with pedestrian in the opposite VS same direction of the traffic ($y_{rep\_opposite} - y_{rep\_same}$)*

Figure 4.35: *Factor influence on driver behaviour CZB [m]. The highlighted area represents the 95% credible interval. Observation refer to small vehicle type, with a pedestrian walking on the line marking*

[-0.47,-0.11]) when an oncoming vehicle is approaching. This result is represented by the data comparison between corpora in Figure 4.35b.
In Figure 4.35c the comparison between the pedestrian walking direction is represented. When the VRU was facing the traffic drivers were passing at a lower distance of about -0.30 m (95% CI [-0.49,-0.12]).

4.3.3 Vehicle speed

To get a descriptive model of factor influencing driver behaviour while passing a pedestrian, data have been separated for pedestrian walking on line marking and for pedestrian being out of the road.

The models that resulted to give the best fit has been characterized by the equation:

$$vehicleSpeed \sim oncomingTraffic + pedestrianDirection \tag{4.3}$$

Representation for the scenario in which a pedestrian is walking on the line is given in Figure 4.36

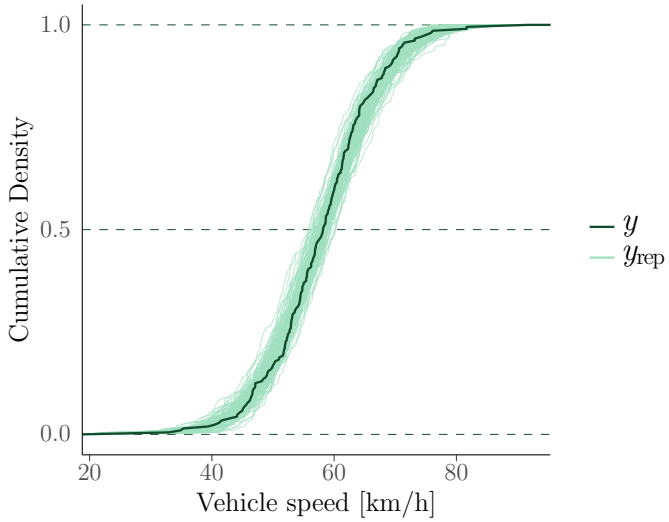

Figure 4.36: *Cumulative density of the actual data (y) together with 200 samples of the posterior predictive distribution (y_{rep}). Observation refer to small vehicle type, with a pedestrian walking on the line marking*

Results related to factor's influence on driver behaviour are represented in Figure 4.37 for both pedestrian walking scenarios. Figure 4.37a shows how the oncoming traffic forces drivers to reduce the speed. The speed reduction is about -2.8 km/h 95% CI [-6.3,0.6] (see Figure 4.37a). On the contrary, when the VRU is walking in the same direction of the vehicle driver are used to pass with a slightly higher speed: 1.6 km/h 95% CI [-1.8,5.1] (see Figure 4.37b). The factors' influence on driver choice of the passing speed are more marked for the condition in which a pedestrian is detected on the road curb. The oncoming traffic presence makes driver to reduce the speed of -4.4 km/h 95% CI [-9.0,-0.1], as represented in Figure 4.37c. As well, drivers are used to reduce the speed of -2.9 km/h 95% CI [-7.3,1.6], when a pedestrian is going in the same direction of the car (see Figure 4.37d).

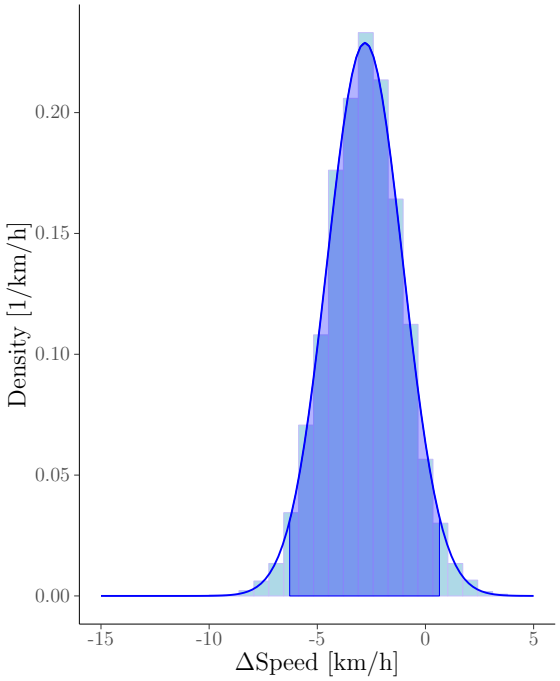

(a) *Difference of distribution between vehicle speed with oncoming traffic present VS oncoming traffic absent*($y_{rep\_present} - y_{rep\_absent}$)

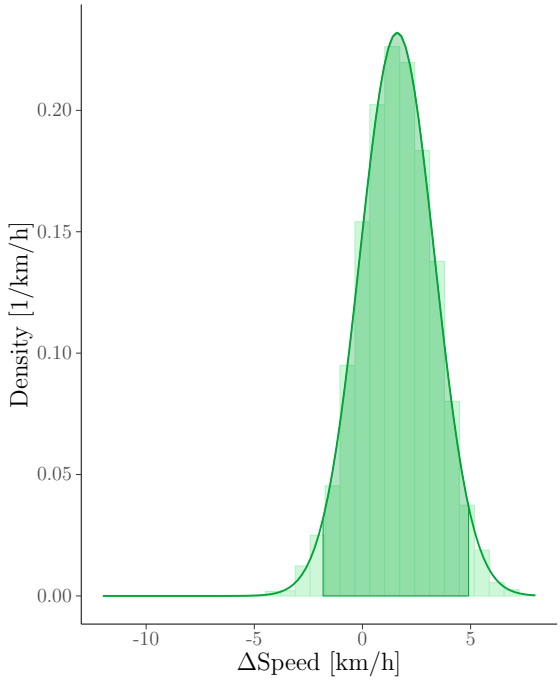

(b) *Difference of distribution between vehicle speed with pedestrian in the same VS opposite direction of the traffic* ($y_{rep\_same} - y_{rep\_opposite}$)

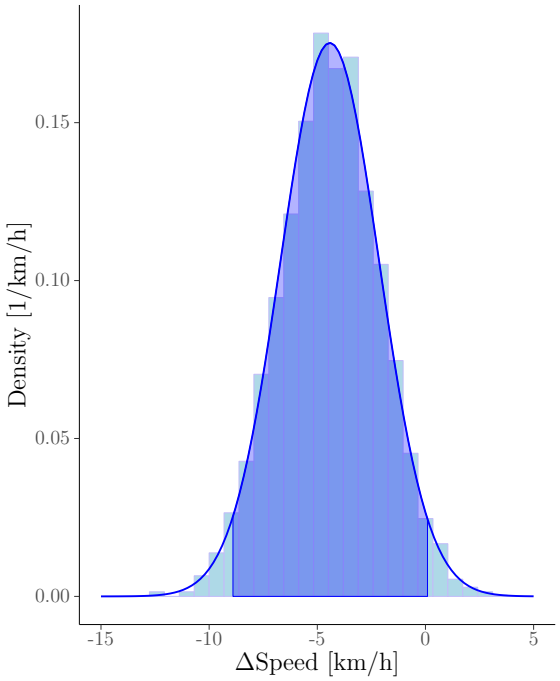

(c) *Difference of distribution between vehicle speed with oncoming traffic present VS oncoming traffic absent*($y_{rep\_present} - y_{rep\_absent}$)

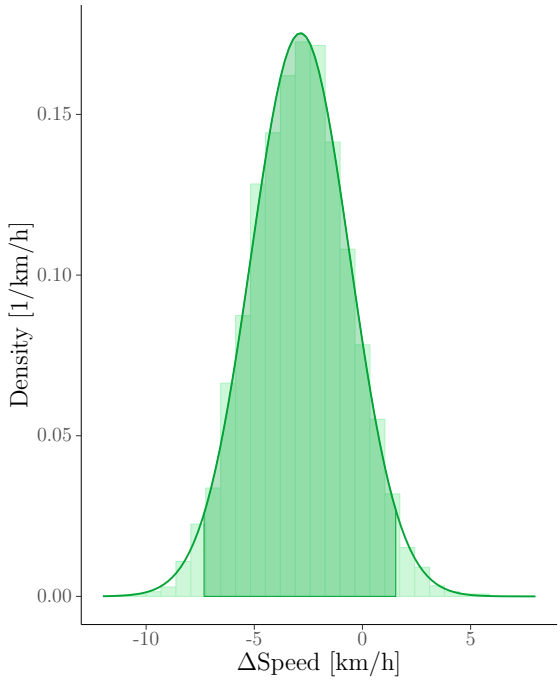

(d) *Difference of distribution between vehicle speed with pedestrian in the same VS opposite direction of the traffic* ($y_{rep\_same} - y_{rep\_opposite}$)

Figure 4.37: *Factor influence on driver behaviour. The highlighted area represents the 95% credible interval. Observation refer to small vehicle type, with a pedestrian walking on the line marking (top) and curb (bottom)*

4.4 Comparative analysis

This section aims to present results comparisons between safety metrics evaluated by means of the two data sets gathered in this study. In the Table 4.10 the minimum lateral clearance (mC) is compared between the pedestrian overtaking events in the NDS and FT. The p-values acquired via two-sample t-test on the data gathered in this study is also listed. The t-test rejects the null hypothesis for all different factors characterizing the scenario of the overtaking manoeuvre. Confidence intervals (c.i.) of the difference of the population means are listed in the table. It is worth highlighting that in the t-test the null hypothesis considers that, for each respective data set, the mean of the measures have the same average value and equal but unknown variances. figure 2

Table 4.10: Comparison of the minimum clearance (mC) between naturalistic data (NDS) and field test experiment (FT). Samples dimension are provided by mean of $N_{Dataset}$.Significant p-values are bold in the table

			mC_{NDS}	mC_{FT}	**p**	**c.i.**
in road position	**Oncoming traffic present**	Mean [m]	0.91	*1.35*	**<0.001**	[-0.61;-0.28]
	$N_{NDS} = 22$ $N_{FT} = 99$	std	±0.33	*±0.35*		
	Oncoming traffic absent	Mean [m]	1.04	*1.65*	**<0.001**	[-0.78;-0.44]
	$N_{NDS} = 35$ $N_{FT} = 109$	std	±0.42	*±0.45*		
	Same walking direction	Mean [m]	1.01	*1.68*	**<0.001**	[-0.85;-0.51]
	$N_{NDS} = 37$ $N_{FT} = 82$	std	±0.43	*±0.42*		
	Opposite walking direction	Mean [m]	0.95	*1.40*	**<0.001**	[-0.63;-0.26]
	$N_{NDS} = 20$ $N_{FT} = 126$	std	±0.31	*±0.41*		

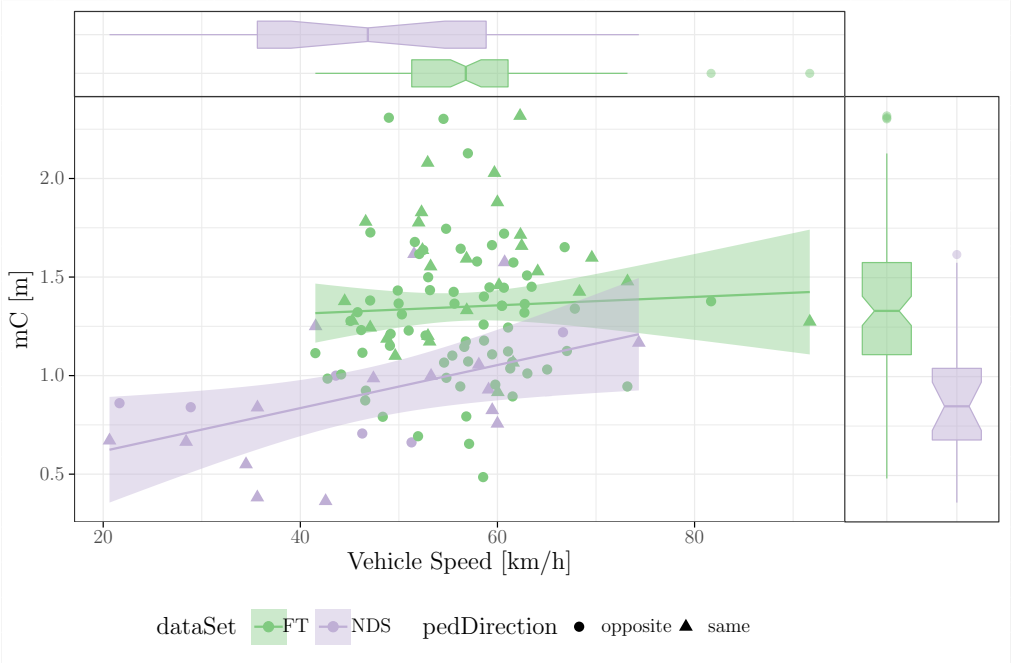

Figure 4.38: *Minimum clearance (mC) and vehicle speed while passing the pedestrian. Data refer to the specific scenario in which an oncoming vehicle was present in the scene.*

5 Discussion

In this chapter, implications of the research activity are presented considering the complementarity of the two data sets analyzed (NDS and FT). The results will be discussed in the Section 5.1. Driver behaviour comparison for the driver interaction with different VRUs (bicyclists and pedestrians) will be outlined in Section 5.2 for the two distinct data sets. Bicycle data were gathered during previously conducted studies [24][25]. In Section 5.4 general remarks associated to each one of the two data sets (NDS and FT) will be presented. Eventually limitations of the project will be outlined (Section 5.4.3).

5.1 Answer to research questions

This thesis project has been based on five main research questions (see Section 1.1.1), for which some hypotheses have been formulated. Thus, the following paragraphs aim at presenting the main findings related to each one of these hypothesis associated to a specific factor of the overtaking scenario.

5.1.1 Hypothesis one

As hypothesized in Section 1.1.1, the factor related to the pedestrian walking position has been assumed influencing the clearance given by the car while performing the manoeuvre. Actually the hypothesis has been verified considering results of the field test data collection, as represented in Figure 4.20, Figure 4.21, Figure 4.22. The main reason for this evidence has been associated to the physical shift of the pedestrian, being he walking away from the road edge (Line marking). Therefore safety can be considered as increased since the leeway is significantly ($C.I. = 95\%$) larger.

The same trend is represented also by the UDRIVE data set. Drivers give a lower clearance to pedestrians that are walking along the road edge. However due to low amount of events in which a driver has been annotated as walking on the curb (N = 6) no actual dependency can be highlighted.

5.1.2 Hypothesis two

The factor related to the pedestrian walking position has been assumed to affect the steering away phase (phase two) during the overtaking manoeuvre. In particular it has been hypothesized that when the pedestrian was walking outside of the road boundaries (which are limited by the line markings) drivers would have not performed any steering away.

From the UDRIVE analysis the steering away phase has been observed for all events. Hence, showing a behaviour that is not consistent with the hypothesis. However the end of the phase two (mDS) was influenced by the pedestrian lateral position with strong evidence, suggesting that the phase two is influenced by this factor (see Table 4.6). With regard to the collection on the Swedish road, no direct evaluation of the overtaking phases has been possible. However, it has to be considered that during the phase two, a driver is deciding which has to be the vehicle position in the lane with respect to the road line markings. Therefore the pedestrian position influence on this driver choice has been evaluated.

When a pedestrian is closer to the center, motorists are driving closer to the road center line, meaning that the perceived position is playing an important role on the trajectory planning (See Figure 4.26). Thus, when a pedestrian is outside the road, walking on the curb, drivers are keeping a lower distance to the road line marking. Therefore this implies that the steering away phase is influenced, having an impact on the driver path planning.

Moreover, the pedestrian position is playing an important influence on the driver's choice of the overtaking speed, with an higher speed for pedestrian located away from the road center. As well, in this second scenario, a clear trend can be noticed between the lateral clearance and the vehicle (small and medium) speed, with a larger clearance at higher speed (see Figure 4.29).

Therefore, as answer to the research question it has to be said that drivers still perform the steering away phase, but the pedestrian walking position is playing a prominent role in the vehicle position in the road with a tendency of having higher speed when the pedestrian is outside the lane.

5.1.3 Hypothesis three

The pedestrian walking direction has been linked to the possibility of having an "eye-contact" during the overtaking event. It has been assumed that the visual contact during the interaction would have affected the minimum clearance while passing the pedestrian. Results related to the field test experiment show that a pedestrian walking in the opposite direction of the vehicle is influencing the driver behaviour with a strong evidence. This is verified only in the scenario in which the pedestrian was walking on the line marking (see Figure 4.35c), and therefore directly present on the road. When the VRU is facing the traffic the leeway decreases, supporting the hypothesis. On the other hand, when a driver perceives that the pedestrian is walking in the same direction, he/she is willing to keep a larger passing distance (Figure 4.22 and Figure4.25). The same trend is observed also in UDRIVE (Figure 4.7a), only for the condition in which no oncoming traffic was present in the scene. This could be associated to the low number of events analyzed.

This behaviour alteration in the driver manoeuvre could be associated to driver intention in keeping a larger comfort boundary for the pedestrian when he/she cannot directly perceive the approaching vehicle. This with the purpose of increasing the comfort felt by the pedestrian in this scenario. The eye contact influence on drivers' comfort boundary has been shown to play an important role also in intersection scenario by Ren et al. in [90]. In the crossing scenario eye-contact influences the drivers' reaction with an higher TTC, thus giving drivers more time to react. In the longitudinal scenario (here analyzed) it is the lack of eye-contact that makes drivers to keep a larger passing distance to the pedestrian. Moreover, the pedestrian walking direction seems to influence also the speed reduction during the approaching phase, as suggested by Figure 4.11.

It is normal recommendation to face the traffic when no dedicated lane is available for pedestrians, and therefore driver could be influenced by the event not being very usual. However, in the French data analysis (associated to the naturalistic database) more than 60% of events occurred with pedestrian going in the same direction of the car.

It has to be noticed, also, that the scenario in which the VRU was walking in the same direction of the car was felt really uncomfortable by the pedestrian during the experiment.

5.1.4 Hypothesis four

In previous studies the oncoming traffic has been shown to be one of the main important factor in drivers' performance [19] [23]. In line with prior findings, it has been hypothesized that the traffic travelling in the opposite direction with respect to the overtaking vehicle would have affected the driver behaviour in the longitudinal interaction with pedestrian as well.

Results reveal that when the oncoming traffic is present, drivers are more likely to reduce the lateral clearance between the EGO vehicle and the VRU (see Figure 4.7b and Figure 4.7a for NDS; see Figure 4.23 and Figure 4.24 for FT). Drivers need to find a trade-off between the distance to the pedestrian and the distance to the oncoming traffic. Considering the field test results, distributions are strongly affected by the oncoming traffic factor (see Figure 4.35b). Considering UDRIVE a clear trend is present in accordance to the field test data.

5.1.5 Hypothesis five

As a response to the fifth research question it has been assumed that the oncoming traffic presence would have affected drivers' choice about the overtaking speed. The influence on the passing speed has been shown influenced by the oncoming traffic, with a lower speed whenever an oncoming vehicle was present in the scene (see Figure 4.37a) The behaviour revealed to be more marked when a pedestrian was walking on the curb (see Figure 4.37c).

As well, the oncoming traffic is shown to affect drivers' decision of the steering away time instant, with a trend characterized by a lower TTC when a vehicle is present in the scene in the opposite lane and approaching the EGO vehicle (see Figure 4.4a). The driver model confirms this trend (see Figure 4.34a).

Furthermore it has to be considered that other factors, like the number of VRUs present in the scene (available in UDRIVE) or the road characteristics could play a significant role on the driver manoeuvre performance. Results associated to the number of VRU overtaken highlight a trend in drivers lateral distance selection (mC). The presence of more than one pedestrian in the scene makes driver choose a larger lateral distance as average tendency (mean = 1.29 m) compared to the events of a single VRU overtaken (mean = 0.98 m). However no influence on the driver behaviour has been associated to this factor.

5.2 Comparative analysis

In this section a comparison between safety metrics evaluated within this project is given. Analogies and contrasts with similar activities carried out in previous studies are provided, focusing on the discussion of possible influencing factors related to different VRUs.

5.2.1 Data comparison within this study

As represented in the Table 4.10, the t-test rejects the null hypothesis for all different factors characterizing the scenario of the overtaking manoeuvre.

Since the tests confirms the alternative hypothesis (populations with different means), it has to be stated that the two data sets contain populations with unequal means. Reasons for this could be related to differences in driver behaviour between the two countries, in which the

data were recorded. However, regarding the UDRIVE data, during the annotation process and video images evaluation it has been noticed that overtaking events were usually happening in secondary rural roads. Namely roads with a single lane for both traffic direction with rarely well define/painted line markings. These roads were characterized by a narrower lane width compared to the data collection performed in Sweden; nonetheless for French data it has not been possible to get reliable measurements of the lane width from vehicle sensor.

Moreover, it has to be considered that this dissimilarity is noticed also in the different speed at which car drivers overtook the VRUs. In UDRIVE data set the average vehicle speed was lower than the speed in the field test collection, with a statistical significance ($p<0.001$ from double t-test). Thus, the two data sets differ both in minimum lateral clearance (see Table 4.10) and in passing speed (mean $V_{NDS} = 50.2km/h$ and mean $V_{FT} = 58.1km/h$) during the overtaking event. Figure 4.38 illustrate previous statements.

The road characteristics could be considered as the main factor causing this difference in behaviour. On the other hand, such a difference could also be related to a possible habit of drivers in UDRIVE in meeting pedestrian on the roads in which the event occurred.

5.2.2 Data comparison with previous studies

This thesis project can be related to previous activities which analyzed driver interaction with a different road user. Therefore, in the following a comparison between driver interrelation with pedestrians and bicyclists is proposed.

Data comparison with NDS bicycle study

Considering that a previous study has been performed over the same NDS database by Nero in [25] a CZB comparison is represented in Table 5.1. This shows a comparison of safety relevant metrics, when a driver is in interaction with a pedestrian or a cyclist. In detail the minimum distance at which drivers start the steer-away phase and the minim clearance during the event are represented.

It stands out that drivers are used to perform the steering control at a larger distance when overtaking a bicycle, especially when no oncoming traffic is present. This could be related to the lower relative speed between car and cyclist, with drivers willing to anticipate the manoeuvre when no other road user is present in the scene. As well, this anticipation of the manoeuvre could be associated to the fact that drivers do not expect the bikes to move much laterally, compared to a pedestrian that can have an erratic behaviour. A similar behaviour is instead shown when the oncoming vehicle is considered in the scenario.

Considering the minimum lateral clearance between drivers and VRUs, results are similar for both interactions when the oncoming traffic is present in the scene. On the other hand, drivers are used to pass at a larger clearance cyclist when no oncoming traffic is detected. Also, as average value, drivers reduce the clearance when they perform flying manoeuvres, behaving in the same way when interacting both with pedestrians and bicyclist.

Table 5.1: Comparison of the comfort zone boundaries between pedestrian an bicyclist evaluated from UDRIVE database. Data refers to the distance at which driver start to steer away (mAG at end of phase one) and minimum lateral clearance while passing (mC)
Bicycle data from Table C.6 in [25]

			mAG_{ped}	mAG_{bic}	mC_{ped}	mC_{bic}
Accelerative	**Oncoming Traffic Present**	Mean [m]	39.8	*39.9*	0.90	*1.04*
	$N_{ped} = 17 \quad N_{bic} = 17$	std	±24.0	*±33.7*	±0.34	*±0.73*
	Oncoming Traffic Absent	Mean [m]	50.6	*64.7*	1.20	*2.00*
	$N_{ped} = 13 \quad N_{bic} = 15$	std	±41.3	*±56.7*	±0.54	*±0.71*
Flying	**Oncoming Traffic Present**	Mean [m]	46.5	*42.0*	1.00	*0.97*
	$N_{ped} = 20 \quad N_{bic} = 8$	std	±20.9	*±36.1*	±0.53	*±0.69*
	Oncoming Traffic Absent	Mean [m]	89.86	*117.8*	0.96	*1.88*
	$N_{ped} = 12 \quad N_{bic} = 39$	std	±52.6	*±104.4*	±7.6	*±0.64*

With reference to the variable of the TTC a comparison with the bicycle study is summarized in Table 5.2. It stands out that driver steering reaction to avoid a possible collision with a pedestrian occurs before (higher TTC) than in the scenario in which a bicycle is present in the scene. In both driver-VRUs interaction it can be noticed an increase of the TTC when no oncoming vehicle is present.

Table 5.2: Comparison of the time to collision (TTC) between pedestrian an bicyclist evaluated from UDRIVE database.
Bicycle data from Table C.1 in [25]

			TTC_{ped}	TTC_{bic}
Accelerative	**Oncoming Traffic Present**	Mean [s]	2.8	*2.0*
	$N_{ped} = 17 \quad N_{bic} = 17$	std	±1.4	*±1.6*
	Oncoming Traffic Absent	Mean [s]	3.7	*2.5*
	$N_{ped} = 13 \quad N_{bic} = 15$	std	±1.7	*±2.0*
Flying	**Oncoming Traffic Present**	Mean [s]	3.5	*1.2*
	$N_{ped} = 20 \quad N_{bic} = 8$	std	±1.4	*±0.6*
	Oncoming Traffic Absent	Mean [s]	4.2	*3.0*
	$N_{ped} = 12 \quad N_{bic} = 39$	std	±2.0	*±2.8*

Data comparison with FT bicycle study

Considering that the same LiDAR used in this study was adopted in a previous data collection by Schindler and Bast [24], results associated to the minimum clearance are evaluated and discussed. Since for the pedestrian data collection all vehicles have been considered performing a flying manoeuvre, bicycle results are limited to this strategy. Moreover, given that the pedestrian walking direction has been shown likely to influence driver behaviour, the Table 5.3 is limited to the scenario in which a VRU is travelling in the same direction of the overtaking vehicle.

The leeway between the car side at the VRU is slightly higher for the pedestrian considering however that the influence of the oncoming traffic is nested in the results. In both conditions however the average distance is consistent with the recommended distance of 1.5 m. However, it has to be considered that the standard deviation is roughly a 0.5 m. This figure points out

that often drivers are prone not to respect such a recommendation, underestimating the severe consequences of a potential collision with both pedestrians and bicyclist.

Table 5.3: Comparison of the comfort zone boundaries between pedestrian an bicyclist evaluated from field data collection. Data refers to minimum lateral clearance while passing (mC). Pedestrian data refers to "small vehicle", with pedestrian walking on the line marking and in the same direction of the traffic. Bicycle data refer to "car" vehicle, cycling next to the road line mearking and in the same direction of the traffic

		mC_{ped}	mC_{bic}
Flying	Mean [m]	1.67	*1.60*
$N_{ped} = 103$ $N_{bic} = 127$	std	± 0.44	± 0.49

5.3 Implication on ADAS

The safety metrics that have been evaluated in this project could be associated to safety system assessment protocols, performed by independent organizations like Euro NCAP.

The TTC evaluated in this project (See Table 4.4 and Figure 4.4b) could suggest that the actual value of 1.7 s for CPLA 25 appears appropriate. Considering flying overtaking manoeuvres, in more than 95% of events drivers reacted by a steering control at a $TTC \geq 1.7s$.

Furthermore, with respect to the minimum clearance in the manoeuvre, a future autonomous steering system could be assessed bearing in mind that only 75% of drivers are used to give at least 1 m to the road user even if the recommend value is usually 1.5 m (see Figure 4.7b) even tough the road characteristic plays also an important role.

The annotated distance at which drivers start the steer away phase reached values above 150 m (see Figure 4.6a) suggesting possible challenges associated to object detection at such a long distance. As well, the correlation between the detection duration of the MobilEye ADAS system and the car speed highlight that sensor performances are strongly associated to vehicle kinematics (see Figure 4.19). Hence, possible system assessment at higher speed, than the actual present in CPLA, could be introduced.

The average speed reduction evaluated for accelerative events (Figure 4.11)could give information useful for self-driving vehicle path planning. As well the speed increase in the returning phase could suggest an expected level of acceleration by car occupant. The large amount of the recorded events as well as the flexible scenario setting during the collection have allowed to quantify the actual influence of a different factors on the driver behaviour.

Considering a possible assistance systems, aimed at supporting the driver in the longitudinal interaction with a pedestrian, some specific factor might be taken into account. First of all, the system should consider the actual position of the pedestrian in the scene. Drivers are used to go faster if a pedestrian is out of the road (on the curb), seldom overstepping the road center line (see Figure 4.26).

Moreover, supposing to have a warning system for lateral passing position of the car with respect to the pedestrian, the triggering threshold could be set differently for each one of the pedestrian walking direction. Larger distance should be set for a VRU detected walking in the same direction of the vehicle (see Figure 4.25) since drivers are likely to give less margin when a pedestrian is facing the vehicle (see Figure 4.35c). This system should also consider in its

algorithm the strong influence of the oncoming traffic presence (see Figure 4.35b), which has proved to affect both drivers' selection of passing distance and vehicle speed (see Figure 4.29).

Furthermore, the mean vehicle trajectory (see Figure 4.17) provides relevant useful information which could be suitable for automated vehicles path-planning, since it represents actual driver behaviour in a natural and non obtrusive driving setting.

5.4 Methodological considerations

As overall consideration it has to be outlined that the evaluation of human behaviour in driving is a complicated task, which can be influenced not only by physical parameters (CZB), but also by the drivers' psychological state. However, the project has been focused on the individuation of the overtaking manoeuvre and their classification using a Naturalistic study like UDRIVE as well as the implementation of a data collection platform that could be used for other purposes, and for which some improvements are suggested.

5.4.1 Naturalistic driving study

The UDRIVE data set has been an important source of information, allowing to have a general understanding of human behaviour while driving in a natural settings. However, if on one side the ecological validity of such data is unquestionable, on the other hand implications arise due to a non complete (360 deg) available observation of the scene.

Event individuation

Considering that UDRIVE is one of the largest data set available in Europe, the detection of the specific scenario under analysis has been a challenging activity. However, the approach that has been adopted resulted to be efficient albeit not optimal. Finding a number of events in the order of hundreds has allowed to highlight that the European database can be suitable also for investigation of the driver-pedestrian interaction in the longitudinal scenario.

The reason behind the choice of the analysis of simply the French data was mainly due to the limited amount of time allotted for this activity. Moreover, to avoid the introduction of possible variability in driver behaviour between different countries, the larger subset of events has been analyzed. However, the post-processing methodology has been implemented so to be applicable for both left-handed and right-handed traffic.

The disparity of event detection between different countries shall be deemed to need an explanatory statement. The main reason could be imputable to the participant selection process within the UDRIVE project. Namely, a larger number of French drivers were living in rural areas compared to other countries. Hence, they were subjected to meet more pedestrians while commuting. Therefore, this has not to be considered as an effect of the data reduction process adopted in this study. In this respect, the same trend has been noticed in previous study devoted to the analysis of the longitudinal scenario involving bicycles. Nevertheless, the disparity between different countries can be related also to different infrastructures available, since events in which a pedestrian was considered on a dedicated area (pavement or pedestrian lane) have been excluded.

Furthermore, within the subset of French overtaking events, a discrepancy associated to single driver manoeuvres has been noticed, with a single driver responsible for a considerable

number of events.

Annotations

Manual annotation has been a necessary step in the data analysis. Several reasons underlay the importance of annotations; first and foremost the manual verification of each event was used to check whether the filtering threshold functioned somewhat accurately (i.e. there were false positives and they should be removed). The second reason was related to the phase definitions: phase one was considered to start when the VRU appeared in the video feed and he/she was detectable by the annotator. As well each event needed to be analyzed combining together on-board camera images and steering wheel signal, which was highly affected by road curvature change in the scenario. In that regards it has to be highlighted that during the activity it has not proven efficient an automatic implementation of the start-end of the different phases. However different phases were recognized matching together the visual information of the video and the signal properties. Therefore results could be slightly affected by annotator's perception of the scene, even though a common annotation approach has been followed by both authors of this activity. The annotation process has been used for evaluation of ME detection, since the sensor was classifying as pedestrian also other road users or traffic signs. For example motorists riding a bike or people riding horses were classified as pedestrian. Moreover, the annotation process has been considered crucial in order to enrich the data about some specific scene factors, like the number of pedestrian overtaken, the position of the pedestrian on the road, the walking direction of the VRU to mention a few.

Overtaking phases

The implemented approach has been an attempt to evaluate drivers behaviour by a direct analysis of which is the driver steering control during the event. The previously defined [19] four phases approach needed to be reviewed since drivers were observed to start the returning phase before having actually passed the pedestrian (see Figure 4.5; however the car-pedestrian lateral distances have been analyzed within an area of $\pm 3m$, which was considered to be the passing phase for bicycle studies [23]. The tendency to start the returning phase before getting past the pedestrian longitudinally has been detected for the majority of drivers (see Figure 4.5). This could be related to the high relative speed between road users, but another factor could also be considered. Due to their experience in time, drivers could have become aware of the response delay of the mechanical system from driver's hand to the front wheels. As a matter of fact a transfer function between front-wheel steering angle on the ground and driver's input to the steering wheel is considered in vehicle dynamics modelling [91]. Therefore, based on observation related to the general trend between drivers, the organization of the manoeuvre could be summarized in: perception, decision making and execution. The perception could be associated to the phase one – approaching. The decision making could be associated to the start of phase two. The execution could then be grouped in two single phases: steering-out (phase two) and steering-in (phase four or returning). Therefore the phase three, as defined in the annotation process (see Section 3.1.3) could be included in the steering-out phase leading to an overall model of three phases altogether.

Pedestrian position extrapolation

In the post processing, the pedestrian position extrapolation has been characterized by multiple assumptions. First and foremost, constant speed and constant walking direction. These were considered possible even though not a complete faithful picture of the scene. It is worth mentioning that no ground truth have been available neither for car trajectory evaluation, nor for pedestrian position estimation in the scene. However, a group of events was selected and for those a map matching between car trajectory and actual road has been executed. Once proved to be reliable, the car trajectory estimation as well as the pedestrian position is space have been analyzed for each event, mainly with the purpose of verifying the pedestrian path fitted through the inliers of ME detection. Thus, a supervised approach has been selected to avoid possible errors in results associated to wrong pedestrian position when transformed into the global reference frame. It is worth highlighting once more that the adoption of the proposed methodology (implementing the scene in a global reference frame) has been necessary in order to evaluate pedestrian position once he/she was out of ME field of view or detection range. This because no other information related to the environment were available for both phases one or two (when pedestrian is detected) and the returning phase (when the VRU is behind the car, and therefore out of sensor detection possibilities).

5.4.2 Field data collection

Three main activities associated to the field data collection are worth to be examined. These are the experimental protocol selection, the equipment performance and data post processing. Referring to the experimental protocol selection, it has to be highlighted the correct hypothesis associated to the pedestrian walking direction. Hence the scenario design could be adopted as well in future studies, also considering test truck experiments.

Sensors and equipment performance

The overall collection platform, implemented using ROS has proved to be reliable in sensor data recording, and therefore its application is suggested also for future implementations. The LiDAR has shown itself to be a convenient device to capture distances in the proximity of the pedestrian. Compared to other sensors such as ultrasonic sensors, it has a wider field of view and higher range. However, in addition to the high cost, some other issues have been identified that need to be taken into account for future experiments. Even if LiDAR specification states that the maximum scanning distance is 80 m, its performances were mainly affected by the relevant motion of the sensor equipment device. Its location over the waist seems not to be optimal and therefore other solutions are encouraged. However, besides equipment motion that was forcing the LiDAR to the detect the ground, other factors are noticed to affect LiDAR detection:

- Road geometry: the LiDAR detection is highly affected by the relative position of the car. Slight changes in height (e.g. hilltops or depressions), drastically decrease detection range. It has to be said that the road selected for the data collection was not perfectly flat, and therefore this could have partially influenced ground removal in the post process activity.

- LiDAR shadow area: every time a surface is detected a shadow area is created behind, avoiding the possibility of detecting other objects at a larger distance. For example multiple overtaking vehicles (piggy backers), could have prevented the detection of the oncoming traffic.

The IMU has provided effective observations, even if a reduced frame rate could be suggested for later studies.

The Camera image has provided useful information as far as vehicle manual annotation is concerned. Best setting angle has been 80 - 90 deg allowing to observe the scene for the whole approaching phase. A possible implementation of computer vision could be applied in order to get an automatic annotation of different vehicle types. However, due to the same motion which has affected LiDAR performances, the camera images should be stabilized (by means of IMU sensor information) in order to get possible estimates of vehicle distances to the road line markings.

The GPS with a rate of 1 Hz, seems not to be very accurate especially in the presence of environmental disturbances, like vegetation next to the road for example. To get a reliable pedestrian tracking over time (by means of sensor fusion with IMU data) an higher GPS rate could be suggested. Overall, GPS data related to the speed over time have been considered to compute the mean pedestrian walking speed in each test scenario. Such a speed has been considered in the vehicle speed computation.

Data post processing

In order to detect vehicle shape and its actual position over time, it has been necessary to fuse IMU and LiDAR data in order to extract pointcloud solely related to the road. Furthermore, one of the main activities in the LiDAR data reduction has been based on the individuation and elimination of ground detection. Due to a possible non proper definition of the reference frame transformation between LiDAR and IMU, ground detection were considered with a positive "z" coordinate in Cartesian 3D space, while the ground itself was assumed to have a "z" value equal zero. Elimination of such ground detections could have caused also the removal of vehicle front-bumper points simultaneously detected in the scene.

Nonetheless the vehicle cluster identification and tracking has proven to be effective also in the classification of events as occurring with oncoming vehicle presence or being the vehicle a piggy backer.

The complete reconstruction of the car side during the overtaking manoeuvre has noticed to be unfeasible due to sensor equipment displacement (in the direction perpendicular to the road) over time. As a matter of fact, the hip motion has been characterized not only by rotations over time (estimated through Madgwick filter) but also by small translations in the direction transverse to the pedestrian body and along the aforementioned "z" axis. Therefore, between frames the vehicle's cluster was affected not only by its longitudinal motion, but also by a slight transverse motion, which has made it impossible to evaluate change in vehicle heading during the manoeuvre.

Furthermore, it has to be considered that during the event the detected area was changing not only related to the front or rear of the vehicle, but also related to the side. Being the 2D laser plane changing over time according to pedestrian walking motion.

As a consequence of all the aforementioned challenges associated to the LiDAR data analysis, the main variable that has been considered is the minimum distance at which the driver is

overtaking the pedestrian. Hence no other evaluation associated to phases definition or related to overtaking strategy have been possible. In other words, to accomplish this task, a self stabilizing gimbal could be adopted allowing the LiDAR to remain as parallel as possible to the road, thus avoiding ground detections while walking.

5.4.3 Limitations

As summary, the reader has to consider that the following activity could have influenced the thesis results:

- Manual annotation - due to possible subjectivity of annotators (NDS)
- Car trajectory reconstruction - due to heading angle estimation in an inertial reference frame (NDS)
- Pedestrian path extrapolation - due to the object detection sensor performance (NDS)
- Vehicle speed while passing - being the speed a derived measure and not a direct sensor measurement (FT)
- Vehicle length and width evaluation - due to a possible not complete shape detection by the LiDAR (FT)

6 Conclusion and future work

6.1 Conclusion

In the recent years, researchers are emphasizing the importance of vulnerable road users safety to reach Vision Zero in Europe. Despite the increased interest and the strong promotion of the interaction between drivers and cyclists in crossing and longitudinal scenario, as well as driver-pedestrian interrelation in crossing scenarios, some research areas still have not yet been analyzed.

Specifically, no research study has been found in the literature related to the longitudinal interaction between drivers and pedestrians. Neither the lateral clearance between pedestrian and vehicle during an overtaking manoeuvre, nor a comprehensive analysis of driver behaviour based on NDS, for such event, have been investigated before.

Achievements can be grouped in term of influencing factors in drivers selection of their comfort zone boundaries. As well relevance has to be given to implications on active system development (AEB) and safety feature assessment.

The driver model developed has shown how drivers' behaviour is influenced by specific factors related to the characteristic of the scenario in which the overtaking manoeuvre needs to be performed. In detail:

- Pedestrian walking position affects driver behaviour. Lateral clearance decreases as a pedestrian walks more toward the middle of the lane.

- Pedestrian walking position affects driver selection of the vehicle position in the lane, with more vehicles overstepping the center line when the pedestrian is closer to the road center. However the behaviour is highly influenced by vehicle's dimensions. As average behaviour, car drivers are used not to reach the road center line (with the vehicle's outermost side) both for a pedestrian walking in the road and out of the road.

- Pedestrian walking direction influences the phase two of the overtaking maneuver. Drivers overtake keeping a larger distance to the pedestrian when no eye-contact is possible.

- Presence of oncoming traffic has a great impact in the performance of the manoeuvre. Drivers are shown to be affected in the selection of the vehicle speed as well as the leeway between car-side and pedestrian, with lower speed and a reduced clearance with the presence of oncoming vehicles. Also, this factor marginally influences the time at which drivers perform the steer away manoeuvre, with manoeuvre carried out earlier when no oncoming traffic is present in the scene.

Implication of these findings have to be related to the Euro NCAP assessment protocol (CPLA) as well as active system development. The $TTC \geq 1.7s$ adopted nowadays in the test protocol CPLA-25 has shown to be consistent with drivers performances. If the road map of Euro NCAP is considered, Automatic Emergency Steering (AES) systems are planned to be tested. A possible future assessment protocol testing AES for the interaction with pedestrians, should consider the influence of specific factors on the driver behaviour, as presented above. As well, the presented vehicle trajectories could be considered for path planning purposes of

automated vehicles. Among the achievements of this project some methodological contributions

can be highlighted. Referring to the NDS, this project outlined the identification process as well as event data extrapolation and CZB evaluation. This was performed by a step wise approach based on the context in which a VRU went out of the field of view/detection range of the ME-system and then determining the VRUs position using the inertial reference frame for data extrapolation. All phases were manually annotated and an area extending from 3 m in front of the pedestrian to -3m behind the VRU was automatically derived. Furthermore, comfort zone measures for each of the four phases were extracted. Additionally, event data enrichment has been applied to each event related to the French country. The main signals that were used in the reduction of the data in this study were the longitudinal and lateral distance to the VRU, both signals from the ME-system. Also lateral acceleration, yaw rate and vehicle speed, from CAN data have been used for segment classification as possible overtaking events. Overall, this work shows the potential of using naturalistic driving data for analysis of vehicles' interaction with pedestrians. Mainly, driver's control of the vehicle has been analyzed suggesting a phase definition based on driver input to the vehicle by mean of the steering action.

Regarding the field test instrumentation, the development of the data collection platform applicable for multiple purposes, has to be considered among the achievements of this thesis. The measurement equipment has proved to be reliable in the recording of synchronized data between different sensors at different rates.

Furthermore a data processing platform for LiDAR data post processing has allowed to detect and track vehicle' clusters over time. This methodology has been applied for the analysis of 481 overtaking maneuvers, allowing to have a detailed evaluation of the minimum lateral clearance.

6.2 Future prospects and research

From the analysis related to the UDRIVE data set, it stood out that drivers are used to have a very short or absent phase three. This suggests that drivers usually are not willing to get parallel to the pedestrian trajectory for a long time, suggesting to split the overtaking manoeuvre in three phases for the overtaking of pedestrians, although previous literature on drivers overtaking vehicles or bicycles proposed four or more phases [19] [23]. This is mainly due to the large relative speed between the vehicle and the road user. The proposal of a three-phase vehicle control strategy could be based on:

- Approaching phase – driver detects the pedestrian in the scene
- Steering out – driver change vehicle's course to avoid a possible collision to the pedestrian
- Steering in – driver returns back to the original position in the lane

This proposal could be consistent with a previous trend noticed in drivers' behaviour classification. When the overtaking manoeuvre of a vehicle has been analyzed, Hegeman suggested the definition of five overtaking phases [20]. Considering the overtaking event of a bicycle Dozza et al. suggested a four phase approach [19]. Hence, it can be reasonable to observe a behavioural modification in driver's control execution when a pedestrian is present in the scene.

The dominant variable which differs among the aforementioned scenarios is the relative speed between the EGO vehicle and the road user that needs to be overtaken. However, a parameter that plays a significant role is the different position of the road user in the lane.

While overtaking a pedestrian, drivers appear to behave as feed forward controllers. Feed forward driven controllers use knowledge of the system it is supposed to control to act directly on it, anticipating changes. Through the analysis of the cabin video in the NDS data set, it was noticed that, if no other threats were present in the scene, drivers comfortably performed the overtaking manoeuvre by mean of a slight steering wheel rotation, usually gazing at the rear view mirror once the manoeuvre has been completed. With reference to an idealized scenario represented in Figure 6.1, this behaviour is considered to be different from the overtaking of another vehicle, where drivers need to properly estimate the leading vehicle speed, and therefore for such events the steering wheel angle is expected to be more marked. Furthermore, the relative speed between road users seems to play an important role in the driver selection of the distances to the pedestrian, leading to a start of the returning phase quite in advance with respect to a car overtaking manoeuvre. Thus, considering driver's main control through steering

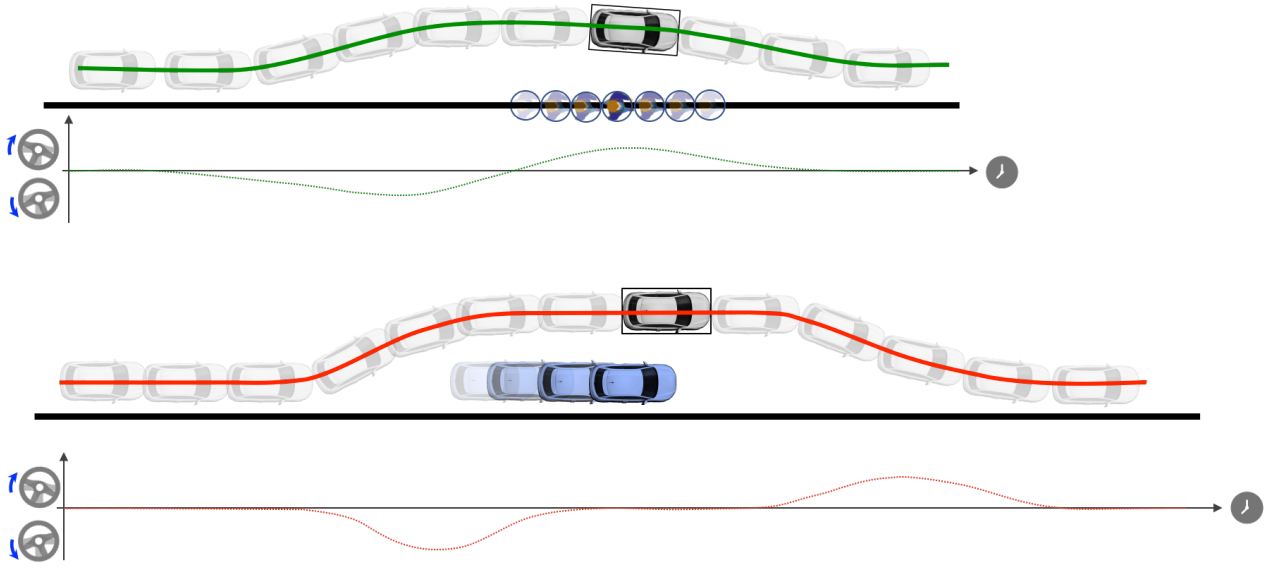

Figure 6.1: *Representation of the overtaking scenario involving two different road user. The representation of the steering wheel signal is given. Difference in the vehicle trajectory is presented for the overtaking of a pedestrian (top) and for overtaking of a vehicle (bottom)*

wheel action, it is proposed an investigation of driver interaction with different road users by mean of an analysis of how the steering control is applied in different events. Furthermore, an analogy with control theory can be investigated in future studies. Since the control action performed by a human controller while overtaking a pedestrian appears to be without much workload, with reference to previous study about transfer functions of human controller [91], the control action is expected to be mainly a proportional action, with very weak derivative action or an integral one (in a proportional, integral, derivative PID control). The development of an accurate driver model associated to the steering wheel action performed by drivers during the overtaking of different road user could be helpful for active safety systems. In detail, such devices could be adopted as driver assistance systems aimed at predict and understand possible driver intentions, and eventually take action in the condition in which no driver expected input

to the vehicle would be noticed. Therefore, an in deep investigation and classification of different behaviour with different user is suggested. This should be done not only in term of comfort zones boundaries, but also in term of trajectory and driver intentions in the path planning. Moreover, in order to properly understand driver's vehicle control and lateral distances to pedestrians, a field test with spontaneous participant driving an equipped vehicle is suggested for further investigations. Indeed, using a LiDAR equipped car together with a CAN-data logger, could provide behavioural information of the driver for the complete duration of the field test. Withal, limitation on the possible number of participants (drivers) and multiple vehicles type would be introduced. As a general recommendation,since the 2D LiDAR installed over pedestrian waist has proven to be not suitable to recognize the four defined phases of an overtaking maneuver, the utilization of a self stabilizing gimbal could be suggested for an improvement in the hardware components. Alternatively, in order to provide the best results, the adoption of a 3D LiDAR for the observation of the scene from a pedestrian point of view could be helpful.

References

[1] C. V. Zegeer and M. Bushell. Pedestrian crash trends and potential countermeasures from around the world. *Accident Analysis & Prevention* **44**.1 (2012), 3–11. ISSN: 0001-4575. DOI: https://doi.org/10.1016/j.aap.2010.12.007. URL: http://www.sciencedirect.com/science/article/pii/S0001457510003842.

[2] J. Bärgman, K. Smith, and J. Werneke. Quantifying drivers' comfort-zone and dread-zone boundaries in left turn across path/opposite direction (LTAP/OD) scenarios. **35** (Nov. 2015), 170–184.

[3] M. L. Aust and J. Engström. A conceptual framework for requirement specification and evaluation of active safety functions. *Theoretical Issues in Ergonomics Science* **12**.1 (2011), 44–65. DOI: 10.1080/14639220903470213. URL: https://doi.org/10.1080/14639220903470213.

[4] M. Peden. *World Report on Road Traffic Injury Prevention*. 2004.

[5] H. Naci, D. Chisholm, and T. D. Baker. Distribution of road traffic deaths by road user group: a global comparison. *Injury Prevention* **15**.1 (2009), 55–59. ISSN: 1353-8047. DOI: 10.1136/ip.2008.018721. URL: http://injuryprevention.bmj.com/content/15/1/55.

[6] National Highway Traffic Safety Administration. Traffic Safety Facts 2015: Speeding. *U.S. Department of Transportation, National Highway Traffic Safety Administration* DOT HS 812 409 (2017), 2006–2014.

[7] K. J. Clifton, C. V. Burnier, and G. Akar. Severity of injury resulting from pedestrian–vehicle crashes: What can we learn from examining the built environment? *Transportation Research Part D: Transport and Environment* **14**.6 (2009), 425–436. ISSN: 1361-9209. DOI: https://doi.org/10.1016/j.trd.2009.01.001. URL: http://www.sciencedirect.com/science/article/pii/S1361920909000157.

[8] National Highway Traffic Safety Administration. Traffic Safety Facts 2008. *Annals of Emergency Medicine* **53**.6 (2009), 214. ISSN: 01960644. DOI: 10.1016/j.annemergmed.2009.04.002.

[9] SafetyNet. Roads (2009), 41.

[10] P. Thomas et al. Dacota: Road Safety Data, Collection, Transfer and Analysis Deliverable 0.1-Final Project Report (Sept. 2013).

[11] the Swedish Transport Administration (2014). URL: http://www.trafikverket.se/Privat/Trafiksakerhet/Olycksstatistik/Vag/.

[12] E. Commission. *Traffic Safety Basic Facts on Main Figures*. European Commission, Directorate General for Transport.

[13] Limpert. *Motor Vehicle Accident Reconstruction and Cause Analysis*. 4th edition. A. The Michie Company, 1994, p. 663.

[14] A. Loukaitou-Sideris, R. Liggett, and H.-G. Sung. Death on the Crosswalk: A Study of Pedestrian-Automobile Collisions in Los Angeles. *Journal of Planning Education and Research* **26**.3 (2007), 338–351. DOI: 10.1177/0739456X06297008. URL: https://doi.org/10.1177/0739456X06297008.

[15] D. Cambridge. *Overtaking definition*. 2018. URL: https://dictionary.cambridge.org/dictionary/english/overtake.

[16] T. R. S. for the Prevention of Accidents. "Road Safety Factsheet, Overtaking". *Calthorpe Road, Edgbaston, Birmingham B15 1RP — Telephone 0121 248 2000*. 2017.

[17] T. M. Matson, T. W. Forbes, and B. D. Greenshields. Overtaking and passing requirements as determined from a moving vehicle. *Highway Research Board Proceedings* **18** (1939).

[18] T. Wilson and W. Best. Driving strategies in overtaking. *Accident Analysis & Prevention* **14**.3 (1982), 179–185. ISSN: 0001-4575. DOI: https://doi.org/10.1016/0001-4575(82)90026-4. URL: http://www.sciencedirect.com/science/article/pii/0001457582900264.

[19] M. Dozza et al. How do drivers overtake cyclists? *Accident Analysis & Prevention* **Volume 88** (2016), 29–36.

[20] G. Hegeman, K. Brookhuis, and S. Hoogendoorn. Opportunities of advanced driver assistance systems towards overtaking. *European journal of transport and infrastructure research EJTIR, 5 (4)* (2005).

[21] K.-H. Chuang et al. The use of a quasi-naturalistic riding method to investigate bicyclists' behaviors when motorists pass. *Accident Analysis & Prevention* **56** (2013), 32–41.

[22] P. Petrov and F. Nashashibi. Planning and nonlinear adaptive control for an automated overtaking maneuver. *Intelligent Transportation Systems (ITSC), 2011 14th International IEEE Conference on* (2011), 662–667.

[23] J. B. M. D. Kovaceva J., Nero G. Drivers overtaking cyclists in the real-world: evidence from a naturalistic driving study. *Article under revision* ().

[24] V. B. Ron Schindler. "Drivers' comfort boundaries when overtaking a cyclist Set-up and verification of a methodology for field data collection and analysis". MA thesis. 2016.

[25] G. Nero. "Quantifying Drivers' Behaviours when Overtaking Bicyclists on Rural Roads A Study Using Naturalistic Driving Data from a Vehicle's Perspective". MA thesis. 2017.

[26] D. Cambridge. *Behaviour definition*. 2018. URL: https://dictionary.cambridge.org/dictionary/english/behaviour.

[27] D. Oxford. *Behaviour definition*. 2018. URL: https://www.collinsdictionary.com/dictionary/english/behaviour.

[28] M. Garcia Ortiz. Prediction of driver behavior (2014).

[29] N. Guéguen, S. Meineri, and C. Eyssartier. A pedestrian's stare and drivers' stopping behavior: A field experiment at the pedestrian crossing. *Safety Science* **75** (2015), 87–89. ISSN: 0925-7535. DOI: https://doi.org/10.1016/j.ssci.2015.01.018. URL: http://www.sciencedirect.com/science/article/pii/S0925753515000193.

[30] N. Guéguen, C. Eyssartier, and S. Meineri. A pedestrian's smile and drivers' behavior: When a smile increases careful driving. *Journal of Safety Research* **56** (2016), 83–88. ISSN: 00224375. DOI: 10.1016/j.jsr.2015.12.005.

[31] S. A. Balk et al. Highlighting Human Form and Motion Information Enhances the Conspicuity of Pedestrians at Night. *Perception* **37**.8 (2008), 1276–1284. DOI: 10.1068/p6017. URL: https://doi.org/10.1068/p6017.

[32] R. A. Tyrrell, J. M. Wood, and T. P. Carberry. On-road measures of pedestrians' estimates of their own nighttime conspicuity. *Journal of Safety Research* **35**.5 (2004), 483–490. ISSN: 0022-4375. DOI: https://doi.org/10.1016/j.jsr.2004.06.004. URL: http://www.sciencedirect.com/science/article/pii/S0022437504000854.

[33] B. E. Hagel et al. The prevalence and reliability of visibility aid and other risk factor data for uninjured cyclists and pedestrians in Edmonton, Alberta, Canada. *Accident Analysis & Prevention* **39**.2 (2007), 284–289. ISSN: 0001-4575. DOI: https://doi.org/

10.1016/j.aap.2006.07.010. URL: http://www.sciencedirect.com/science/article/pii/S0001457506001345.

[34] J. M. Wood, R. A. Tyrrell, and T. P. Carberry. Limitations in Drivers' Ability to Recognize Pedestrians at Night. *Human Factors* **47**.3 (2005), 644–653. DOI: 10.1518/001872005774859980. URL: https://doi.org/10.1518/001872005774859980.

[35] D. Shinar. *Traffic Safety and Human Behavior: Second Edition*. Emerald Publishing Limited, 2017. ISBN: 9781786352217. URL: https://books.google.se/books?id=1CUpDwAAQBAJ.

[36] D. Stewart, C. J. Cudworth, and J. R. Lishman. Misperception of Time-to-Collision by Drivers in Pedestrian Accidents. *Perception* **22**.10 (1993), 1227–1244. DOI: 10.1068/p221227. URL: https://doi.org/10.1068/p221227.

[37] J. J. Gibson. *The Perception Of The Visual World*. Boston: Houghton Mifflin, 1950.

[38] W. D. Hollnagel E. *Joint Cognitive Systems*. Boca Raton, 2005.

[39] H. E. Engström J. A General Conceptual Framework for Modelling Behavioural Effects of Driver Support Functions. *In: Cacciabue P.C. (eds) Modelling Driver Behaviour in Automotive Environments.* (2007). DOI: https://doi.org/10.1007/978-1-84628-618-6_4.

[40] J. A. Michon. "A Critical View of Driver Behavior Models: What Do We Know, What Should We Do?" *Human Behavior and Traffic Safety*. Ed. by L. Evans and R. C. Schwing. Boston, MA: Springer US, 1985, pp. 485–524. ISBN: 978-1-4613-2173-6. DOI: 10.1007/978-1-4613-2173-6_19. URL: https://doi.org/10.1007/978-1-4613-2173-6%7B%5C_%7D19.

[41] S. Breker et al. *Problems of elderly in relation to the driving task and relevant critical scenarios*. Tech. rep. D1.1. School of Health Science, Jönköping University, HHJ, Dep. of Rehabilitation, 2003, p. 124.

[42] E. Bekiaris, A. Amditis, and M. Panou. DRIVABILITY: a new concept for modelling driving performance. *Cognition, Technology & Work* **5** (2003), 152–161.

[43] P. Cisek. Cortical mechanisms of action selection: the affordance competition hypothesis. *Philosophical Transactions of the Royal Society of London B: Biological Sciences* **362**.1485 (2007), 1585–1599. ISSN: 0962-8436. DOI: 10.1098/rstb.2007.2054. URL: http://rstb.royalsocietypublishing.org/content/362/1485/1585.

[44] G. K. S. A. Da Lio M. Mazzalai A. Biologically Guided Driver Modeling: the Stop Behavior of Human Car Drivers. *IEEE Transactions on Intelligent Transportation Systems* **362**.1485 (2017), 1585–1599. DOI: 0.1109/TITS.2017.2751526. URL: https://ieeexplore.ieee.org/document/8057588/?denied.

[45] A. H. P. M. Marti Geoffrey and G. Montagne. Drivers' Decision-Making When Attempting to Cross an Intersection Results from Choice between Affordances. **8**.1026 (2014). DOI: doi:10.3389/fnhum.2014.01026.

[46] D. T. McRuer et al. New Results in Driver Steering Control Models. *Human Factors* **19**.4 (1977), 381–397. DOI: 10.1177/001872087701900406. URL: https://doi.org/10.1177/001872087701900406.

[47] U. Kjellén. The deviation concept in occupational accident control-II. *Accident Analysis & Prevention* **16** (1984), 289–306.

[48] J. J. Gibson and L. E. Crooks. A Theoretical Field-Analysis of Automobile-Driving. *The American Journal of Psychology* **51**.3 (1938), 453–471. ISSN: 00029556. URL: http://www.jstor.org/stable/1416145.

[49] V. Papakostopoulos, N. Marmaras, and D. Nathanael. The "field of safe travel" revisited: interpreting driving behaviour performance through a holistic approach. *Transport Reviews* **37**.6 (2017), 695–714. DOI: 10.1080/01441647.2017.1289992. URL: https://doi.org/10.1080/01441647.2017.1289992.

[50] I. BROWN. A review of: "Road-User Behavior and Traffic Accidents", By R. NÄÄTÄNEN and H. SUMMALA. (Amsterdam: NORTH-HOLLAND PUBLISHING CO., 1976.) [Pp. ix270.] $27•95. *Ergonomics* **20**.6 (1977), 698–700. DOI: 10.1080/00140137708931684. URL: https://doi.org/10.1080/00140137708931684.

[51] H. Summala. "Towards Understanding Motivational and Emotional Factors in Driver Behaviour: Comfort Through Satisficing". *Modelling Driver Behaviour in Automotive Environments: Critical Issues in Driver Interactions with Intelligent Transport Systems*. Ed. by P. C. Cacciabue. London: Springer London, 2007, pp. 189–207. ISBN: 978-1-84628-618-6. DOI: 10.1007/978-1-84628-618-6_11. URL: https://doi.org/10.1007/978-1-84628-618-6%7B%5C_%7D11.

[52] T. Vaa. "Modelling Driver Behaviour on Basis of Emotions and Feelings: Intelligent Transport Systems and Behavioural Adaptations". *Modelling Driver Behaviour in Automotive Environments: Critical Issues in Driver Interactions with Intelligent Transport Systems*. Ed. by P. C. Cacciabue. London: Springer London, 2007, pp. 208–232. ISBN: 978-1-84628-618-6. DOI: 10.1007/978-1-84628-618-6_12. URL: https://doi.org/10.1007/978-1-84628-618-6%7B%5C_%7D12.

[53] I. Walker. Drivers overtaking bicyclists: Objective data on the effects of riding position, helmet use, vehicle type and apparent gender. *Accident Analysis & Prevention* **39**.2 (2007), 417–425. ISSN: 0001-4575. DOI: https://doi.org/10.1016/j.aap.2006.08.010. URL: http://www.sciencedirect.com/science/article/pii/S0001457506001540.

[54] Mehta, Kushal. "Analysis of Passing Distances between Bicycles and Motorized Vehicles on Urban Arterials". MA thesis. 2015. URL: http://hdl.handle.net/10012/9111.

[55] D. A. Gordon and T. M. Mast. Drivers' Judgments in Overtaking and Passing. *Human Factors: The Journal of Human Factors and Ergonomics Society* **12**.3 (1970), 341–346. ISSN: 15478181. DOI: 10.1177/001872087001200310.

[56] M. L. A. S. Dombrovskis. "Understanding and Improving Driver Compliance with Safety System Feedback". *Proceedings of the 23rd Enhanced Safety of Vehicles (ESV) Conference, Seoul, Republic of Korea, paper number 13-0455*. Vol. 51. 13-0455. 2013. URL: http://www-esv.nhtsa.dot.gov/Proceedings/23/isv7/main.htm.

[57] A. Doshi and M. M. Trivedi. Tactical Driver Behavior Prediction and Intent Inference: A Review. *IEEE Conference on Intelligent Transportation Systems, Proceedings, ITSC* (2011), 1892–1897.

[58] L. Fridman et al. {MIT} Autonomous Vehicle Technology Study: Large-Scale Deep Learning Based Analysis of Driver Behavior and Interaction with Automation. *CoRR* **abs/1711.0** (2017). arXiv: 1711.06976. URL: http://arxiv.org/abs/1711.06976.

[59] K. Dietmayer. Predicting of machine perception for automated driving. *Autonomous Driving* (2016), 407–424.

[60] D. Gerónimo, A. López, and A. D. Sappa. Computer vision approaches to pedestrian detection: visible spectrum survey. *Iberian Conference on Pattern Recognition and Image Analysis* (2007), 547–554.

[61] A. Shashua, Y. Gdalyahu, and G. Hayun. Pedestrian detection for driving assistance systems: single-frame classification and system level performance. *IEEE Intelligent Vehicles Symposium, 2004* (2004), 1–6.

[62] Y.-C. Kuo et al. Pedestrian Collision Warning of Advanced Driver Assistance Systems. *Computer, Consumer and Control (IS3C), 2016 International Symposium on* (2016), 740–743.

[63] C. Harris and M. Stephens. "A combined corner and edge detector". *In Proc. of Fourth Alvey Vision Conference*. 1988, pp. 147–151.

[64] D. Julong. Introduction to grey system theory. *The Journal of grey system* **1**.1 (1989), 1–24.

[65] J. Bärgman et al. How does glance behavior influence crash and injury risk? A 'what-if'counterfactual simulation using crashes and near-crashes from SHRP2. *Transportation Research Part F: Traffic Psychology and Behaviour* **35** (2015), 152–169.

[66] I. Van Schagen and F. Sagberg. The potential benefits of naturalistic driving for road safety research: Theoretical and empirical considerations and challenges for the future. *Procedia-Social and Behavioral Sciences* **48** (2012), 692–701.

[67] T. A. Dingus et al. Driver crash risk factors and prevalence evaluation using naturalistic driving data. *Proceedings of the National Academy of Sciences* **113**.10 (2016), 2636–2641.

[68] M. de Rycke. *The UDRIVE dataset and key analysis results*. Tech. rep. D41.1. European Commission, 2018, p. 120.

[69] E. NCAP. *Euro NCAP 2025 Roadmap*. Tech. rep. D41.1. Brussels, 2018, p. 19.

[70] P. Seiniger et al. ASPECSS - Assessment methodologies for forward looking Integrated Pedestrian and further extension to Cyclists Safety. *Aspecss D2.5* (2014), 74. ISSN: 00295493. DOI: 10.1016/j.nucengdes.2011.01.052.

[71] W. By et al. European Commission (2013).

[72] E. NCAP. *VRU test protocols*. 2018. URL: https://www.euroncap.com/en/vehicle-safety/the-ratings-explained/vulnerable-road-user-vru-protection/.

[73] Euro NCAP. EUROPEAN NEW CAR ASSESSMENT PROGRAMME (Euro NCAP) - Test Protocol AEB VRU systems. Version 2.0 (2017).

[74] EuroNCAP. European new car assessment programme, assement protocol for pedestrian protection. June (2011).

[75] E.-c. U. Partners. *deliverables download*. 2018. URL: http://www.udrive.eu/index.php/udrive-library/deliverables?start=20.

[76] C. Partner Clément Val. *What are the challenges to have a good database?* 2018. URL: http://www.udrive.eu/index.php?option=com_content&view=article&id=111.

[77] R. Rajamani. "Lateral vehicle dynamics". *Vehicle Dynamics and control*. Springer, 2012, pp. 15–46.

[78] M. A. Fischler and R. C. Bolles. "Random sample consensus: a paradigm for model fitting with applications to image analysis and automated cartography". *Readings in computer vision*. Elsevier, 1987, pp. 726–740.

[79] J.-O. Nilsson et al. Foot-mounted INS for everybody-an open-source embedded implementation. *Position Location and Navigation Symposium (PLANS), 2012 IEEE/ION* (2012), 140–145.

[80] S. O. H. Madgwick, A. J. L. Harrison, and R. Vaidyanathan. Estimation of IMU and MARG orientation using a gradient descent algorithm. *Rehabilitation Robotics (ICORR), 2011 IEEE International Conference on* (2011), 1–7.

[81] C. C. A. 3. Dirk Thomas. *ROS introduction*. 2014. URL: http://wiki.ros.org/ROS/Introduction.

[82] S. Krakowiak. What is middleware. *ObjectWeb. org. http://middleware. objectweb. org* (2003).

[83] A. Bhaumik. *From AI to Robotics*. Boca Raton: CRC Press, 2018, p. 162. ISBN: 9781482251487. URL: https://books.google.se/books?id=0mlQDwAAQBAJ.

[84] A. M. Romero. *ROS Concepts*. 2014. URL: http://wiki.ros.org/ROS/Concepts.

[85] R. Alexander. *RTC-Real time clock for bike logger*. 2017. URL: https://github.com/feuerblitz7/cycle-data-logger.

[86] R. Anitha, S. Arunachalam, and P. Radhakrishnan. Critical parameters influencing the quality of prototypes in fused deposition modelling. *Journal of Materials Processing Technology* **118**.1-3 (2001), 385–388.

[87] Replycating-Rapid-prototyping. *Extruders*. 2015. URL: http://reprap.org/wiki/Category:Extruders.

[88] B. Efron. Bayes' theorem in the 21st century. *Science* **340**.6137 (2013), 1177–1178.

[89] A. Gelman et al. *Bayesian data analysis*. CRC press, 2013.

[90] Z. Ren, X. Jiang, and W. Wang. Analysis of the Influence of Pedestrians' eye Contact on Drivers' Comfort Boundary During the Crossing Conflict. *Procedia engineering* **137** (2016), 399–406.

[91] M. Abe. *Vehicle Handling Dynamics: Theory and Application*. Elsevier Science, 2015. ISBN: 9780081003732. URL: https://books.google.se/books?id=yOzHBQAAQBAJ.

[92] A. Dockhorn, C. Braune, and R. Kruse. "An alternating optimization approach based on hierarchical adaptations of dbscan". *Computational Intelligence, 2015 IEEE Symposium Series on*. IEEE. 2015, pp. 749–755.

[93] V. Papakostopoulos, N. Marmaras, and D. Nathanael. The "field of safe travel" revisited: interpreting driving behaviour performance through a holistic approach. *Transport Reviews* **37**.6 (2017), 695–714. ISSN: 14645327. DOI: 10.1080/01441647.2017.1289992. URL: https://doi.org/10.1080/01441647.2017.1289992.

[94] A. Nguyen and B. Le. *3D point cloud segmentation: A survey*. 2013.

[95] T. Shamir. How should an autonomous vehicle overtake a slower moving vehicle: Design and analysis of an optimal trajectory. *IEEE Transactions on Automatic Control* **49**.4 (2004), 607–610.

[96] D. P. Felzenszwalb Pedro F; Huttenlocher. Effcient Graph-Based Image Segmentation. *International Journal of Computer Vision* **59**.2 (2004), 167–181. URL: http://link.springer.com/article/10.1023/B:VISI.0000022288.19776.77.

[97] J. C. Pinheiro and D. M. Bates. "Linear Mixed-Effects Models: Basic Concepts and Examples". *Mixed-Effects Models in Sand S-PLUS*. 2000, pp. 3–56.

[98] B. Bhanu et al. "Range data processing: Representation of surfaces by edges". *Proceedings of the IEEE International Pattern Recognition Conference*. 1986, pp. 236–238.

[99] J. C. Pinheiro and D. M. Bates. "Mixed-Effects Models in S and S-PLUS". *Mixed-Effects Models in S and S-PLUS*. 2000.

[100] G. Nero. Quantifying Drivers ' Behaviours when Overtaking Bicyclists on Rural Roads A Study Using Naturalistic Driving Data from a Vehicle ' s Perspective (2017).